REC-ERC-77-8

ATMOSPHERIC SIMULATION USING STRATIFIED LIQUID MODELS

Engineering and Research Center
Bureau of Reclamation

July 1977

MS-230 (1-76)
Bureau of Reclamation

TECHNICAL REPORT STANDARD TITLE PAGE

1. REPORT NO. REC-ERC-77-8	2. GOVERNMENT ACCESSION NO.	3. RECIPIENT'S CATALOG NO.
4. TITLE AND SUBTITLE Atmospheric Simulation Using Stratified Liquid Models		5. REPORT DATE July 1977
		6. PERFORMING ORGANIZATION CODE
7. AUTHOR(S) H. T. Falvey and R. A. Dodge		8. PERFORMING ORGANIZATION REPORT NO. REC-ERC-77-8
9. PERFORMING ORGANIZATION NAME AND ADDRESS Engineering and Research Center Bureau of Reclamation Denver, Colorado 80225		10. WORK UNIT NO.
		11. CONTRACT OR GRANT NO.
12. SPONSORING AGENCY NAME AND ADDRESS Same		13. TYPE OF REPORT AND PERIOD COVERED
		14. SPONSORING AGENCY CODE

15. SUPPLEMENTARY NOTES

16. ABSTRACT

Analytical and laboratory studies were made to demonstrate the feasibility of using stratified liquids and distorted scale maps of an area to simulate mesoscale (2 to 20 kilometres) atmospheric phenomena. Techniques and instrumentation were developed for creating velocity gradients, creating density gradients, for visualization, and for making measurements. The effectiveness of both aerial and ground seeding station locations was investigated for various pilot study areas of Project Skywater.

17. KEY WORDS AND DOCUMENT ANALYSIS

a. *DESCRIPTORS*-- / *atmospheric research/ *model studies/ *field investigations/ weather modification/ cloud seeding/ similitude

b. *IDENTIFIERS*-- / Project Skywater/ Leadville-Climax Pilot Project/ Sierra Cooperative Pilot Project/ Colorado River Basin Pilot Project

c. *COSATI Field/Group* 04B *COWRR:* 0402.1

18. DISTRIBUTION STATEMENT *Available from the National Technical Information Service, Operations Division, Springfield, Virginia 22151.*	19. SECURITY CLASS (THIS REPORT) *UNCLASSIFIED*	21. NO. OF PAGES 96
	20. SECURITY CLASS (THIS PAGE) *UNCLASSIFIED*	22. PRICE

REC-ERC-77-8

ATMOSPHERIC SIMULATION USING STRATIFIED LIQUID MODELS

by

H. T. Falvey

R. A. Dodge

July 1977

Hydraulics Branch
Division of General Research
Engineering and Research Center
Denver, Colorado

SI METRIC

UNITED STATES DEPARTMENT OF THE INTERIOR * BUREAU OF RECLAMATION

ACKNOWLEDGMENT

The concept of using a stratified liquid model to help study cloud seeding from ground stations was conceived by Dr. H. T. Falvey when he was Head, Hydraulics Research Section. He performed the theoretical analyses, designed the laboratory facility, and developed the optical method needed to measure density profiles.

R. H. Kuemmich did considerable work in developing, testing, and installing instrumentation.

W. M. Batts did the photography for documentation and for measuring density profiles.

R. A. Dodge was in charge of the model investigations under the supervision of J. C. Schuster, the current Head, Hydraulic Research Section.

P. Julius converted the numerous photographic data into suitable form to produce the color overlay maps in this report.

The incisive analysis of Dr. Peter Lissaman, Aerovironment, Inc., Pasadena, Calif., concerning the development of the optical method to measure density gradients, is gratefully acknowledged.

The continual interest and help by the Division of Atmospheric Water Resources Management during these studies, as well as their critical review of this report, is greatly appreciated.

Final editing and preparation of the manuscript for publication was performed by R. D. Mohr of the Technical Services and Publications Branch.

CONTENTS

CONTENTS—Continued

CONTENTS—Continued

TABLES

FIGURES

CONTENTS—Continued

TABLES

FIGURES

CONTENTS—Continued

FIGURES IN APPENDICES

PURPOSE

Analytical and laboratory studies were made to determine the feasibility of using stratified liquids and distorted scale maps of an area to simulate mesoscale (2 to 20 kilometers) atmospheric phenomena. Techniques and instrumentation were developed for creating velocity gradients, creating density gradients, for visualization, and for making measurements. The ultimate goal was to investigate the effectiveness of both aerial and ground seeding station locations for various pilot study areas.

INTRODUCTION

Background

Models have been used to simulate atmospheric phenomena for almost half a century. One of the earliest investigations was by Abe [1] [1], who modeled the air currents and cloud formations around Mount Fujiyama in Japan.

In general, two types of scale models have been employed. The first and most common type uses air as the working fluid. With this type of model, flow patterns, eddies, and diffusion characteristics can be studied. Because of difficulties in establishing density gradients, this type of model is usually limited to studies in the lowest layer of the atmosphere. Air models are extremely useful in studying flows around buildings and of diffusion from ground sources.

The second type of model uses liquid as the working fluid. Liquid models have their greatest range of applicability where gravity effects are significant. Studies in the past have included (1) wave motion at and mixing across a density interface, (2) the progress of a density flow (such as a dust cloud or a cold front), and (3) the effect of a schematic mountain range upon successively higher thermal zones of the atmosphere [8]. These models can even include Coriolis forces by rotating the entire tank.

The Bureau model and studies which are described in this report were designed to study orographic deflection of atmospheric flow. The distance scale studied in nature was of the order of 2 to 20 kilometers. Cermak [3] defines this as mesoscale phenomena.

The Bureau model used a stratified liquid to simulate the entire depth of the atmosphere. The purpose of the model was to study mean flow patterns and the patterns of the major circulations. The model flow patterns that are simulated represent the flow patterns at only one instant during the time history of a storm. Thus, the development of a storm can only be simulated by making several runs with various density gradients. It is recognized that the model cannot exactly reproduce the flow conditions over the mountains. However, the surface geometry and stratifications in the atmosphere introduce complexities in the flow patterns that are so great that even a qualitative reproduction of the flow field is beneficial.

The topography is simulated with commercially available plastic relief maps having a 2:1 vertical distortion. The maps can be rotated to change wind direction, density gradients can be varied, and the horizontal curvature of the free stream line trajectories can be reproduced.

Work Plan and General Objectives

To achieve the goals of these studies, model laws and similitude were investigated first. Then, operational and measuring techniques were developed. A facility was then designed to verify the model using the Leadville-Climax, Colo., field data. Tests were then performed on ground seeding stations for the Colorado River Basin Pilot Project of Project Skywater. Following these steps, a series of studies was performed with an improved facility to investigate transport phenomena in winter orographic storms of the Sierra Nevada. The Sierra Cooperative Pilot Project is also a part of Project Skywater.

CONCLUSIONS

The technique of simulating the atmosphere with a stratified liquid was developed and verified during the course of these investigations. Conclusions from these investigations can have a profound effect on locating future ground seeder sites and deciding when to use airborne seeders. Detailed conclusions are discussed later in this report.

MODEL SIMILITUDE

General

For a model to truly represent actual conditions, it must be geometrically, kinematically, and dynamically

[1] Numbers in brackets refer to items in the bibliography.

similar to the prototype. If the model deviates from the prototype in any one of these three areas of similitude, then more care must be taken to interpret the model results. However, if the deviation is too large, the model does not represent the prototype and no amount of interpretation will yield the correct results.

Velocity and Density Gradient Similitude

Atmospheric equation of state.—The theory upon which the model is based was developed by Claus [4]. His studies, as well as some fundamental considerations, have been summarized by Yih [12]. Only the major details will be reproduced here.

For a nonviscous fluid, the equations of motion in rectangular coordinates can be given in vector notation as

$$\rho\left(\frac{\partial u_i}{\partial t} + [u \cdot \nabla u]_i\right) = -\frac{\partial p}{\partial x_i} + \rho X_i \qquad (1)$$

where

p = pressure,
t = time,
u = velocity,
x = coordinate direction,
X = body force per unit mass,
ρ = density of fluid, and
∇ = vector or differential operator known as "nabla" or "del"

subscript

i = 1, 2, and 3 and refer to three orthogonal coordinates such as the x, y, and z directions in rectangular coordinates, respectively.

Equation (1), representing three equations, is applicable for both stratified liquids and gases. The density in the equation is not necessarily constant. For compressible fluids, an equation of state is needed to define the variation of density with elevation or pressure. For stratified liquids, the expression involves a definition of density with depth.

The equation of state for a compressible fluid requires the assumption that the atmosphere behaves like a polytropic process in a perfect gas. Thus,

$$p/\rho^n = p_o/\rho_o^n = \text{constant} \qquad (2)$$

where the subscript o refers to conditions at a reference point, usually the ground. The value n is considered constant for a discrete layer of the atmosphere. However, the absolute value of n varies with the atmospheric conditions. For instance, n can have the following values for various processes:

Constant pressure . . . . $n = 0$
Isothermal (no change in temperature) . . . . $n = 1$
Isentropic (no change in entropy) . . . . $n = k = C_p/C_v > 1$
Constant volume . . . . $n = \infty$

C_p = specific heat at constant pressure
C_v = specific heat at constant volume

For dry air, k is the ratio of the specific heats, C_p/C_v, and is equal to 1.4.

The difference in entropy S between any two states is given by Soo [11] in the relation

$$pv^k = p_o v_o{}^k e^{(S-S_o)/C_v} \qquad (3)$$

where

v = specific volume
e = 2.71828

Let

$$p_o v_o{}^k = C_1$$

Then,

$$pv^n v^{k-n} = C_1 e^{(S-S_o)/C_v}$$

Taking the kth root and substituting $(1/\rho)$ for v gives after some rearrangement,

$$(\rho^n/p)^{1/k} \rho^{(k-n)/n} = C_2 e^{(S_o-S)/C_p}$$

However, since (ρ^n/p) is a constant,

$$\rho^{(k-n)/n} = C_3 e^{(S_o-S)/C_p}$$

Referenced to conditions at the ground level,

$$(\rho/\rho_o)^{(k-n)/n} = C_4 e^{(S_o-S)/C_p} \qquad (4)$$

C_1, C_2, C_3, and C_4 in the above equations are constants.

The right side of equation (4) is an expression which indicates the variation of entropy in the atmosphere with elevation. Entropy can be regarded as a mathematical expression which can be conveniently used to describe quantitatively the ability of the atmosphere to change its energy level. Since entropy is a property, changes in its value are independent of the actual way in which the change was accomplished. Thus, entropy can be used to describe a dry adiabatic atmosphere, a pseudomoist atmosphere, or any other atmosphere that may not even obey reversible gas laws. Equation (4) can be regarded as the equation of state for the polytropic compressible atmosphere.

Richardson number criteria.—Most investigators rely upon a Richardson number to create models of the atmosphere. This number incorporates density variations and velocity gradients into one expression. The Richardson number R is defined as

$$R = -\frac{g}{\rho_a}\left(\frac{\partial \rho}{\partial y}\right)\left(\frac{\partial u_x}{\partial y}\right)^{-2} \tag{5}$$

where

g = acceleration of gravity
ρ_a = average density

Claus [4], in numerical studies of linear equations, discovered a method of essentially breaking the Richardson number criterion into two parts. He found that the flow of an incompressible fluid with stratification in density is similar to the flow of a compressible fluid with stratification of entropy if:

(1) The potential density distribution of the compressible fluid is identical with the potential density distribution of the incompressible fluid, and

(2) The velocity profiles are nearly identical.

For a compressible fluid, the potential density is defined as the resulting density when a parcel of the fluid is brought isentropically to a reference elevation. Potential density has a similar significance as potential temperature, which is a commonly used concept in meteorology. Since the atmosphere is to be simulated with density variations in a liquid, the concept of potential density is the appropriate parameter to be used in this case.

If the reference pressure is defined as the ground level pressure, then the potential density is given by

$$\rho_{pot} = \rho(p_o/p)^{1/k}$$

Similarly, the potential density at any height divided by the potential density at the ground is

$$\rho_{pot}/(\rho_{pot})_o = (\rho/\rho_o)\,(p_o/p)^{1/k} = e^{(S_o - S/C_p)} \tag{6}$$

Comparing equation (6) with equation (4) reveals that the potential density distribution in a polytropic atmosphere is given by

$$\text{Relative density} = \rho_{pot}\,/\,(\rho_{pot})_o = (\rho/\rho_o)^{(k-n)/k}$$

In terms of temperature T and pressure p, if $n \neq k$, then

$$\text{Relative density} = \left(\frac{T_o}{T}\cdot\frac{p}{p_o}\right)^{(k-n)/k} \tag{7a}$$

For $n = k$,

$$\text{Relative density} = \frac{T_o}{T}\left(\frac{p}{p_o}\right)^{\frac{k-1}{k}} = 1 \tag{7b}$$

The temperature in equations (7a) and (7b) must be expressed on the Kelvin scale.

With an incompressible fluid, its relative density is defined simply as the ratio of the density at any elevation to the density at some fixed elevation. Therefore, the entropy gradient of the atmosphere can be properly simulated when the density distribution in the incompressible fluid matches the potential density distribution in the atmosphere as computed from equation (7). Data from radiosondes can be used for input into the equation to compute the relative density at a series of elevations in the atmosphere. Details of the procedure are outlined in appendix B.

The second criterion of Claus requires that the velocity profiles are nearly identical. Thus, as a first approximation, boundary layers should be established in the model where boundary layers exist in the atmosphere. However, identical velocity profiles do not have to be established within the boundary layers.

The maximum velocity in the model can be determined from the Richardson similitude considerations. If each term in the Richardson number, equation (5), is made dimensionless, the following expression results:

$$R = -\frac{gH}{U^2}\left(\frac{\rho_o}{\rho_a}\right)\frac{\partial(\rho/\rho_o)}{\partial(y/H)}\left[\frac{\partial(y/H)}{\partial(U_x/U)}\right]^2 \qquad (8)$$

where

H = distance from sea level elevation to the tropopause,
U = maximum free stream or geostrophic velocity, and
ρ_o = density at the earth's surface.

Equation (8) clearly shows that the conditions of Claus [4] and Yih [12] are directly related to the Richardson number similitude. The term gH/U^2 is the reciprocal of the Froude parameter. This dimensionless parameter arises whenever gravitational effects are significant. For example, see equation (18c).

If the variation in density and in velocity with height is to be similar in the model and the atmosphere, then similitude of the Richardson number requires that

$$U_m = U_{atm}\left(\frac{H_m}{H_{atm}}\right)^{1/2} \qquad (9)$$

where the subscript m refers to model values and atm to atmospheric values.

Equation (9) shows that if maps with a vertical distortion are used to simulate the topography, the velocity scaling is based upon the vertical and not the horizontal scale ratio.

Reynolds similitude.—Reynolds similitude refers to the fluid turbulence. No effort was made to achieve Reynolds similarity. Therefore, flow phenomena related to turbulence such as diffusivity, spreading of a plume, and boundary layer development was not expected to be determined from the model. Only mainstream or plume centerline flow would be represented.

Geometric Similitude

For convenience, commercially available relief maps were used. Therefore, geometric similitude was not maintained in the model. These maps had 2:1 vertical distortion in the scale. Originally the study was planned to investigate the effects of distortion in the model. The flow over several simple geometric shapes was to be compared with the flow over equivalent distorted shapes. The comparative method, while frequently used in laboratory practice, is deficient since the question of extrapolating the data to prototype scales is not definitely resolved.

Another frequently used method to investigate the effects of vertical exaggeration is to calibrate the model using prototype measurements. This method, while not the most scientific, is certainly the most practical. For instance, river models are often distorted as much as 5:1. The bed roughness in the model is varied until a historical event can be duplicated. The main deficiency of this method is the difficulty in obtaining accurate field measurements.

This latter method was chosen to determine if the maps with a 2:1 vertical exaggeration could be used to obtain an accurate representation of field conditions.

Coriolis and Pressure Field Simulation

The motion of the atmosphere is described by Newton's second law which must be written relative to an inertial coordinate system. If the motion is viewed from a moving coordinate system, the basic relationships must account for this movement. To simulate atmospheric motions on a mesoscale, the relationship of the earth to the sun can be considered as an inertial coordinate system. The rotation of the earth is then considered as a moving coordinate system. The velocity of an element of the atmosphere can be described relative to an observer traveling with the moving coordinate system. In this case, the absolute velocity is the vector sum of the movement of the earth and the velocity of the particle as observed from the earth, or

$$\vec{V_a} = \vec{V} + \vec{V_e} \qquad (10)$$

where

$\vec{V_a}$ = absolute velocity,
$\vec{V}$ = observed velocity, and
$\vec{V_e}$ = velocity of the surface of the earth.

The acceleration of the particle in vector notation is given by:

$$\frac{d\vec{V_a}}{dt}\text{ (fixed system)} = \frac{d\vec{V_a}}{dt}\text{ (rotating system)} + \vec{\Omega} \times \vec{V_a} \qquad (11)$$

Substituting equation (10) into equation (11) reduces to:

$$\frac{d\vec{V}_a}{dt} = \frac{d\vec{V}}{dt} + 2\vec{\Omega} X \vec{V} - \vec{\Omega}^2 R \qquad (12)$$

where

$\vec{\Omega}$ = angular velocity of the earth,
R = distance of particle from earth's axis, and
X = signifies a cross vector product.

From Newton's second law, the sum of the forces is equal to the mass times the acceleration. In terms of force per unit mass, this is expressed as

$$\vec{b} + \vec{g} + \vec{F} = \frac{d\vec{V}_a}{dt} \qquad (13a)$$

where

$\vec{b}$ = pressure force,
$\vec{g}$ = gravitational force, and
$\vec{F}$ = frictional forces.

With respect to the observed velocities, the equation becomes

$$\frac{d\vec{V}}{dt} + 2\vec{\Omega} X \vec{V} - \vec{\Omega}^2 R = \vec{b} + \vec{g} + \vec{F} \qquad (13b)$$

Equation (13b) is the expanded form of equation (1) for the horizontal component of flow.

This development has not yet considered the coordinate system in which the observations are made. Normally, the choice of a coordinate system is made to coincide with the spherical coordinate system of the earth. However, some advantages can be derived by using another coordinate system to describe the atmospheric motion. For instance, the coordinates can be fixed relative to the point of observation on the surface of the earth. It is possible to describe the atmospheric motion relative to this point by using a natural coordinate system. A natural coordinate system is defined in terms of the trajectory of a particle. At the coordinate origin, the velocity vector lies tangent to the trajectory. The tangent is called the s axis. This axis forms one of three mutually perpendicular axes. The other two are the n and m axes where n is in the plane of the motion and m is directed perpendicular to the plane. This coordinate system was used in the model. The coordinate origin was taken to be a point near the center of the target area.

The equations of horizontal motion in the natural coordinate system (neglecting friction) are:

$$\frac{dV}{dt} = -\nu \frac{\partial p}{\partial s} \qquad (14a)$$

$$K_H V^2 = -\nu \frac{\partial p}{\partial n} - fV \qquad (14b)$$

and

$$-\frac{V^2}{a} = -\nu \frac{\partial p}{\partial z} - g - 2u\,\Omega \cos \Phi \qquad (14c)$$

where

V = instantaneous velocity vector relative to the observer, m/s
ν = specific volume of air, kg/m^3
p = pressure, Pa (pascals)
$K_H = 1/R_H$ = horizontal curvature of trajectory
R_H = horizontal radius of curvature of trajectory
f = Coriolis parameter = $2\,\Omega \sin \Phi$
Ω = angular velocity of Earth = $2\,\pi$ radians per 86 400 seconds
Φ = latitude of coordinate center
a = radius of Earth = 6370 km
u = component of velocity vector V in the easterly direction

The term "horizontal" in the above definitions refers to surfaces that are parallel to mean sea level.

Realizing that the terms V^2/a and $2u\Omega \cos \Phi$ are small, gives the following equations for steady flow:

$$0 = \nu \frac{\partial p}{\partial s} \qquad (15a)$$

$$K_H V^2 = -\nu \frac{\partial p}{\partial n} - fV \qquad (15b)$$

and

$$0 = -\nu \frac{\partial p}{\partial z} - g \qquad (15c)$$

For the most general case, the tangent to the particle trajectory does not coincide with the tangent to the isobars on weather maps. The system of equations can be transformed for use with isobaric maps by defining N as the coordinate direction of the horizontal pressure gradient. The angle that the wind makes with the isobars is defined as θ. If the wind is deflected toward lower pressures, θ is positive. For deflections toward higher pressures, θ is negative. Using this new notation:

$$-\nu \frac{\partial p}{\partial s} = -\nu \frac{\partial p}{\partial N} \sin \theta$$

and

$$-\nu \frac{\partial p}{\partial n} = -\nu \frac{\partial p}{\partial N} \cos \theta$$

Substituting these equations into equation (15) gives

$$\frac{dV}{dt} = -\nu \frac{\partial p}{\partial N} \sin \theta \qquad (16a)$$

$$K_H V^2 = -\nu \frac{\partial p}{\partial N} \cos \theta - fV \qquad (16b)$$

and

$$0 = -\nu \frac{\partial p}{\partial z} - g \qquad (16c)$$

Equation (16) can be normalized in such a fashion that all of the variables, both independent and dependent, are approximately unity over the domain of concern. This is accomplished by defining the following dimensionless variables:

$$\begin{array}{llll} \overline{z} = z/H & & \overline{g} = g/g_o \\ \overline{V} = V/U & & \overline{t} = t\Omega_o \\ \overline{K} = LK_H & & \overline{p} = p/p_o \\ \overline{N} = N/L & & \overline{\Omega} = \Omega/\Omega_o \\ & & \overline{\nu} = \nu/\nu_o \end{array}$$

where

g_o = gravitational constant = 9.8 m/s^2
U = maximum wind velocity
L = maximum horizontal length in domain of interest
p_o = standard atmospheric pressure at sea level
Ω_o = angular velocity of the Earth = 7.272×10^{-5} rad/s
ν_o = specific volume of air at sea level pressure and temperature = 0.773 m^3/kg at 0 $^{\circ}$C
H = height of atmosphere from sea level = 11 km
z = vertical coordinate

Substitution of these variables into equation (16) gives:

$$\Omega_o U \frac{d\overline{V}}{dt} = -\frac{\nu_o p_o}{L} \frac{\partial \overline{p}}{\partial \overline{N}} \sin \theta \qquad (17a)$$

$$\frac{U^2}{L} \overline{K} \overline{V}^2 = -\frac{\nu_o p_o}{L} \frac{\partial \overline{p}}{\partial \overline{N}} \cos \theta - 2 \sin \Phi \, \Omega_o U \overline{V} \overline{\Omega} \qquad (17b)$$

and

$$0 = \frac{\nu_o p_o}{H} \frac{\partial \overline{p}}{\partial \overline{z}} - g_o \overline{g} \qquad (17c)$$

Equation (17) can in turn be made dimensionless term-wise by dividing each term by the coefficient of one term. This process results in the following:

$$\frac{d\overline{V}}{dt} = -\left(\frac{\nu_o p_o}{U^2}\right) \cdot \left(\frac{U}{\Omega_o L}\right) \frac{\partial \overline{p}}{\partial \overline{N}} \sin \theta \qquad (18a)$$

$$\overline{K} \overline{V}^2 = -\left(\frac{\nu_o p_o}{U^2}\right) \frac{\partial \overline{p}}{\partial \overline{N}} - 2 \sin \theta \left(\frac{\Omega_o L}{U}\right) \overline{\Omega} \, \overline{V} \qquad (18b)$$

and

$$0 = -\left(\frac{\nu_o p_o}{U^2}\right) \cdot \left(\frac{U^2}{g_o H}\right) \frac{\partial \overline{p}}{\partial \overline{z}} - \overline{g} \qquad (18c)$$

The dimensionless parameters are generally defined as follows:

$$\frac{\nu_o p_o}{U^2} = \text{pressure parameter}$$

$$\frac{\Omega_o L}{U} = \text{Rossby parameter}$$

$$\frac{U^2}{g_o H} = \text{Froude parameter}$$

The group of flow conditions which is described by equation (18) is called a "class" of flow conditions. This particular class describes the frictionless flow of horizontal particle motion in a rotating coordinate system acted upon by pressure gradients. A single flow condition of this class is determined by the specific set of values taken by the pressure, Rossby, and Froude parameters. Thus, when these parameters are specified, a specific flow condition is specified. It should be noted that the value of each dimensionless variable (V, for instance) is unique for each specified flow condition.

In the conventional method of designing a model, careful attention is paid to properly reproducing the magnitudes of the dimensionless parameters. If this is done reasonably well, the model represents a solution of the normalized differential equation. That is, dimensionless velocities, flow directions, etc., in the model are identical with the corresponding dimensionless quantities in the atmosphere. Arx [2] demonstrates, for instance, how rapidly a model must be rotated about its axis to properly simulate tidal and Coriolis effects in marginal and small mediterranean seas of the Earth. This rotation is necessary to maintain equality of the Rossby number in the model and in nature.

The liquid simulation model was designed from a slightly different concept. Instead of reproducing the magnitudes of the dimensionless parameters, their resultant effect at a given elevation is reproduced. This is achieved by duplicating, in the model, the horizontal curvature and velocities observed in the field. This procedure is based upon the assumption that if the flow condition in the model (in dimensionless terms) reproduces a specified flow condition measured in the field at a given elevation, then the flow conditions at all elevations are properly simulated. Therefore, the liquid simulation model essentially duplicates the Coriolis and pressure fields implicitly. This technique can be viewed as one in which known flow conditions at one elevation (the upper atmosphere) are extrapolated into an area where the flow conditions are unknown (near the ground).

Summary

The boundary conditions which must be met in the model simulation are:

(1) correct variation of entropy with elevation,

(2) correct free stream velocity, and

(3) correct horizontal curvature of the free stream trajectory.

The simulation of the correct variation of entropy requires that the density at any elevation in the liquid relative to the ground level reference density vary as

$$(\rho/\rho_o)_{liquid} = \left(\frac{T_o}{T} \cdot \frac{p_o}{p}\right)_{air}^{\frac{k-n}{n}}$$

The correct free stream velocity is determined from the Froude parameter. The model velocity V_m is given by:

$$V_m = V_p\,(H_m/H_{atm})^{1/2}$$

For a vertical scale of 1:125 000, the model velocity is given by:

$$V_m = \frac{V_{atm}}{353.6}$$

For example, with a field velocity of 25 m/s the model velocity is 71 mm/s.

The establishment of the correct horizontal free stream trajectory is limited in the model. The horizontal radius of curvature R_m in the model varies between 0 and 2 metres. The correlation between the model and the field values is based upon a simple geometric ratio:

$$R_m = R_p \frac{L_m}{L_{atm}}$$

The ratio L_m/L_{atm} represents the relationship between horizontal lengths in the model and in the atmosphere. With a horizontal scale of 1:250 000, the model radius of curvature is

$$R_m = \frac{R_{atm}}{250\,000}$$

For example, with a free stream trajectory radius of curvature of 355 km in the atmosphere, the model value is 1.42 m (fig. 1).

LABORATORY APPARATUS AND TECHNIQUES

Laboratory Facility

The model (fig. 2) includes a tank 150 mm deep having a diameter of 4000 mm. The liquid used to simulate the atmosphere enters the tank through four inlet ports in the floor. The depth of the liquid above sea level is about 88 mm, which roughly corresponds to the boundary between the atmosphere and the troposphere when a vertical scale of 1:125 000 is used. Motion in the model is generated by a rotating disk floating on the liquid. The clearance between the disk and the tank wall is about 3 mm. Originally, three d-c electric motors mounted on the disk provided the required driving torque and kept the disk centered in the tank. For the Sierra studies, the disk was driven by a variable speed motor through a vertical spindle located at the center of the disk. This arrangement greatly improved the smoothness of rotation and control of the rotational velocity.

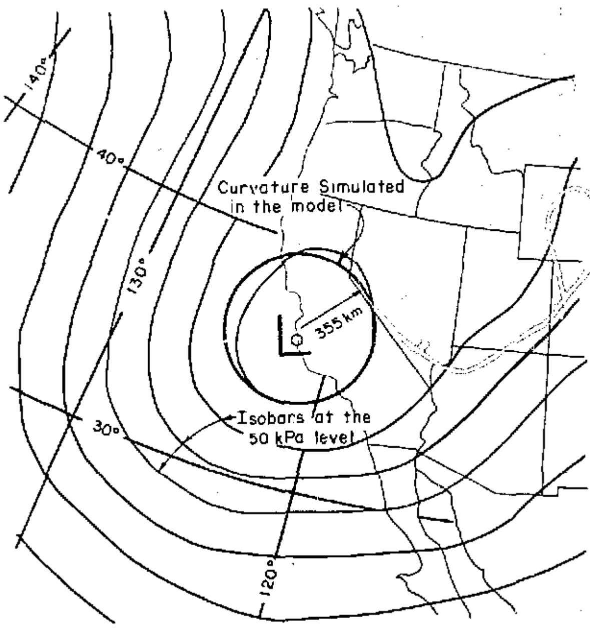

Figure 1.—Comparison of free stream curvature in model with typical atmospheric conditions.

Producing Potential Flow

Rouse [9] shows that a velocity potential, that is potential flow, exists if the flow is laminar and if there is no appreciable acceleration in the direction of motion. Schlichting [10], who studied the flow induced by a rotating disk, found that the flow remained laminar up to a rotational Reynolds number R_r of 100 000 with homogeneous fluids.

The rotational Reynolds number is defined as

$$R_r = \frac{r^2 \omega}{\nu}$$

where

r = radius of disk, m
ω = angular velocity, rad/s
ν = kinematic viscosity, m^2/s

The shear induced rotational flow can be divided into three distinct zones: (1) a boundary layer about 20 mm thick at the upper plate, (2) an intermediate core, and (3) a boundary layer at the floor about 20 mm thick.

The velocity in the intermediate core region is about one-half the disk velocity.

Thus, the model must be designed to provide a disk speed of twice the speed of the desired free stream wind velocity as scaled by equation (9) and/or the Richardson number. In addition, to avoid boundary layer effects the model must be elevated sufficiently to place it in the intermediate core zone.

If the disk is rotated at too large a rotational speed, turbulence develops just below the disk. This tends to destratify the gradient and destroys the potential flow field. Experimentally, the upper limit for the rotational Reynolds number of the disk with stratified fluids was determined to be 200 000. The maximum rotational speed of the disk is thus 90 seconds per revolution using the kinematic viscosity for freshwater. This condition puts an upper limit on the maximum upper air velocities in the atmosphere which can be simulated.

Producing Density Gradients

Various methods have been used by experimenters to achieve density variations in liquid models. For instance, a mixture of stanisol and carbon tetrachloride (with a specific gravity of 1.59) has been used with water in two density studies. Clay slurries have also been used with water. These methods produce distinct density discontinuities. However, density gradients are more commonly produced with saline solutions or by temperature gradients within the fluid. Density gradients produced by temperature can be easier to measure, and a noncorrosive liquid such as water can be used in the model. The maximum attainable density difference through the use of temperature, however, is about 3 percent. With the height of the troposphere at 11 000 metres and no temperature inversions, the change in relative density which must be attained in a model simulation is about 8 percent. Therefore, highly concentrated saline solutions must be used to produce the required density gradients for proper atmospheric simulation.

The original method of producing a density gradient consisted of floating a freshwater layer on top of a 150 000 mg/ℓ saline solution. Molecular diffusion was then utilized in producing the desired density gradient. A computer program based on Fickian diffusion was written to predict the density gradient as a function of time. The computer program PRO 1532-HATM, documented in appendix C, performs these computations. Figure C-1 in appendix C shows the change of relative concentration with time as computed using the program. Although the density

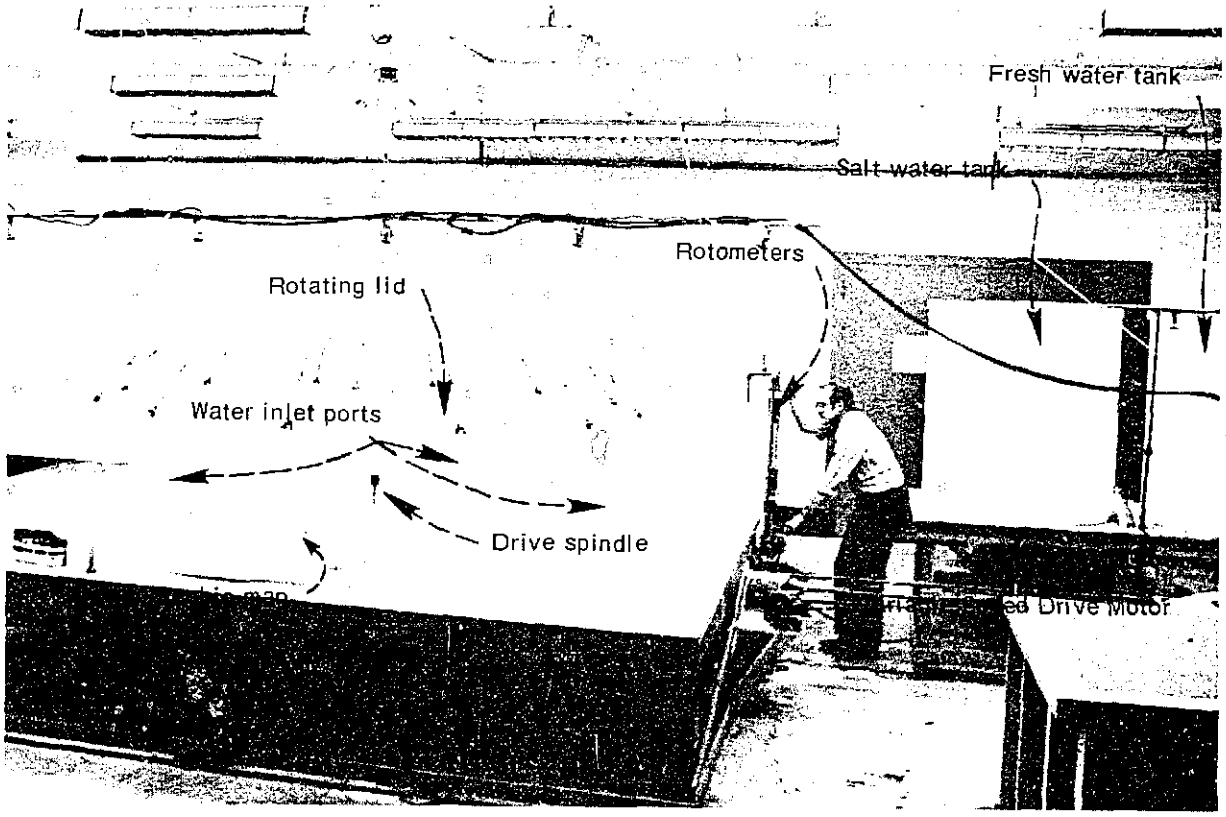

Figure 2.—Laboratory test facility. Photo P801-D-71983

gradient produced in this manner does not duplicate exactly the potential density distribution of simple atmospheric profiles, the difference is small enough to be ignored for all practical purposes. The time to establish a desired gradient was about 20 hours.

The more complex distributions required for the Sierra studies resulted in the development of a different laboratory technique to produce the density gradients. For this technique, the flow from two tanks was mixed and their resultant product introduced into the model. One tank held freshwater at room temperature, and the other contained a saline solution at the maximum required density. The flow from each tank was controlled with a valve. The individual flow rates were metered by two separate rotameters. By properly adjusting the valves, any desired density could be achieved. As with the previous technique, the lighter fluid was introduced before the more dense fluids. The total time from the initiation of filling until the model could be run was about 3 hours.

Velocity Measurements and Seeding Representation

Three methods were tried to trace the plume trajectories. One method was to generate a sheet of hydrogen bubbles of about 0.1-mm diameter. The probe was a fencelike array of platinum wires pulsed with an electric current. The current electrolyzed the saline fluid, generating hydrogen bubbles. The bubbles are soluble in water and disappear after about 3 seconds. The path of the bubbles can be recorded photographically for later analysis and velocity determinations. Observation of the bubbles was difficult because they are white and the quantity produced was not sufficient to produce a dense sheet. Also, the horizontal velocities in the model were small relative to the rise velocity of the bubbles.

The second method involved the use of tellurium probes. When pulsed with a current, the probe produced a single dense, black streak of tellurium ions which have a low settling rate. These probes were fabricated by melting tellurium in glass tubes and drawing them down to capillary size to essentially represent point sources. The glass around the tellurium capillary tips was then etched off using hydrofluoric acid. Difficulty was experienced with these probes from spontaneous fracturing caused by stress relief during and after etching. Control of capillary size was not good and each probe required a different voltage to produce required streaking intensity. They were prone to cannonading or bursting when pulsed, probably because hydrogen formed between the glass and tellurium or within fracture cracks in the tellurium.

Because of the above difficulties, the tellurium probes were replaced with small dye injection tubes. Small bottles were coated on the inside with a mixture of alcohol and dye and allowed to dry. Fluid was slowly siphoned from the seeding stations on the map, mixed with the dye in the bottles, and then reinjected into the model. Thus, the dye plumes had very nearly the same density that existed at the seeding stations. Using three types of dyes helped to distinguish between seeding station dye tracks. The three dyes used were Alphazurine A, Pontycil Pink B, and Fluorescein. Only the Fluorescein required extra care to prevent significant density change due to the weight of dye.

Dye injection tubes placed flush with the map surface simulated ground seeders. Aerial seeding was simulated by injection tubes which projected variable distances above the map surface, figure 3. Since the dye cloud follows the plume trajectory, the cloud indicates what would have occurred downwind if aerial seeding had been performed anywhere along the path of the cloud. The height of the aerial seeders could be changed during a run by adjusting the height of the injection tube which passed through suitable seals in the tank floor.

Measuring Density Gradients

Three ways of determining density gradients were considered. One method uses spheres having various densities. The spheres float at a depth corresponding to their respective density. Two suppliers of plastic products were contacted; however, no source of color-coded spheres with the required densities was found.

Conductivity probes were considered. These probes were difficult to platinize, they polarized and were difficult to calibrate. These probes were invasive and disturbed the flow.

Because of the above difficulties, an optical method was developed to measure the density gradients. The method is based on the diffraction of light when it passes through a density gradient. By measuring the amount a light beam is diffracted from a known location, the gradient can be determined through a trial and error process involving a numerical integration. This method is described in appendix A and a computer program for performing the numerical integration is also included. This method is practically noninvasive and provides a continuous record with respect to elevation rather than discrete sample points. Figure 4 shows how sloping straight rods appear to the viewer looking through the side of the tank. The greater the stratification gradient, the greater the distortion.

Measuring Elevation

Determining the elevation of dye tracks or plumes in a density stratified liquid is difficult because of diffraction distortion when viewing the plumes from the side of the tank. However, by placing graduated rods near the dye paths, elevations could be determined by sighting the path against the rods, figure 5.

Preparing Maps

The three-dimensional plastic relief maps used in the studies needed reinforcing before being placed in the atmospheric model. To reinforce the maps it was necessary to provide them with a backing material while simultaneously maintaining good control on the elevation of the topography. Elevation control was obtained by selecting 20 to 30 critical topographic features on each map. Nails were hammered into plywood sheets at locations which were the mirror image of the selected critical points. The heads of the nails protruded a distance which corresponded to the difference between a control elevation and the elevation of the selected point. The control elevation was chosen somewhat higher than the highest topographic feature on the map. The maps were then turned upside down, supported on the nails, and filled with lightweight concrete prepared by mixing vermiculite with portland cement.

The lightweight concrete was easily drilled and grooved to accept the metal seeder tubing and its associated plastic connecting tubing.

Difficulties were encountered because of lack of bond between the concrete and the plastic map. Originally, clear plastic cement was injected through the map to

Photo P801-D-77862

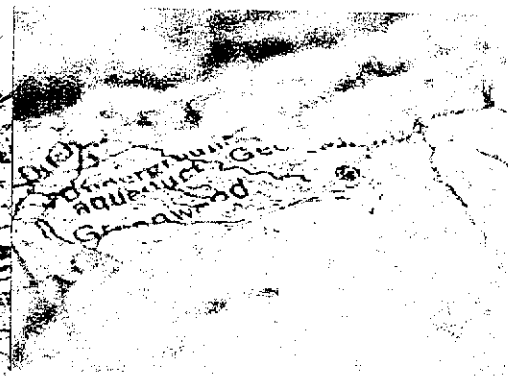

Photo P801-D-77860

a.—Ground seeder simulation.

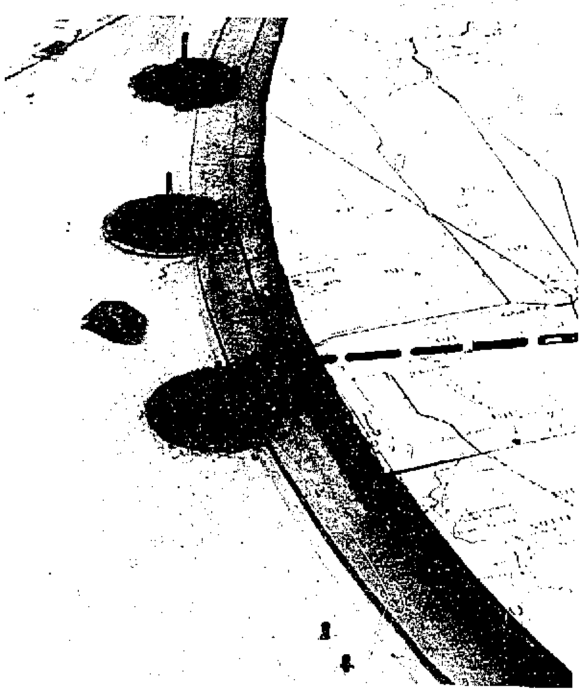

Photo P801-D-77859

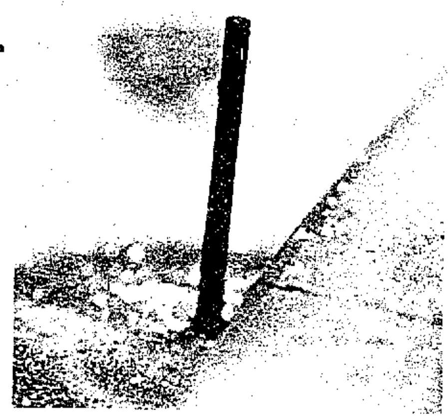

Photo P801-D-77861

b.—Airborne seeder simulation.

Figure 3.—Simulation of seeders.

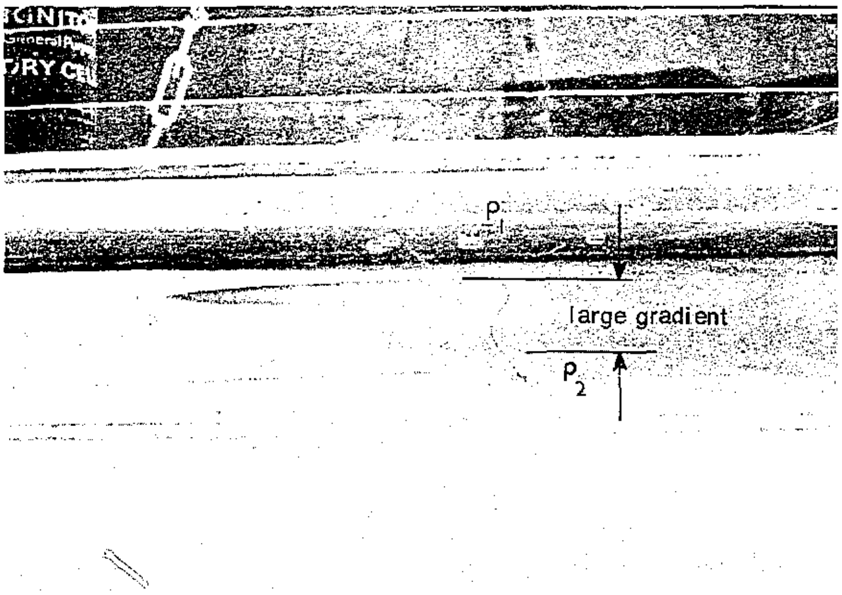

a.—Narrow density gradient. Photo P801-D-77864

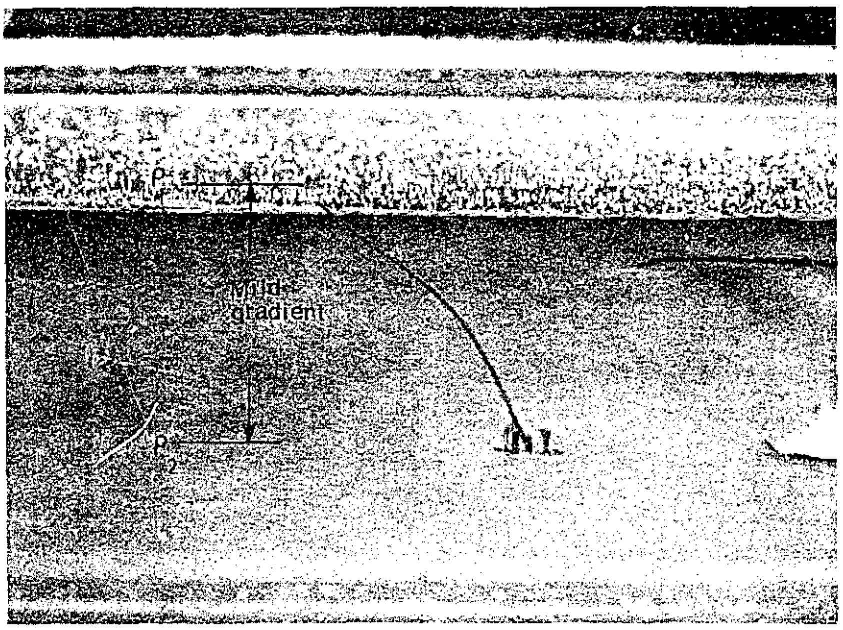

b.—Thick density gradient. Photo I 801-D-77865

Figure 4.—Visual distortion in stratified fluids.

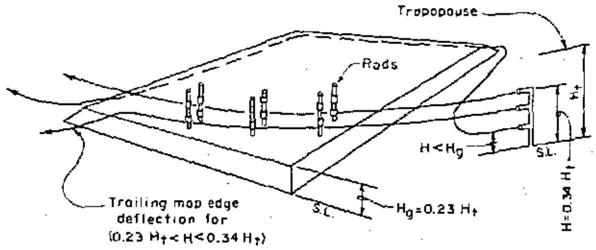

Figure 5.—Elevation rods used to investigate map.

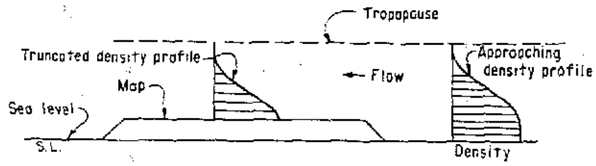

Figure 6.—Truncation of density profiles.

provide bonding to the concrete. Subsequent maps were coated on the inside with epoxy resin to provide bond. This procedure was much better but eventually the plastic separated from the concrete. The best results were obtained by mixing some concrete repair epoxy into the lightweight concrete. The inside of the plastic map was coated with the same epoxy before placing the concrete. Maps prepared in this manner maintained their bond after more than 12 months of continuous immersion. The continuous immersion of the maps in freshwater is recommended. This prevents the formation of salt crystals which distort and fracture the concrete.

A mixture of plaster of paris, fiberglass, and ceramic tile latex grout was also tried as a backing material. This material gradually dissolved or eroded away under very low water velocities.

STUDIES OF MAP SIZE

Effect of Blockage by the Maps

The physical presence of the plastic relief map in the tank presents the possibility that the fluid might be induced to flow over the map in a peculiar way. It is desired that the trajectories over an actual relief map be influenced by the topography only and not by the placement of the map in the tank. Therefore, studies were made of free stream trajectories over a flat relief map. It was assumed that blockage and tank boundary effects were insignificant if the trajectory was not deflected.

A 500- by 750-mm map was constructed with a plane upper face located 20 mm above the tank floor. The map was oriented with its long dimension rotated 40° from being perpendicular to the free stream direction. Density gradients similar to those shown in figure 6 were established in the tank.

It was found that the map does not affect the free stream trajectory at the leading edge of the map, figure 5. However, at the trailing edge of the map, the trajectory was deflected 50 mm away from the center of rotation for plumes located between elevations H/H_t = 0.23 and H/H_t = 0.34. Here, H_t is the elevation of the troposphere. The lower limit of 0.23 corresponds with the elevation of the top of the blank map.

These tests also showed that flow laminae remain at their density elevations and will flow around obstacles rather than pass over them (see the trace $H<H_g$ fig. 5). This effect is so strong that the map essentially truncates the approaching density profiles, figure 6. The effect is noticed even though the angle between the slope to the top of the map and the tank floor is less than 45°. This effect can be used to eliminate undesirable lower portions of density profiles.

It was concluded from these studies that blockage effects due to placement of maps within the tank are not significant when the longest dimension of the model is less than or equal to 1 m and when the distance from the map to the wall of the tank is greater than 80 mm.

Boundary Limitations

In wind tunnel models, the flow is normally confined between two parallel walls. If a barrier is constructed with its axis perpendicular to a wind tunnel axis, all flow is forced over the barrier. Whereas, in nature, the flow could actually pass around a mountain barrier. This condition illustrates one extreme boundary limitation that the test facility can exert on the simulation.

The liquid simulation model discussed in this report represents the opposite extreme with respect to boundary limitations imposed by the test facility. In this case, flow can pass around barriers even though they would actually stagnate behind them in nature. For an extreme example, consider atmospheric flow into a box canyon. In this case, the flow will stagnate at the head of the canyon. If only a portion of the canyon were simulated, then the model could indicate a flow through the canyon when actually none existed. For this reason, care must be taken in interpreting flow conditions that are observed near the edges of the maps.

LEADVILLE-CLIMAX MODEL VERIFICATION STUDY

Purpose

The purpose of these studies was to verify that accurate simulations of plume trajectories can be performed using stratified liquids. Since field studies had already been performed in the Leadville-Climax, Colo. area, it was decided to attempt a simulation of the atmospheric conditions which existed during the field studies. The verification consisted of three essential parts. First, it was necessary to establish that a capability existed to simulate the stability conditions which are present in the atmosphere. Secondly, it was necessary to demonstrate that observed model velocities and velocity distributions correlated with atmospheric measurements. Finally, field observations of plume trajectories from seeding stations located at Minturn, Red Cliff, and Camp Hale had to correspond with plume trajectories in the model. Based upon these studies it is possible to draw some basic generalizations concerning the behavior of the plume trajectory for various topographic conditions in the field.

Capability to Simulate Desired Density Distribution

The simulation of the atmosphere depends very strongly on the ability to achieve a distribution of density in the model which is identical to the distribution of potential density in the atmosphere. To study the flexibility of simulating the atmosphere in the model, two approaches were taken. The first was to try to simulate the distribution actually observed in the field. The second was to compare the distributions achieved with several mathematical or conceptual descriptions of the atmosphere.

The first approach included filling the model half full with freshwater and allowing the water to attain room temperature. Then the filling of the model was completed by the addition of the salt solution at room temperature beneath the freshwater layer. Computations, assuming Fickian molecular diffusion, were used to predict a given gradient at a later time. An attempt was made to reproduce Camp Hale radiosonde data for two observed cases. These cases were: (1) storms with temperature inversions, and (2) storms without temperature inversions. For case (1), the distribution in the model was close to, but not identical to, the atmospheric distribution above the 4500-metre level. This distribution corresponded with a model diffusion time of approximately 5 hours. The distribution simulating case (2) was also close below 4500 metres, but deviated above that elevation, figure 7a. This distribution corresponded with a total diffusion time of 25 hours.

The results indicate that better simulations could have been achieved after total diffusion times of approximately 8 and 30 hours for cases (1) and (2), respectively. Two probable reasons for the discrepancy between the computer prediction and the observations in the physical model are: (1) the mathematical model does not account for mixing which occurs during filling, and (2) the mathematical model assumes that the density gradient upstream from the physical model is truncated at the elevation of the top of the physical model. Actually, some of the denser fluid from below the map surface flows up onto the map. In addition, the actual diffusion coefficient may not have been equal to the assumed value of 0.00109 mm^2/s.

Conceptual mathematical models of the atmosphere compare poorly with distributions obtained in the model, figure 7b. The slope of the distribution in the model for the case without inversions was approximately parallel with that of the mathematical models. However, below 4500 metres the comparison was very poor. The difference can probably be explained by the fact that the conceptual models do not properly account for mixing in the lower layers.

From these studies, it has been concluded that realistic atmospheric density distributions can be simulated in the model. Furthermore, sufficient additional knowledge has been gained to facilitate the simulation of a given atmospheric distribution.

Velocity and Plume Movement Simulation

The rotating disk which induces the free stream velocities was adjusted to turn at a rate which simulated a 15-m/s wind velocity at an elevation of 5000 metres over the center of the map. The scale of the circular motion corresponded with a 425-km radius of curvature of the free stream wind trajectories. The map was oriented so that the free stream flow came from an azimuth of 320° and the center of curvature was to the west. Thus, the model simulated the anticyclonic motion with a low-pressure area being centered around Page, Ariz.

The comparison of the model with the field measurements resulted in the following observations:

1. The mean motion of the dye axis in the model and the silver iodide plume in the atmosphere was similar, figure 8.

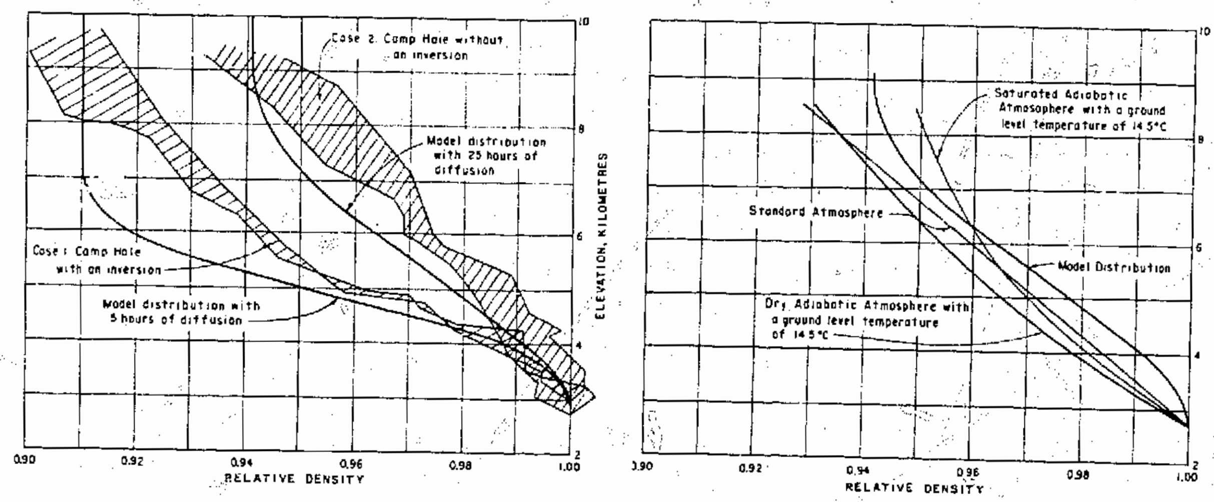

a.—Comparison with radiosonde data

b.—Comparison with conceptual models of the atmosphere

Figure 7.—Density gradients, Leadville-Climax.

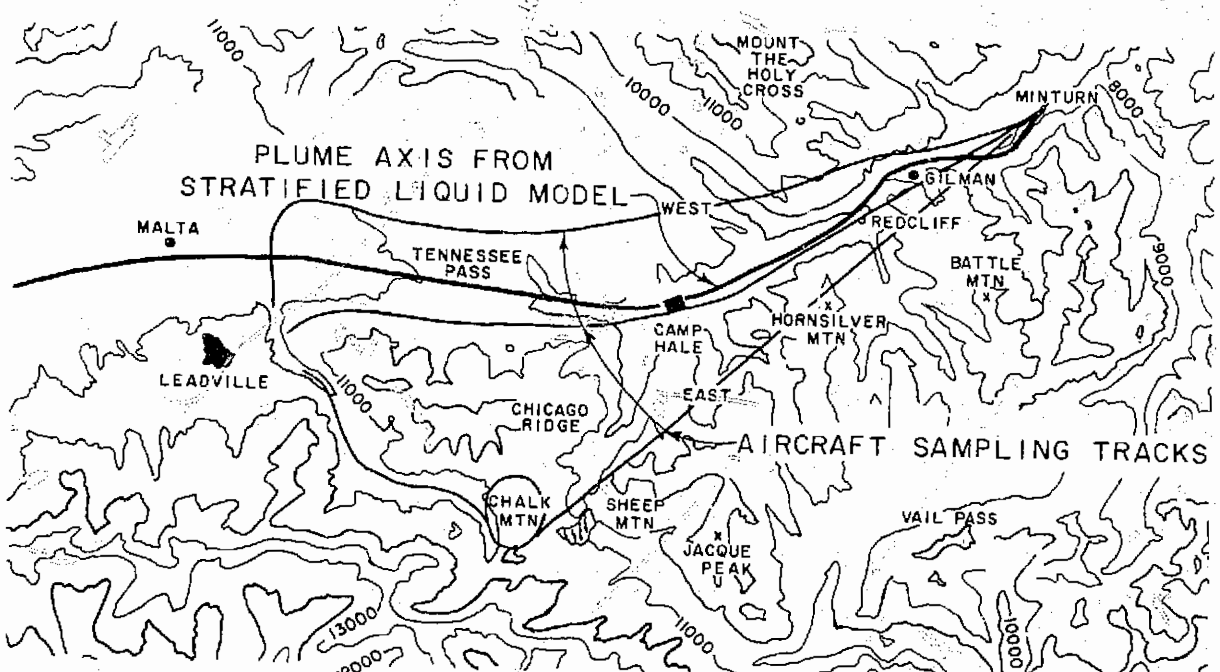

Figure 8.—Plume trajectory, Leadville-Climax.

Orgill, Cermak, and Grant [7] described the field observations as follows: "The flights on March 16 as well as the other two sampling days indicated that the seeding material filled the main valley downstream from Minturn. The main axis of the plume was located between Chicago Ridge and Tennessee Pass region. The material was transported some 40 km downwind toward Malta, but for some unknown reason quickly dissipated or was lost in the Arkansas River Valley. However, it is very probable that the material was transported upward and horizontally toward the Chicago Ridge region."

2. After a model time corresponding to approximately 9 months' real time, dye still lingered in the valleys. Field studies indicated a high background count of silver iodide after 1 year.

3. Valley velocities measured in the model ranged between 2.0 and 5.0 m/s. Equivalent field measurements ranged between 2.0 and 6.0 m/s, figure 9.

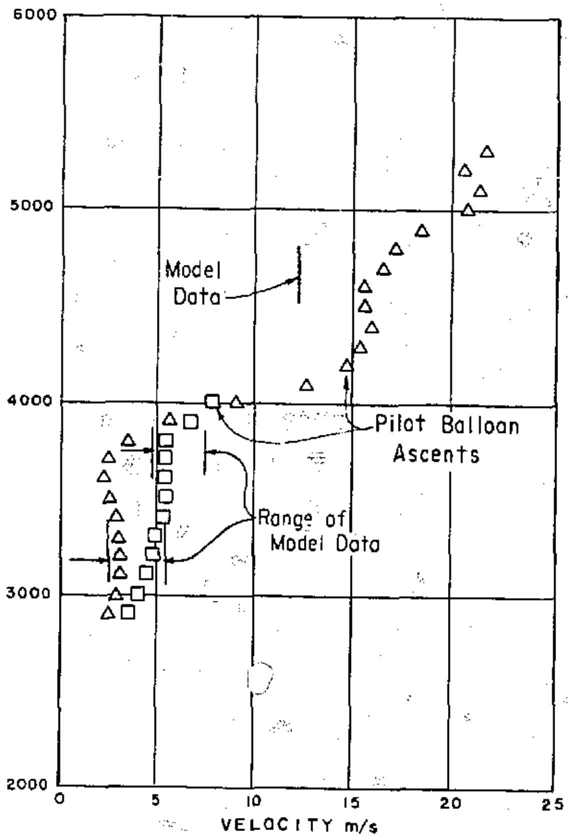

Figure 9.—Model velocities, Leadville-Climax.

4. Movement of dye into transverse valleys was noted in the model. Evidence of similar movement was noted in the field.

Based on these observations, the liquid model satisfactorily simulated conditions observed in the field and the 2:1 vertical scale exaggeration of the topographic maps apparently did not invalidate the model results.

Influence of Topography on Plume Trajectory

Observations of the model indicated that flow layers in stratified flow tend to remain at the potential density level in which they were generated. Thus, material released in or near valleys alined in the same direction as the flow tended to be channelized. Since the model did not indicate any material reached the high elevation targets located above the valleys, transport into these areas would be dependent on turbulent dispersion not simulated by the model. In addition, material released into valleys normal to free stream flows tended to stagnate. Here again, the transport of material to higher elevations would be dependent on turbulent dispersion.

In addition to showing mainstream flow, the model clearly shows disturbances including initial lee wave action. However, the amplification of the lee waves, shown in figure 10, into turbulence was precluded by the model design. To take advantage of the lee wave spreading action, as shown in figure 11, seeding should be performed upstream from and near the elevation of obstructing range crests. Spreading occurs as the plume passes each successive mountain range. This spreading is due to convective transport and not from diffusion processes. In the atmosphere, the spreading would probably be even greater due to the turbulent diffusion which is present in the atmosphere but not in the model.

COLORADO RIVER BASIN PILOT PROJECT

Purpose

The first and largest of the pilot studies under Project Skywater was conducted in the San Juan Mountains of southwestern Colorado. Seeding operations began in the 1970-71 winter season and were terminated in the 1974-75 season. The purpose of the atmospheric simulation studies was to provide qualitative data concerning the mean trajectory paths from selected seeders. These data could then be used later to assist in interpreting the observations made during field operations.

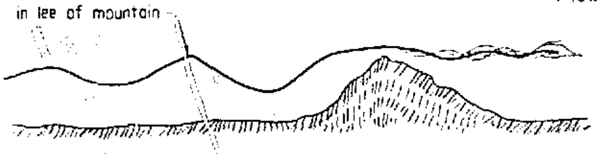

a.—Lee wave disturbance caused by mountain obstruction.

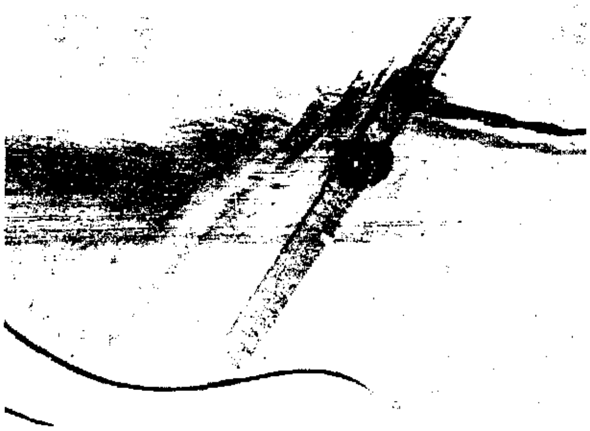

b.—Lee wave over triangular prism. Photo P801-D-77869

Figure 10.—Dispersion with lee waves.

Test Parameters

The San Juan seeding and target area topography map, as shown in figure 12, was put into the test facility. All seeding stations were installed but not all were used.

December 18, 1971 radiosonde storm data for Durango, Colo., was used to determine the required map orientation, lid velocity, and predict molecular diffusion time, figure 13. These radiosonde data indicated that a wind direction from 215° and a free stream velocity of 20 m/s were desirable. However, due to the critical Reynolds number limitation, the maximum attainable free stream velocity was 15 m/s. This velocity and 215° wind direction were used for three tests at different diffusion times. Twenty hours of diffusion were used to simulate the December radiosonde data.

Two additional tests were performed which indicate the sensitivity of the results to the simulation of the atmospheric conditions. For one series, the model atmosphere was thoroughly mixed to simulate a very deep, neutrally stable atmosphere. In another set of tests, 64 hours of diffusion were used to represent a density profile intermediate between the storm profile data and the deep, neutrally stable atmosphere.

These three relative density profiles are shown in figure 14. The map was oriented to simulate a low-pressure area to the northwest of the target area.

Storm Profile Test

The plume trajectory from station 21, as shown in figure 15, traveled over the Continental Divide from Wolf Creek Pass toward Del Norte. The plume from seeding station 33 traveled south along U.S. Highway No. 84 to the junction with State Highway No. 17 over Cumbres Pass to Antonito in the San Luis Valley. The plumes from stations 25, 12, and 4 went over Durango along U.S. Highway No. 160 to Hesperus and then north. The plume from station 16 more or less stagnated, with some drift into the Durango plume.

Test with Intermediate Density Gradient

During this test, the plume from station 21, figure 16, went over the high country from Wolf Creek Pass toward Del Norte. The plumes from seeding stations 28 and 33 followed the valley along U.S. Highway No. 84 to the junction of State Highway No. 17, then over Cumbres Pass to Antonito in the San Luis Valley. The plume from station 14 went over the high country near Wiemuchi Pass. The plumes from stations 25, 27, and 4 followed U.S. Highway No. 160 west over Durango towards Cortez, and then at about Hesperus went north. The plume from station 16 more or less stagnated, with some drift into the Durango plume.

Test with Completely Neutral Atmosphere

All the plumes from stations 12, 16, 21, 25, 27, 28, and 33 traveled over the high country and in the general direction of the free stream flow, figure 17. The station 4 plume followed U.S. Highway No. 550 to Ouray.

Field Studies

During the period February-March 1974, Hobbs, et al. [5] made ice nucleus measurements in the San Juans to investigate the dispersal in time and space of the silver iodide from ground generations. These studies showed that the silver iodide did not reach the cloud level under stable conditions. For marginally stable conditions, the silver iodide entered the clouds too close to the target area to be effective. To investigate the reason for the lack of dispersal of the silver iodide, dynamical and microphysical process studies were conducted during the next winter period by Marwitz, et al. [6].

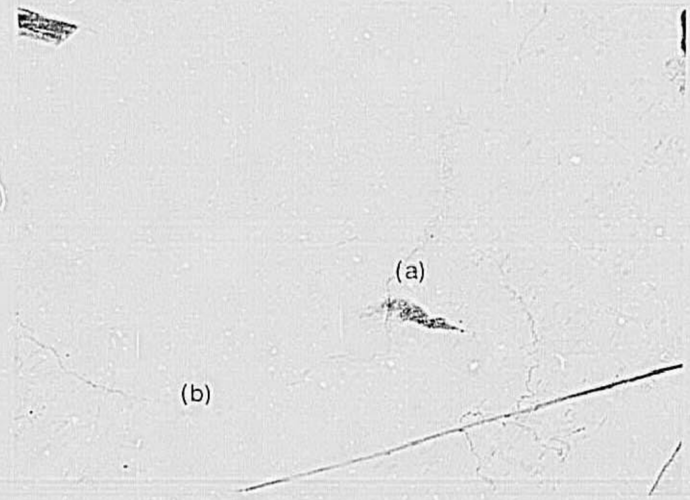

Initially, the plume from Castle Peak spreads just east of Eagle (a). There was also a stream track (not visible) over Camp Hale (b). Photo P801-D-77866

After 15 hours (time in nature), the lee wave action spreads the plume over high country as it crosses successive mountain ranges. Photo P801-D-77867

After 24 hours, the trajectory extends to Aspen (c). Photo P801-D-77868

Figure 11.—Lee wave action over topography map.

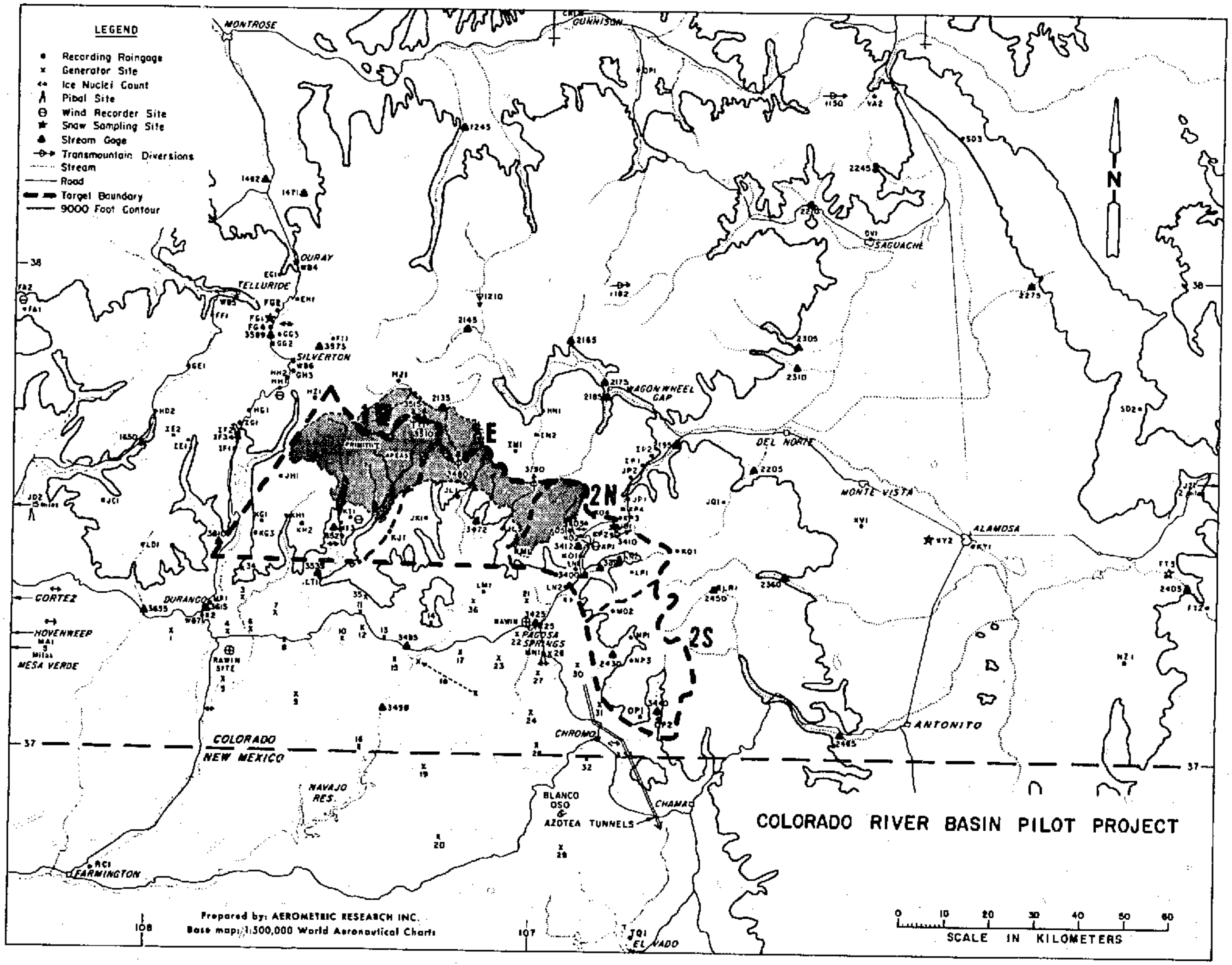

Figure 12.—San Juan seed station and target area location map.

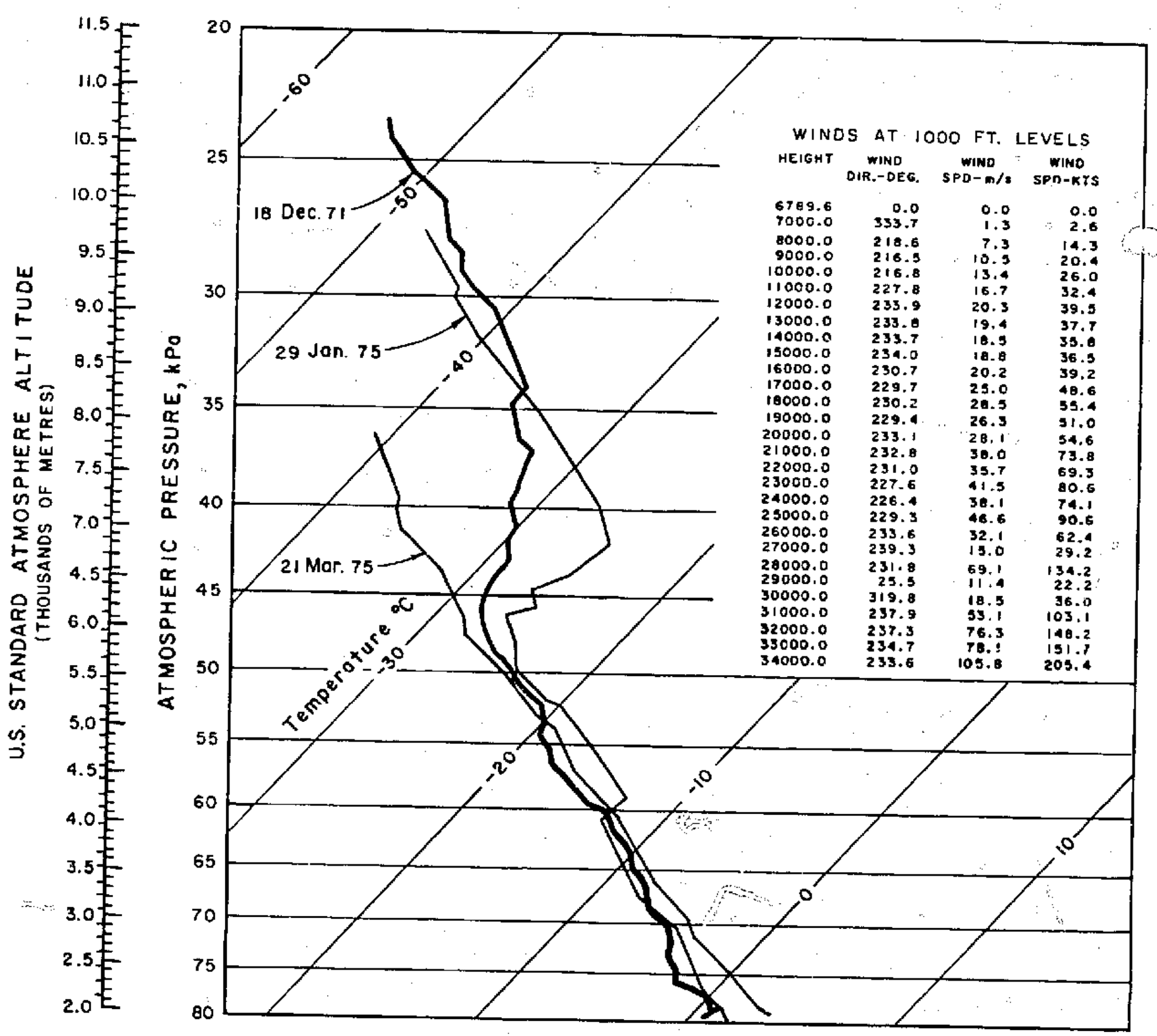

WINDS AT 1000 FT. LEVELS

HEIGHT	WIND DIR.-DEG.	WIND SPD-m/s	WIND SPD-KTS
6789.6	0.0	0.0	0.0
7000.0	333.7	1.3	2.6
8000.0	218.6	7.3	14.3
9000.0	216.5	10.5	20.4
10000.0	216.8	13.4	26.0
11000.0	227.8	16.7	32.4
12000.0	233.9	20.3	39.5
13000.0	233.8	19.4	37.7
14000.0	233.7	18.5	35.8
15000.0	234.0	18.8	36.5
16000.0	230.7	20.2	39.2
17000.0	229.7	25.0	48.6
18000.0	230.2	28.5	55.4
19000.0	229.4	26.3	51.0
20000.0	233.1	28.1	54.6
21000.0	232.8	38.0	73.8
22000.0	231.0	35.7	69.3
23000.0	227.6	41.5	80.6
24000.0	226.4	38.1	74.1
25000.0	229.3	46.6	90.6
26000.0	233.6	32.1	62.4
27000.0	239.3	15.0	29.2
28000.0	231.8	69.1	134.2
29000.0	25.5	11.4	22.2
30000.0	319.8	18.5	36.0
31000.0	237.9	53.1	103.1
32000.0	237.3	76.3	148.2
33000.0	234.7	78.1	151.7
34000.0	233.6	105.8	205.4

Figure 13.—Atmospheric profiles, San Juan studies.

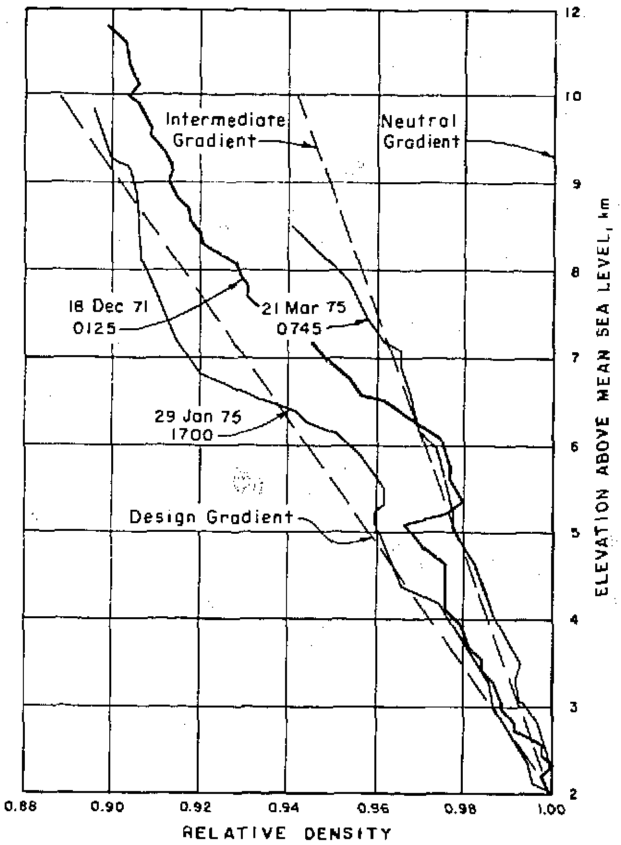

Figure 14.—Relative density profiles, San Juan studies.

Two of the storms observed by Marwitz correspond very well with density profiles established in the model, figure 14. The January 1975 storm was seeded at the time indicated by the profile. The March 1975 storm was seeded about 3 hours after the profile was observed. Therefore, these two conditions represent storms which indicated a good potential for cloud seeding based upon the criteria being used at the time of these field studies.

Based upon the wind vectors measured in the field, Marwitz concluded that a downslope condition existed during the January storm, figure 18. In addition, he postulated that a convergence line formed over Pagosa Springs. The mean trajectories of seeders in this region were around the target area to the northwest. However, there were insufficient dye tracks in the model to make a definite conclusion concerning the presence of a downslope flow, figure 15. It should be noted, nevertheless, that the trajectory from seeder 21 was up and over Wolf Creek Pass. The plume trajectories which tend to flow from Pagosa Springs to Durango could be interpreted as being indicative of the convergence line postulated by Marwitz.

For the March storm, Marwitz concluded that most of the flow passed up and over the Continental Divide, figure 19. The model, on the other hand, indicated a very complex flow field, figure 16. Several areas existed where the flow was practically stagnant. The tendency for flow over the target area was greater than for the January storm. However, flow around the target area to the northwest and into the San Luis Valley was still the predominant characteristic observed in the model.

SIERRA COOPERATIVE PILOT PROJECT

Purpose

The winter weather modification programs have indicated that the proper placement of seeders is extremely important for a successful operation. Therefore, for the Sierra Nevada studies, a detailed investigation of seeder locations is being conducted prior to the seeding operation. The purposes of these investigations are to:

1. Describe the probable distribution of seeding materials within and near the American River Basin released from air and ground seeders,

2. Specify meteorological conditions for which airborne seeding is required, and

3. Determine the optimum ground-based generator locations and airborne seeder tracks.

The initial part of these investigations is the model studies described herein. These model studies will be followed by field studies to determine the trajectory and diffusion characteristics during storm periods and in clear air situations.

Some differences are to be expected between the model and field study results because of the storm characteristics in the Sierra Nevadas. The most important factor which could cause differences are band passages and their embedded convection. It has been observed that precipitation in the Central Valley of California tends to form in bands. These bands cross the valley ahead of the weather fronts. The bands are oriented roughly parallel to the upper slopes of the Sierra Nevada. Embedded within the general surface wind field, predicted by the model, are wind shifts

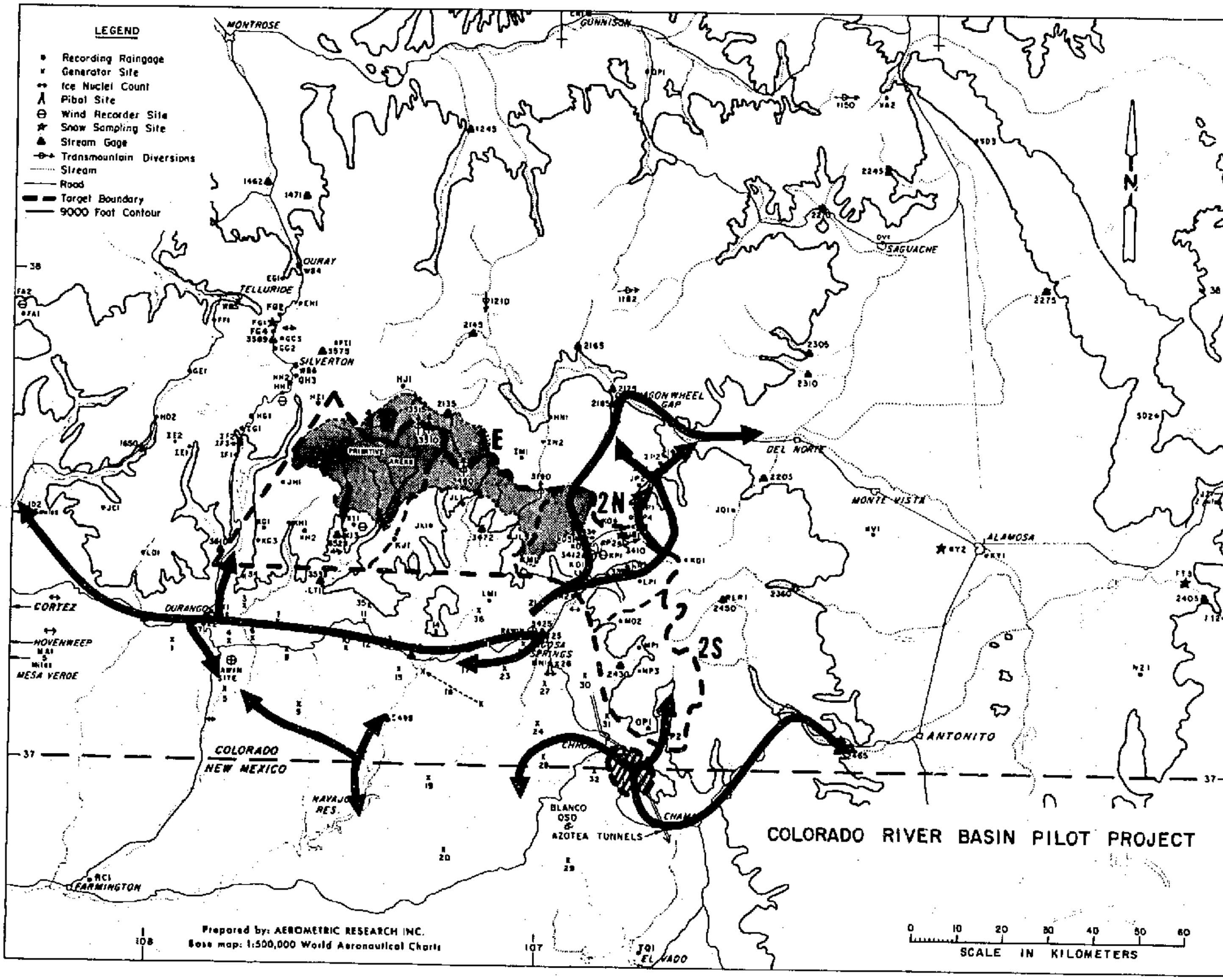

Figure 15.—Ground level trajectories—stable atmosphere.

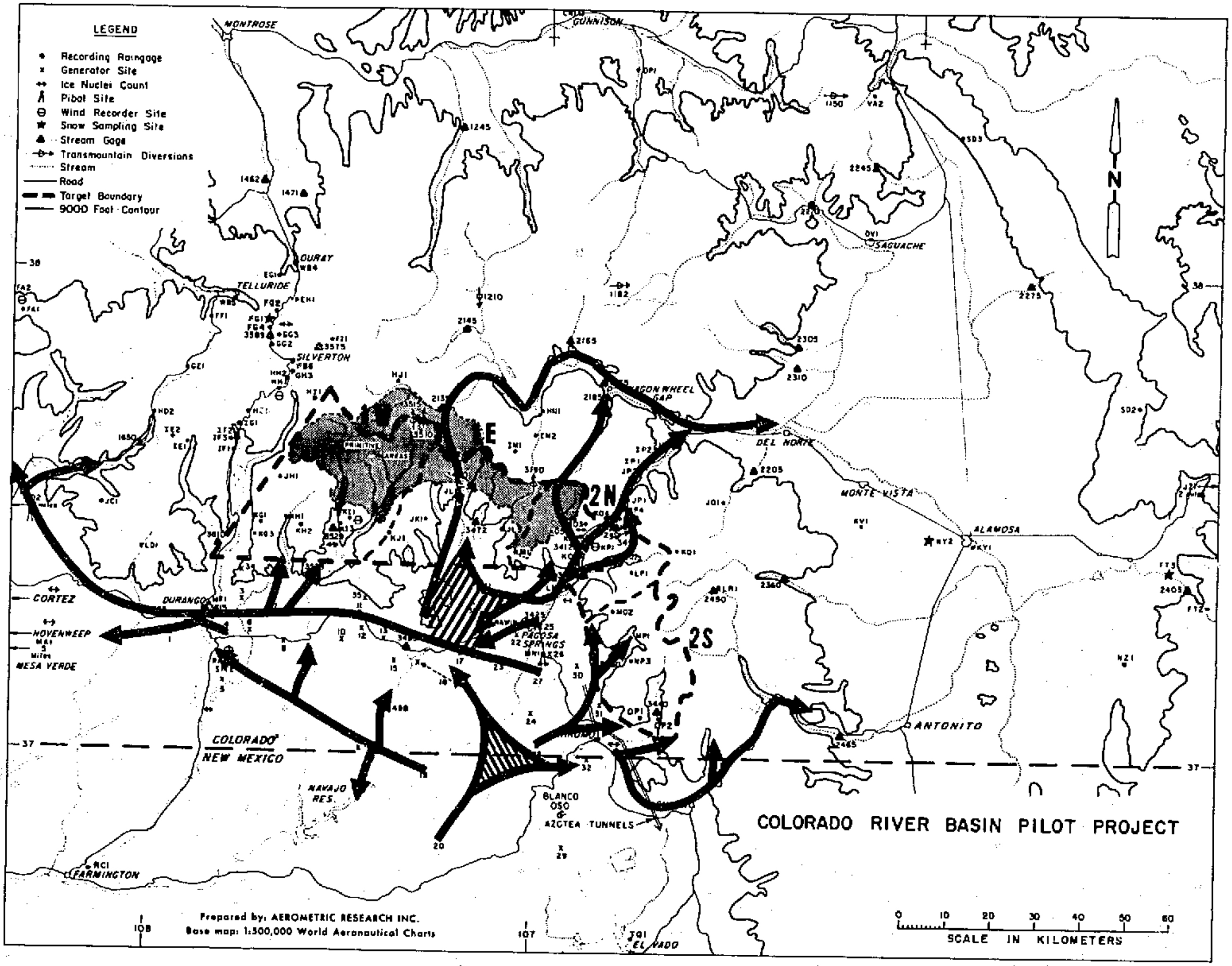

Figure 16.--Ground level trajectories--intermediately stable atmosphere.

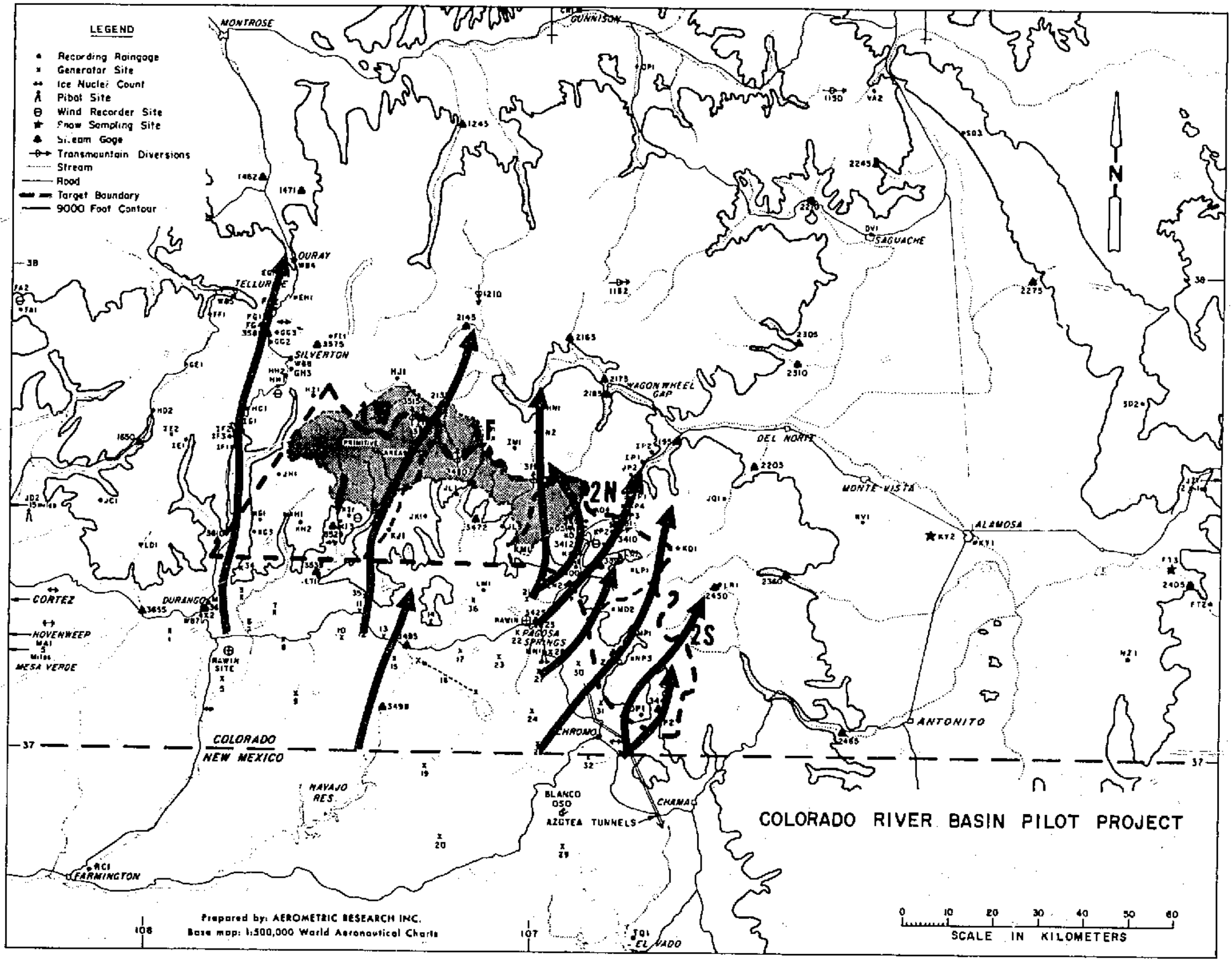

Figure 17.—Ground level trajectories—neutrally stable atmosphere.

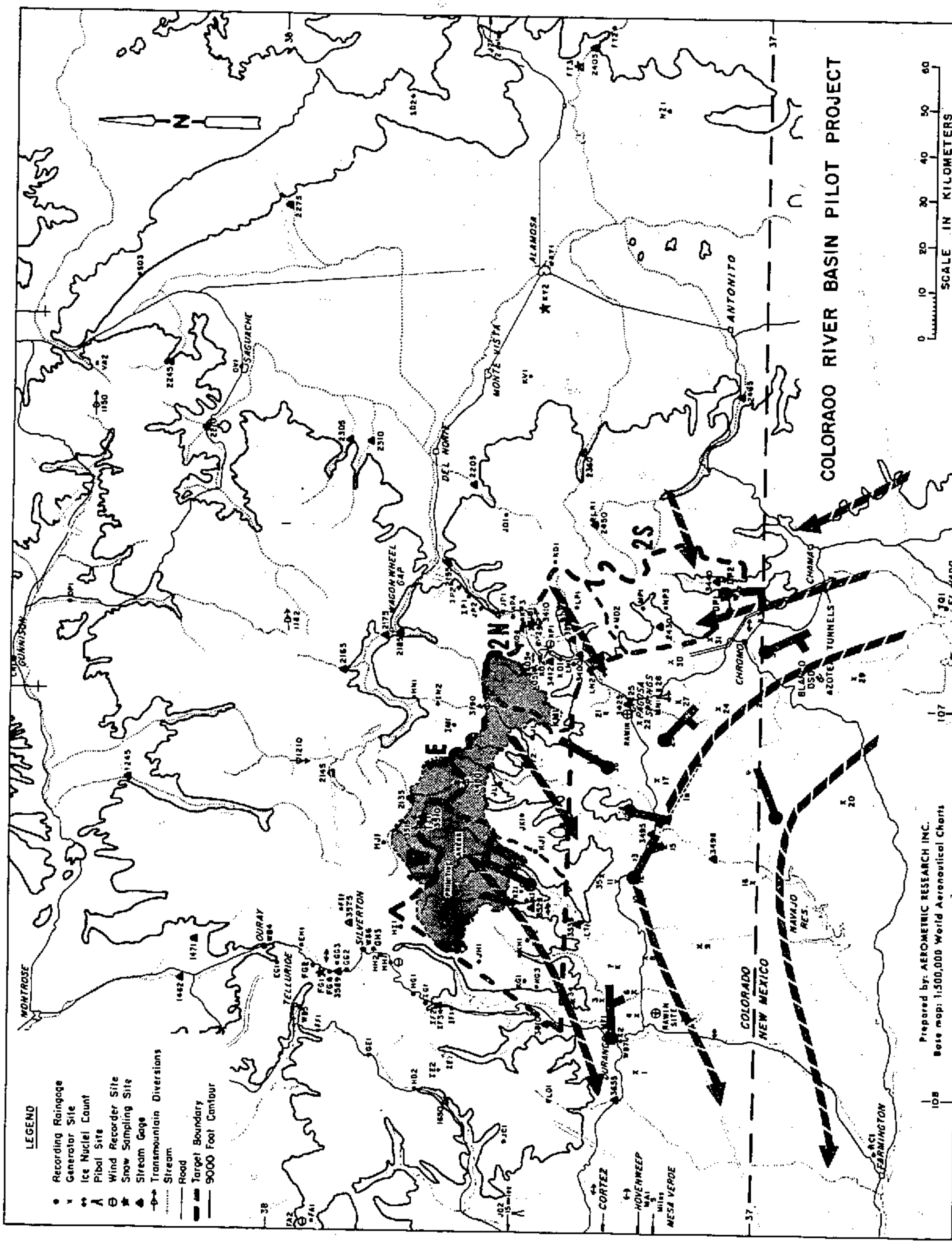

Figure 18.—Field observations, San Juan studies, January 1975 storm.

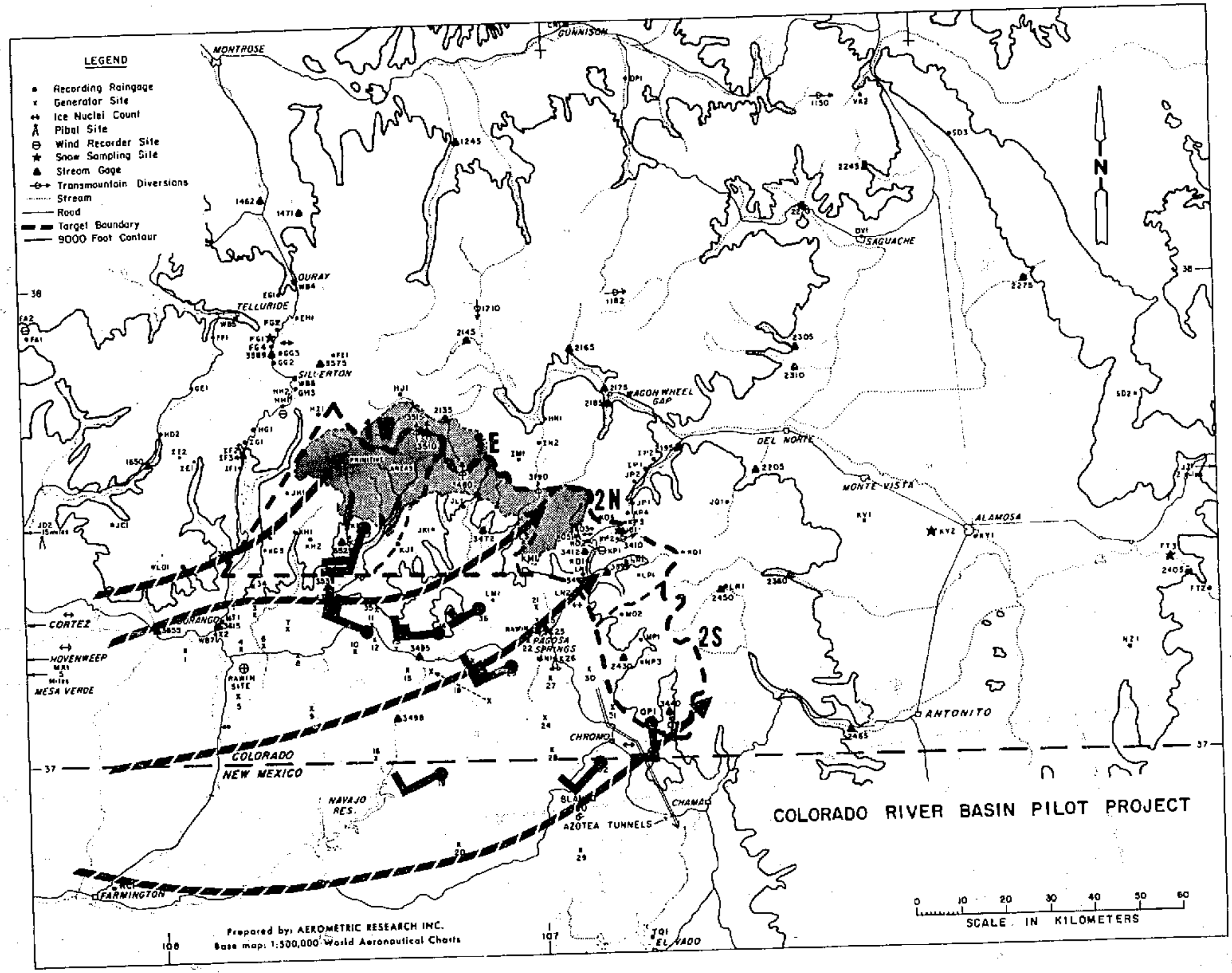

Figure 19.—Field observations, San Juan studies, March 1975 storm.

caused by convergence associated with the prefrontal bands. These localized wind shifts could have a profound effect upon the seeder trajectories as predicted by the model. However, the model studies should prove useful in determining locations to start searching for the plumes during field operations.

Model Parameters

The topography was oriented in the tank to simulate cyclonic curvature of the wind fields as they encounter the Sierra Nevada barrier. A disk-shaped section of the Earth's surface with a diameter of 250 km was used in the simulation. The model was located in the tank to simulate a 350-km radius of curvature of the wind field trajectory over the middle of the American River Basin.

The wind velocity, which had to be simulated, was determined from a statistical sample of storms observed during the CENSARE (Central Sierra Research Experiment) Project. The data were supplied by the Division of Atmospheric Water Resources Management. The median wind velocity was 26 m/s at the 50-kPa (500-mbar) level. The maximum wind velocity that would be achieved in the model over the center of the target area was 15.5 m/s. Thus, the simulations were limited by the maximum velocity limitation of the model. The velocity vectors in the subsequent figures have been normalized with respect to the wind velocity at the 50-kPa level. In this manner, the results can be applied to any specific wind field observed in the field.

An analysis of many atmospheric conditions from the CENSARE Project revealed that a storm history could be simulated with several representative atmospheric profiles, figures 20 and 21. The profiles tested in the model represent the two extreme conditions and an average poststorm condition.

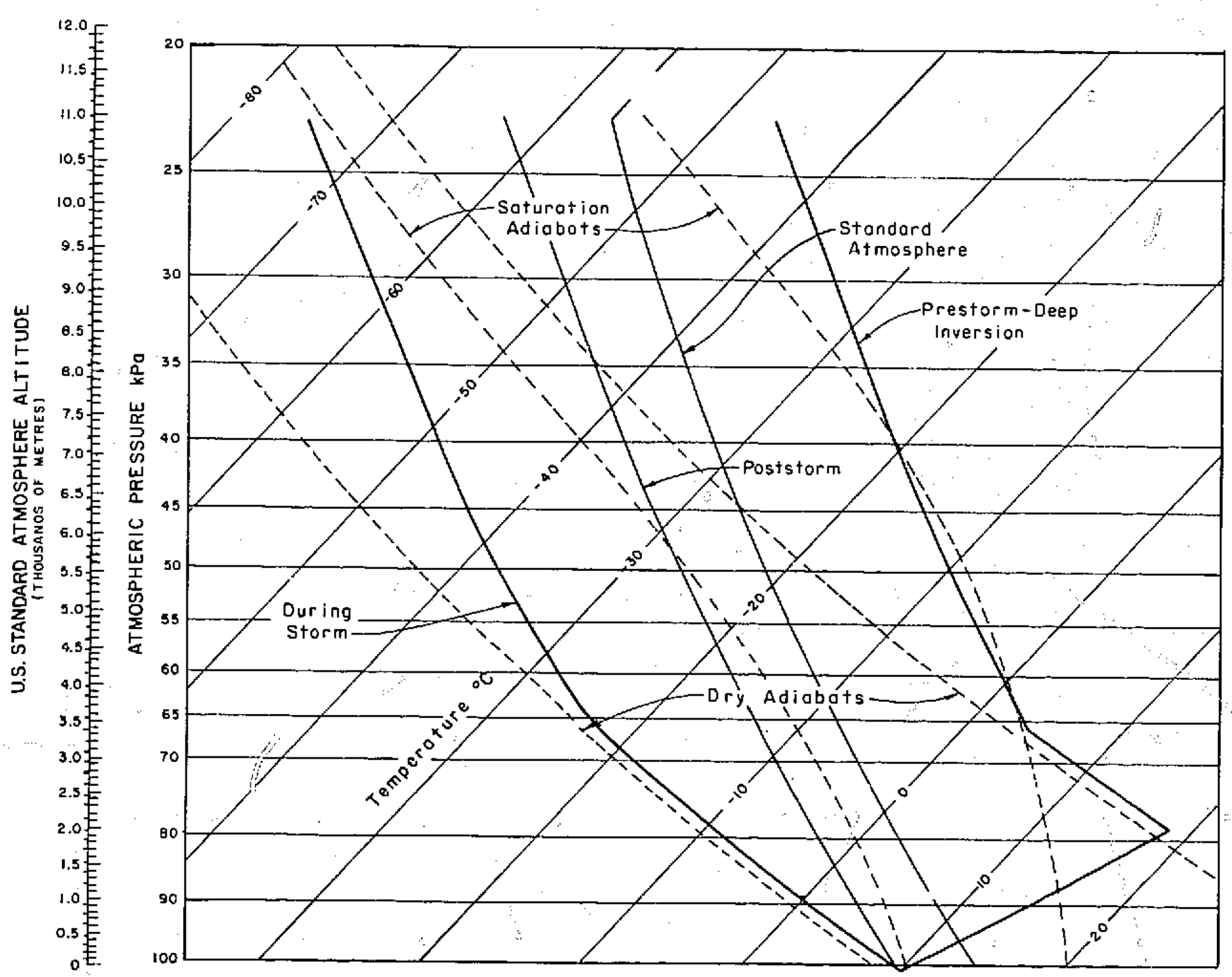

Figure 20.—Atmospheric profiles, Sierra Nevada studies.

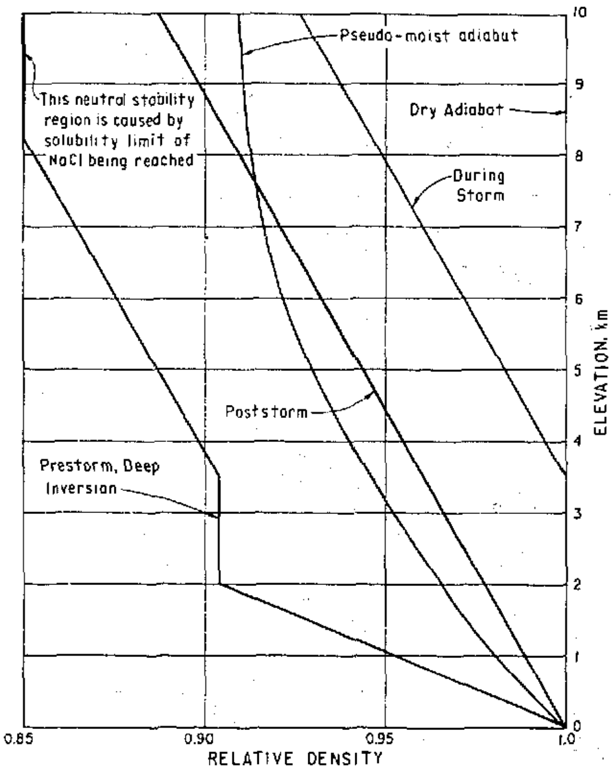

Figure 21.—Relative densities, Sierra Nevada.

The direction of the approaching wind could be varied by rotating the topography about the center of the target area. The center of the target area was assumed to be located at 725 000 metres east and 4 322 500 metres north, Universal Transverse Mercator Grid, zone 10. The approaching wind direction could be varied in azimuth from 185° to 305°. Generally, experiments were conducted at 15° intervals between these two extremes.

Both ground seeders and airborne seeders were simulated, figure 3. The list of ground seeders and their location are given in table I. During the course of an experiment, only a selected number of seeders was used. Normally these included a set of low-level seeders (less than 1200 metres), a set of intermediate level seeders (between 1200 and 1800 metres), and a set of high-level seeders (greater than 1800 meters). The crest of the mountain barrier in the study region is at an elevation of about 2600 metres. The airborne seeders had their origins upwind of the topography at nine fixed locations. The elevations of the airborne seeders were arranged in three adjacent sets with three seeders for each set. The elevation of the most southern seeder of each set was fixed at 500 metres, the middle seeder at 1500 metres, and the most northern seeder at 2500 metres. Tests with airborne seeders were conducted at only a few of the 15° incremental settings. Above 4000 metres the seeder trajectory essentially coincided with the free stream trajectory.

In figures 22 through 38, the ground seeders are differentiated by the elevation of the seeder location. The low-level seeders are designated by blue lines, the intermediate-level seeders by red lines, and the high-level seeders by green lines. The airborne seeders are also differentiated in the same manner according to elevation. The blue lines correspond with 500 metres, the red lines with 1500 metres, and the green lines with 2500 metres. The brown lines designate the 50-kPa trajectory.

Prestorm Trajectories with Deep Inversion

Combined airborne and ground seeder trajectories were determined for wind directions from 260° and 305°. Ground seeder trajectories were determined for the 245°, 260°, and 305° wind directions, figures 22 through 26.

All plume trajectories from ground seeders tended to flow around the Sierra Nevada barrier in the vicinity of the target area. Those trajectories which do cross the barrier do so only at the low points in the barrier.

Only airborne plume trajectories above the 2500-m elevation passed over the target area. Some divergence of the flow field was experienced over the target area at the 2500-m elevation. However, the divergence was small enough so that the physical location of the seeder source was not extremely critical. Since the trajectories were deflected somewhat from the free stream direction, figures 23 and 25 should be used to estimate the required aircraft location for a given wind direction. At 1500 metres and below, the airborne seeder trajectories were deflected around the target area. Depending upon the wind direction, they either passed up or down the valley and crossed the barrier at the low points in the barrier.

Trajectories During Storm

Combined airborne and ground seeder trajectories were determined for wind directions from 245°, 275°, and 305°, figures 27 through 32.

With this atmospheric condition, ground seeder plume trajectories passed over the target area for all wind directions. With a wind azimuth of 275°, the

Table 1.—*Ground seeder locations, Sierra Nevada*

Seeder No.	Coordinates East m x 10^{-2}	Coordinates North m x 10^{-2}	Description
1	7091	42 957	South Fork, American River
2	7054	43 263	Peavine Ridge
3	6893	42 931	South Fork, American River, Canyon
4	7437	42 789	State Highway No. 88
5	7458	43 595	Truckee River, U.S. Highway No. 40
6	6714	43 284	Buck Mountain (694)
7	7098	43 140	Rubicon River Canyon
8	7157	42 775	Steely Fork, Consumnes River (1475)
9	6910	43 380	North Fork, American River Canyon
10	6508	42 219	Lodi
11	6570	43 612	Oregon Hill
12	7404	42 596	Stanislaus National Forest, between Blue and Moore Creeks (1918)
13	6985	43 340	Forest Hill Divide (1409)
14	2600	43 500	Washoe Lake (1532)
15	6977	43 494	Blue Canyon, U.S. Highway No. 80
16	7234	43 247	Rubicon Road
17	7103	42 931	Pollack Pines
18	6951	43 200	American Bar Reservoir
19	7353	42 954	Kyburz, Canyon
20	7503	42 597	Mattley Meadow (2408)
21	6349	44 038	Big Bar Mountain
22	7100	43 023	Saddle Mountain (1879)
23	6545	44 112	Grizzly Mountain
24	6535	43 250	Rock Mountain
25	6870	43 760	Table Mountain
26	7210	43 000	Soft Silver Creek
27	7190	43 318	French Meadows Reservoir
28	6450	43 949	Shute Mountain
29	6317	43 753	Kelly Ridge
30	7500	42 651	Salt Spring River
31	6472	43 000	Orchard Creek, U.S. Highway No. 99
32	7018	43 850	Sierra Buttes (2617)
33	6858	43 543	State Highway No. 20
34	6013	43 409	Sutter Buttes
35	6926	42 496	Westover Airfield (Amador)
36	7248	43 024	Eldorado (1876)
37	6698	43 390	Peardale
38	7162	43 374	Sunflower Hill
39	7161	42 855	Baltic Peak (1548)
40	7444	42 689	Cole Creek Canyon
41	6666	42 620	Bridge House, State Highway No. 76
42	7303	42 468	Blue Mountain (1847)
43	6816	42 188	Power Station, State Highway No. 8
44	6892	43 390	Moody Ridge
45	7575	43 317	Lake Tahoe (1899)
46	7304	42 867	Iron Mountain
47	6750	42 875	Pine Hill
48	6290	42 786	Valley Acres, Natomas Airport
49	6858	43 074	Georgetown Divide Ditch
50	6775	43 191	North Fork, American River Canyon
51	7133	43 444	North Fork, American River Canyon
52	6559	42 830	Hank Exchange
53	5993	43 193	Ralston Ridge
54	6971	42 717	Aukum Mountain
55	7267	43 256	Bunker Hill (2293)

Notes: Target center 725 000 metres east and 4 322 500 metres north.
Numbers in parentheses are elevations in metres.

trajectories were approximtely perpendicular to the Sierra Nevada boundary. Seeders located north of the target area had trajectories that passed over the target area for wind azimuths greater than 275°. Seeder trajectories from locations on the southern boundary of the target area passed over the target area for wind azimuths less than 275°.

Airborne seeder trajectories tended to diverge over the target area. This effect enhances the spreading of the material over the area. However, the physical location of the airborne seeder is extremely critical and is strongly dependent upon the wind direction.

Poststorm Trajectories Without Inversions

Combined airborne and ground seeder trajectories were determined for wind directions from 245°, 275°, and 305°, figures 33 through 38.

For the 245° wind direction, an extreme amount of lateral transport of the plume was observed with the low elevation seeders. With the exception of a few high-level seeders located south of the target area, all the seeder trajectories passed into the Yuba River Basin. With the 275° wind direction, extensive pooling around seeders was observed. The flow field tended to be around and not over the Sierra Nevada barrier in the target area. Only with the 305° wind was there an indication of ground seeder trajectories entering the upper regions of the target area.

At the 1500-m elevation, the airborne seed material tended to pool along an axis which parallels the crest of the Sierra Nevadas. Above 2500 metres, the airborne seeder trajectories passed over the target area. Some care would need to be exercised with high-level seeding to hit a specific target area.

DETAILED CONCLUSIONS

Studies of Map Size

The purpose of these studies was to investigate the effect of the model on the approaching density and velocity profiles. The conclusions are as follows:

1. The tests with a blank map that represented a flat average topography elevation showed that flow laminae remain at their density elevations and will generally flow around obstacles rather than flowing over them.

2. The damming effect tends to truncate approaching density profiles, although some of the more dense fluid from below the map top flows up onto the map.

3. The damming effect does not significantly deflect upstream flow that is at a higher elevation than the map. However, downstream from the map a horizontal deflection away from the center of rotation was noted.

Leadville-Climax Verification Model

The purpose of this study was to verify that the model could reproduce observed atmospheric flow fields. The conclusions were:

1. In the valleys, model velocities scaled to prototype values when the free stream velocity conformed with Richardson scaling.

2. Mainstream transport, in or near valleys which were parallel to the free stream flow, followed the valley flow at the potential density levels at which they were generated. Thus, transport of material to higher elevation target areas would be highly dependent upon turbulent diffusion which was not simulated in the model.

3. Plumes stagnated in the bottom of valleys which were normal to the free stream flow.

4. The 2:1 vertical distortion in the model scale apparently does not adversely affect the simulation of the flow trajectories and velocities.

5. In addition to showing mainstream flow, the model clearly shows lee wave action. Lee waves, over ranges oriented at an angle to the free stream flow, caused the plume trajectories to spread laterally.

6. Plume trajectories observed with the model will occur in the atmosphere. Spreading about the plume axis will be augmented in the atmosphere by turbulent diffusion.

San Juan Model

The purpose of these studies was to simulate ground seeding operations. The results that follow are to be used in interpreting field observations.

1. Ground level trajectories were determined for atmospheric conditions which were typical of storms that were candidates for seeding. The predominant flow characteristic was the merging of individual seeder plumes into one long plume that

formed near Pagosa Springs, extended westward over Durango, and passed around the western border of the target area.

2. Trajectories from seeders located near the east end of the target boundary passed eastward over Cumbres Pass into the San Luis Valley.

3. The only trajectories to pass northward through the target area came from seeders located at elevations higher than 2300 metres.

Sierra Nevada Model

The purpose of these studies was to provide guidance for field tracer and dispersion investigations. The results were:

1. During storm periods, ground seeder trajectories from properly located sites pass over the entire target area.

2. During prestorm periods with deep inversions and during poststorm periods, the trajectories from most ground-based generators remain below the 1800-m elevation.

3. Airborne seeder trajectories can be made to pass over the target area for all atmospheric conditions when the airborne seeder is located at or above 2500 metres.

4. Airborne seeder trajectories can be made to pass over the target area only during storm conditions for airborne seeders located at or below 1500 metres.

APPLICATIONS

The application of the model to investigate both ground and airborne seeder locations for a wide variety of atmospheric conditions has been demonstrated in this report. Further development of the simulation techniques could lead to the capability to investigate locally developed convection cells.

The model also has application in the field of energy production by the wind. All the existing wind surveys are primarily based upon data from airports. Since airports are located in low wind areas, the survey results tend to underestimate the true wind potential. Because of its ability to yield quantitative results with respect to surface wind fields, the model could be used to identify prospective sites for wind farms.

Satellite photographs have been useful in defining the path of air pollution from both point sources (such as coal-fired powerplants) and diffuse sources (such as metropolitan areas). The model could be used in a similar manner to trace pollutant trajectories over distances up to 200 km. The model would be especially advantageous for simulations during storm periods since the trajectories are not visible to satellites during these periods.

A continuing area of concern in air travel is the presence of CAT (clear air turbulence) when it is least expected. It was observed during operation of the model that a transition from laminar to turbulent flow could occur locally under certain atmospheric conditions and wind velocities. This implies that the model might be used to obtain some generalized atmospheric characteristics that are necessary for the generation of CAT.

BIBLIOGRAPHY

[1] Abe, Masanao, "Mountain Clouds, Their Forms and Connected Air Current," Bull. Cent. Meteorol. Obs., Tokyo, vol. 7, No. 3, 1929.

[2] Von Arx, W. S., "An Introduction to Physical Oceanography," Addison Wesley, 1964.

[3] Cermak, J. E., "Laboratory Simulation of the Atmosphere Boundary Layer," American Institute of Aeronautics and Astronautics, report No. CDP69-70 JEC80, Fluid Dynamics and Diffusion Laboratory, Colorado State University, Fort Collins, 1970.

[4] Claus, A. J., "Large-Amplitude Motion of a Compressible Fluid in the Atmosphere," J. Fluid Mech., vol. 19, pp. 267-289, 1964.

[5] Hobbs, P. V., Radke, L. F., Fleming, J. R., and Atkinson, D. G., "Contributions from the Cloud Physics Group, Airborne Ice Nucleus and Cloud Microstructure Measurements in Natural and Artificially Seeded Situations Over the San Juan Mountains of Colorado," University of Washington, Seattle, Research Report X, 1975.

[6] Marwitz, J. D., Cooper, W. A., and Saunders, C.P.R., "Final Report to Division of Atmospheric Water Resources Management, Bureau of Reclamation," contract No. 14-06-6801, University of Wyoming, Laramie, 3 vol., 1976.

[7] Orgill, M. M., Cermak, J. E., and Grant, L. O., "Research and Development Technique for Estimating Airflow and Diffusion Parameters in Connection with the Atmospheric Water Resources Program," Annual Report CER70-71MMO-JEL-LO623, Fluid Dynamics and Diffusion Laboratory, Colorado State University, Fort Collins, 1970.

[8] Rouse, Hunter, "Model Techniques in Meteorological Research," Compendium of Meteorology, Boston, Am. Meteorol. Soc., pp. 1249-1254, 1951.

[9] Rouse, Hunter, "Fluid Mechanics for Hydraulic Engineers," Engineering Societies Monograph, McGraw-Hill, 422 pp, 1961.

[10] Schlichting, Hermann, "Boundary Layer Theory," 6th edition, McGraw-Hill, 1968.

[11] Soo, S. L., "Thermodynamics of Engineering Science," Prentice Hall, Inc., 1959.

[12] Yih, Chin-Shun, "Dynamics of Nonhomogeneous Fluids" McMillan Lo, 1965.

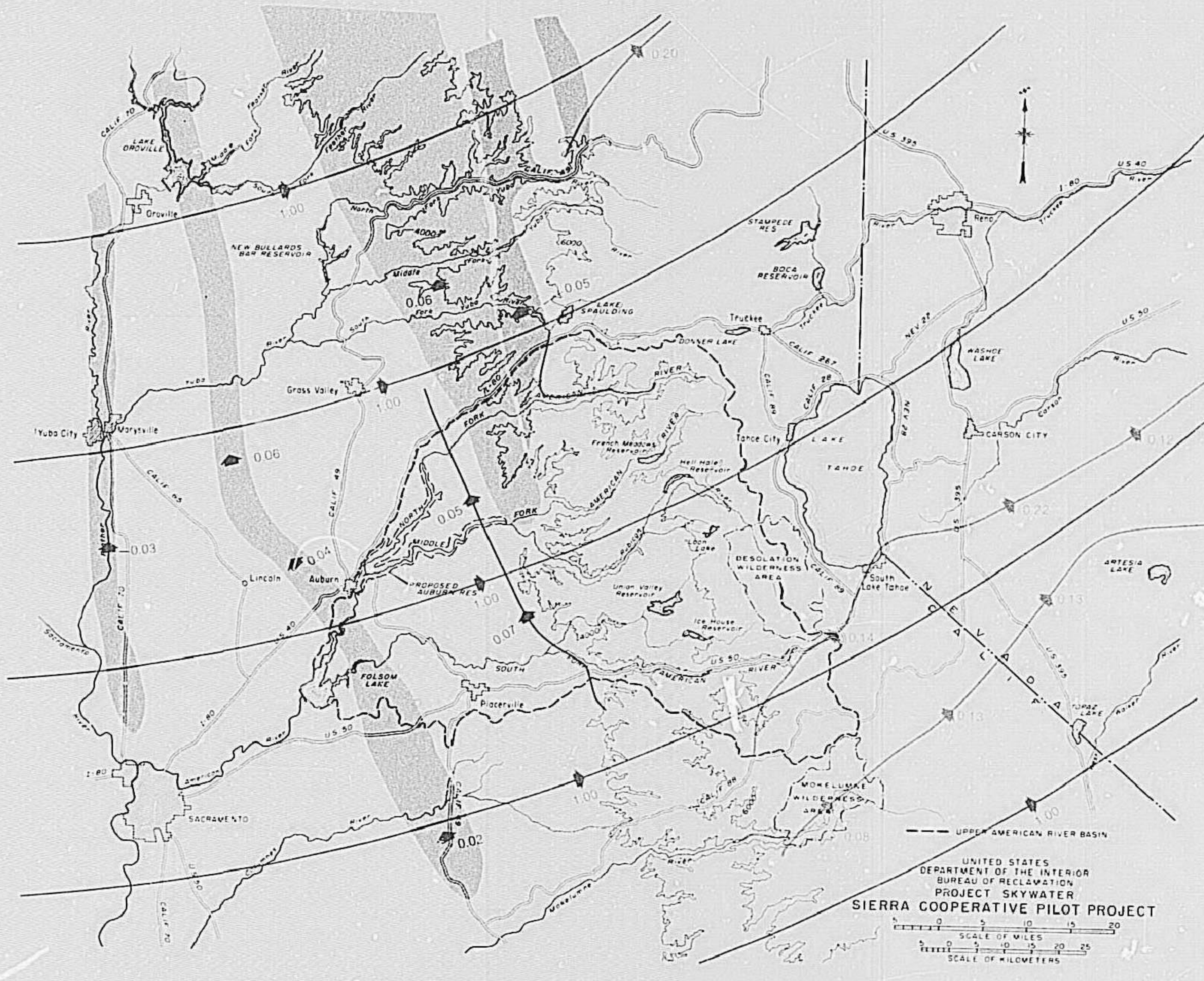

Figure 22.–Ground seeder trajectories, 245° wind, prestorm with deep inversion.

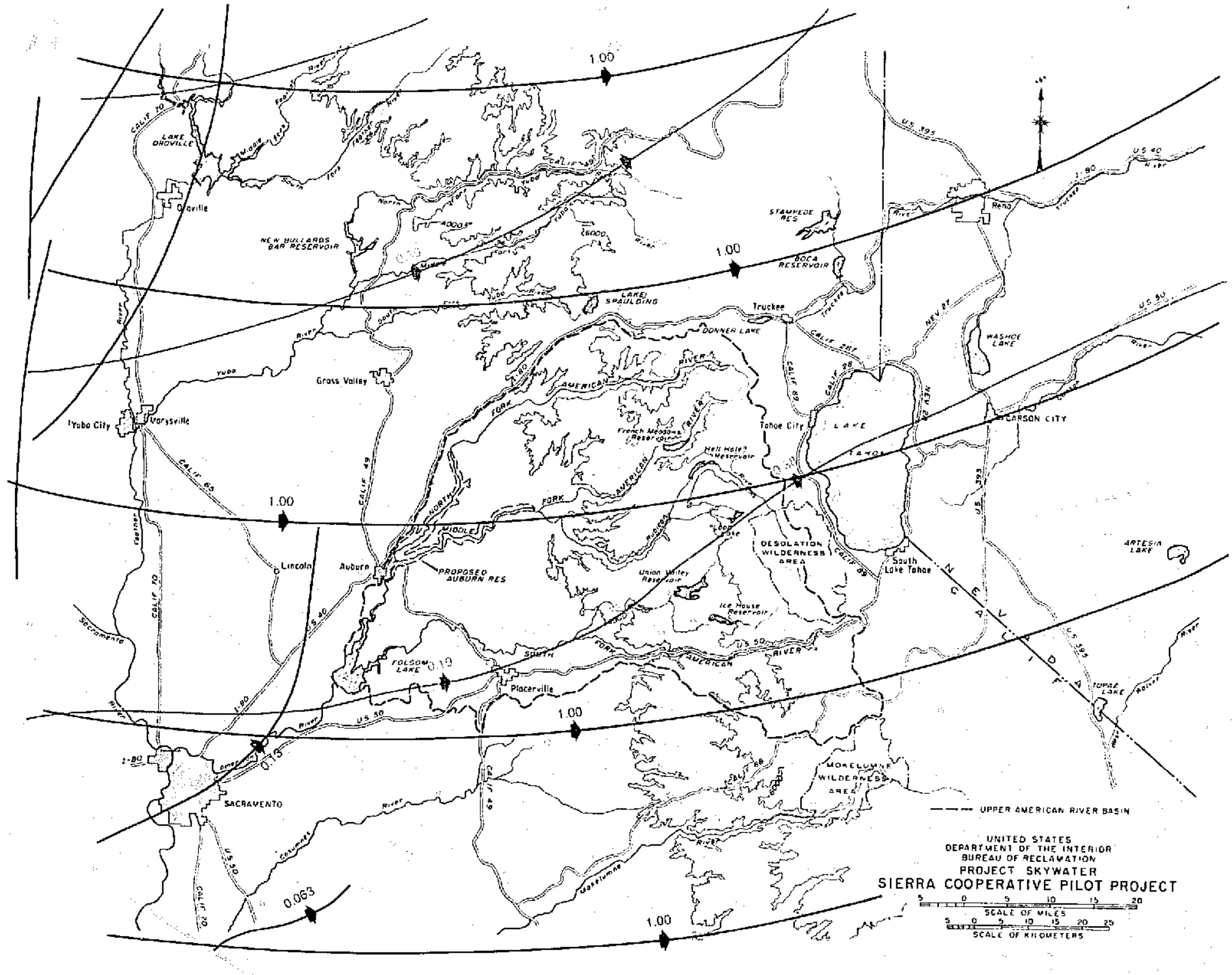

Figure 23.—Airborne seeder trajectories, 260° wind, prestorm with deep inversion.

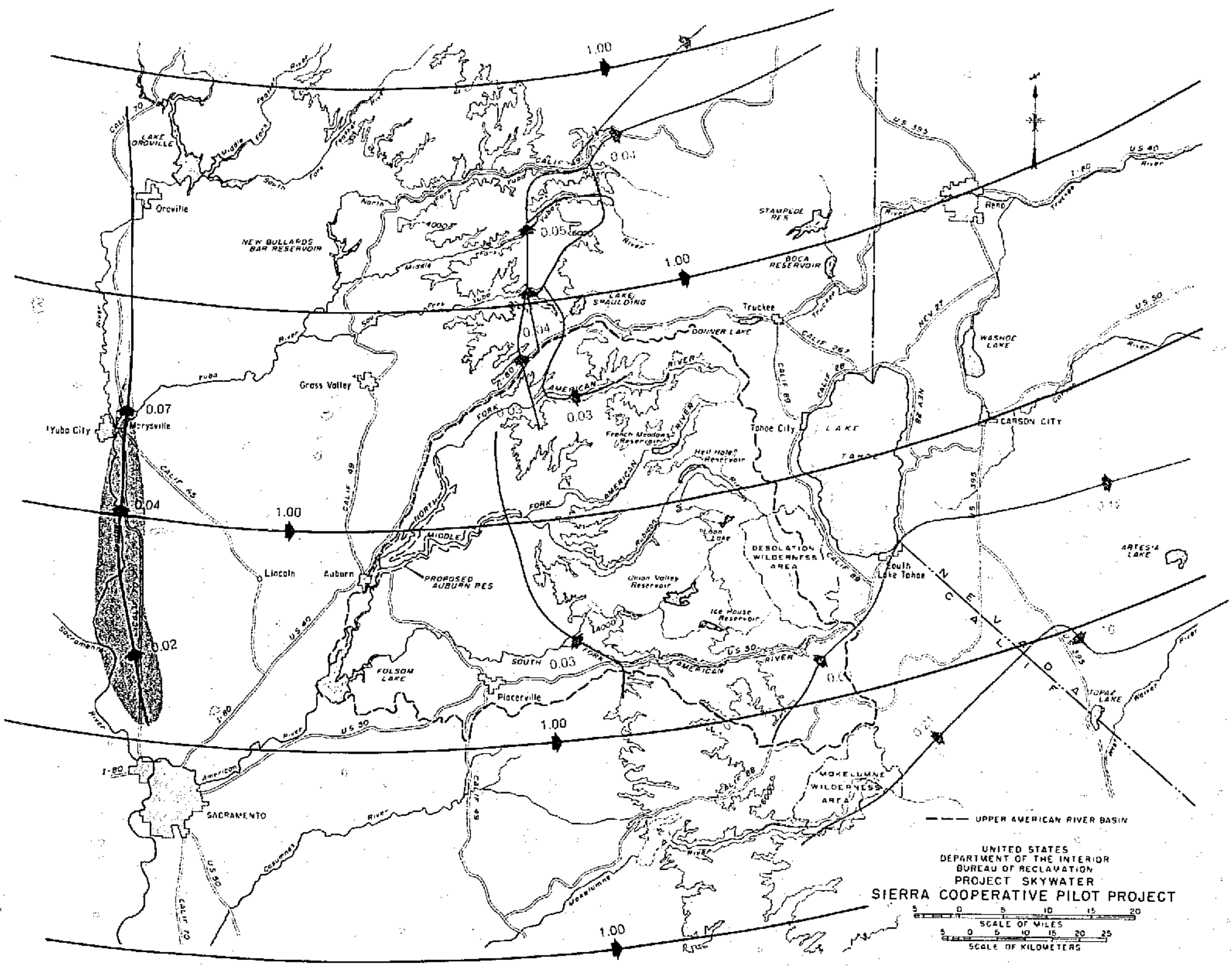

Figure 24.--Ground seeder trajectories, 260° wind, prestorm with deep inversion.

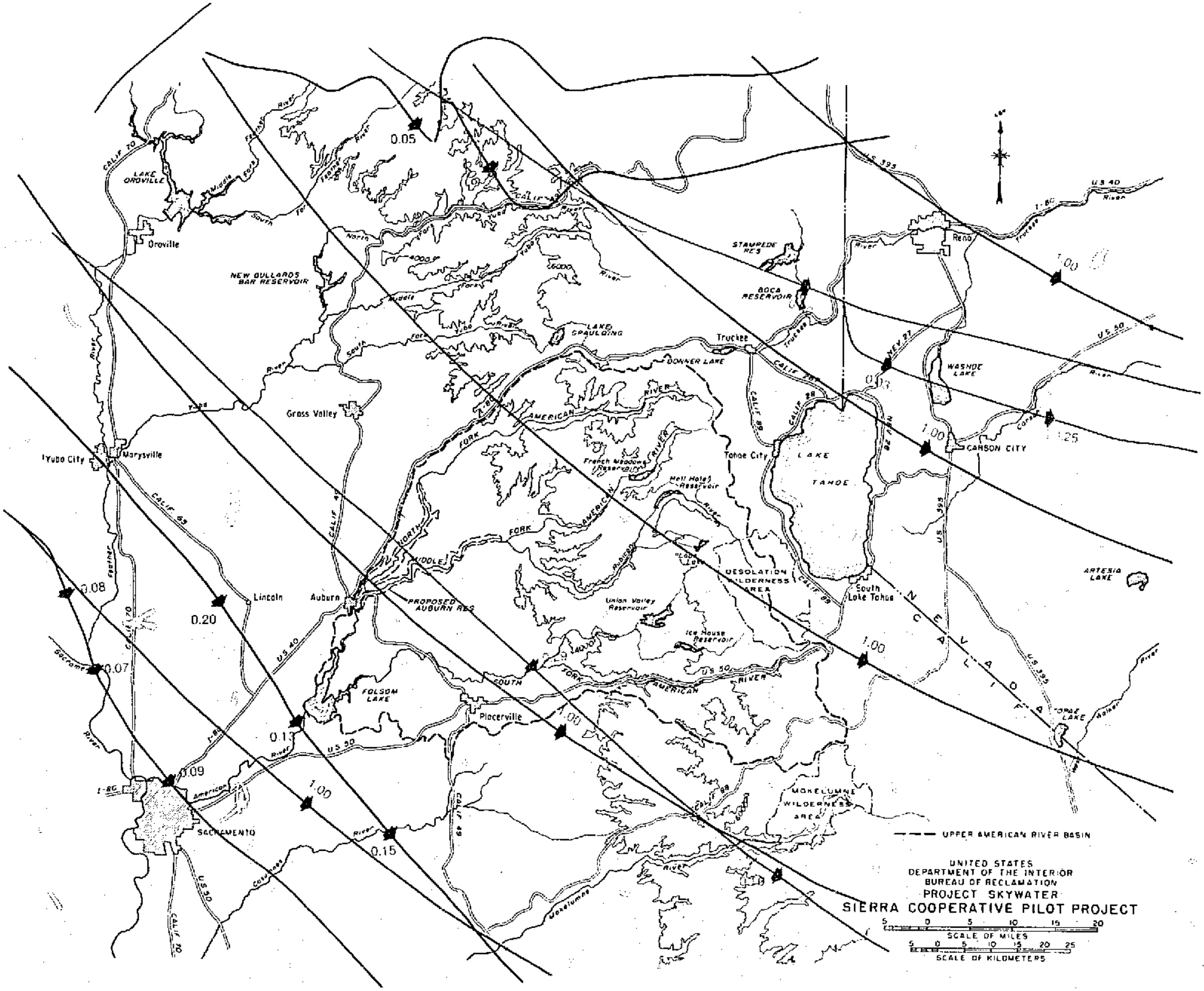

Figure 25.—Airborne seeder trajectories, 305° wind, prestorm with deep inversion.

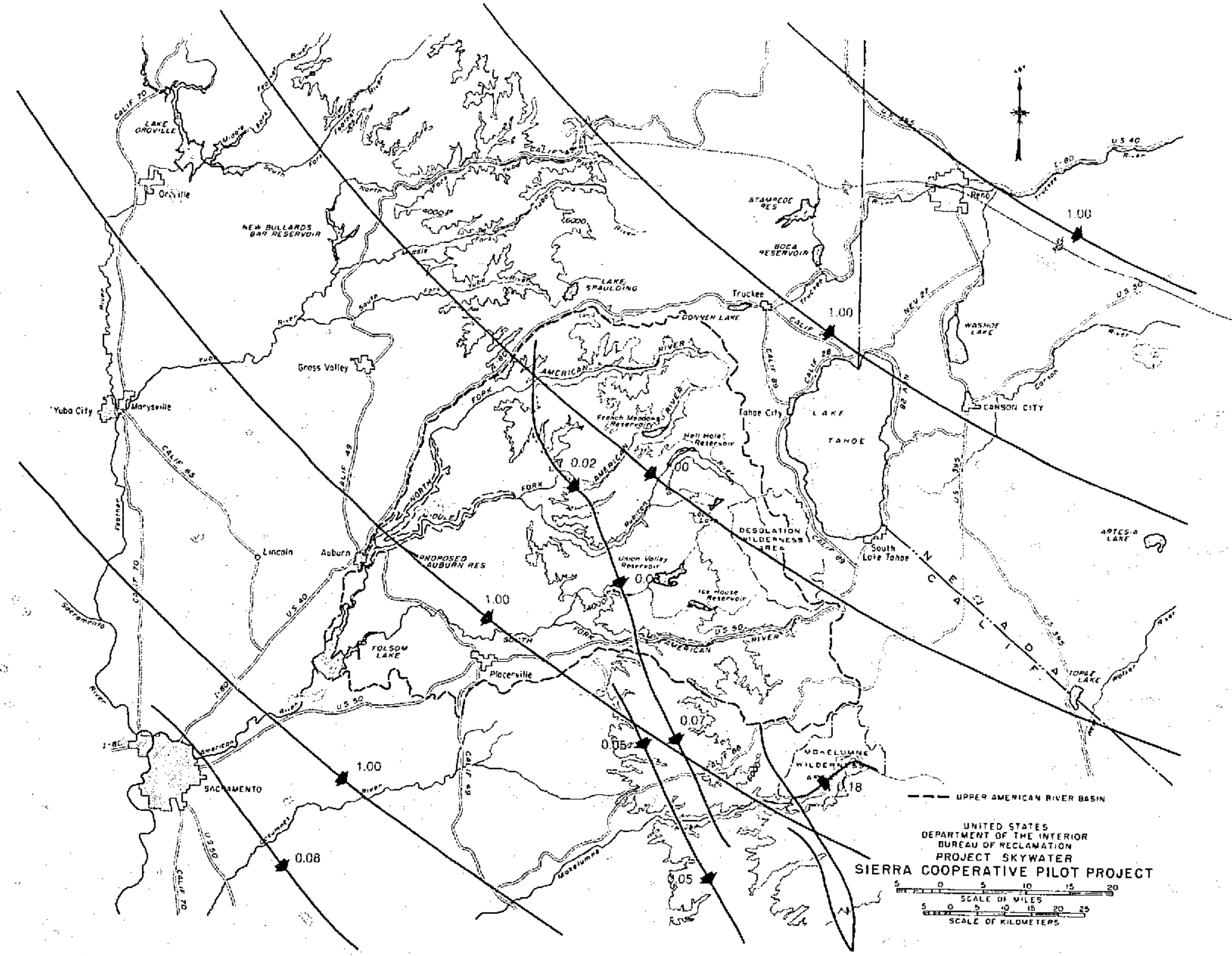

Figure 26.—Ground seeder trajectories, 305° wind, prestorm with deep inversion.

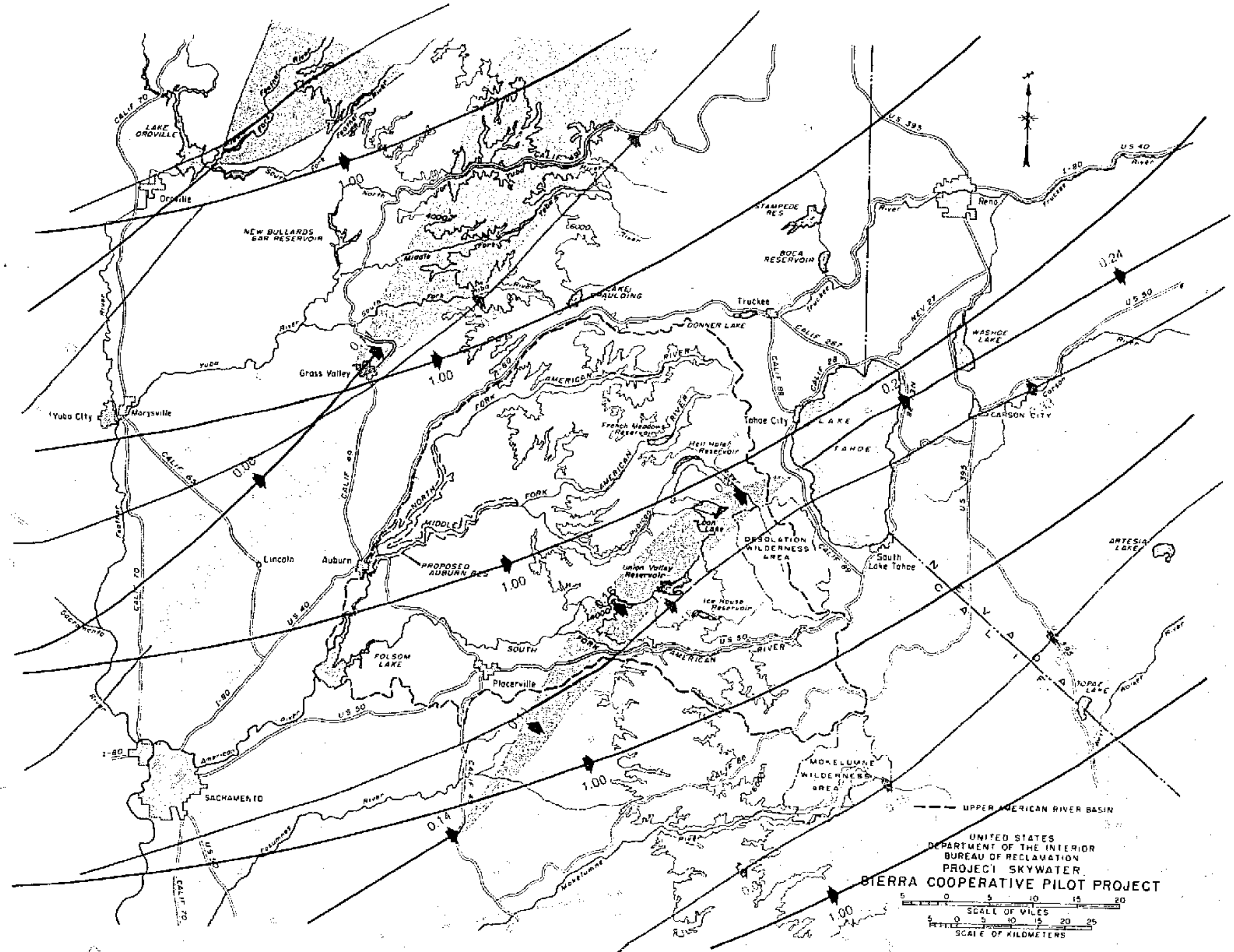

Figure 27.—Airborne seeder trajectories, 245° wind, during storm.

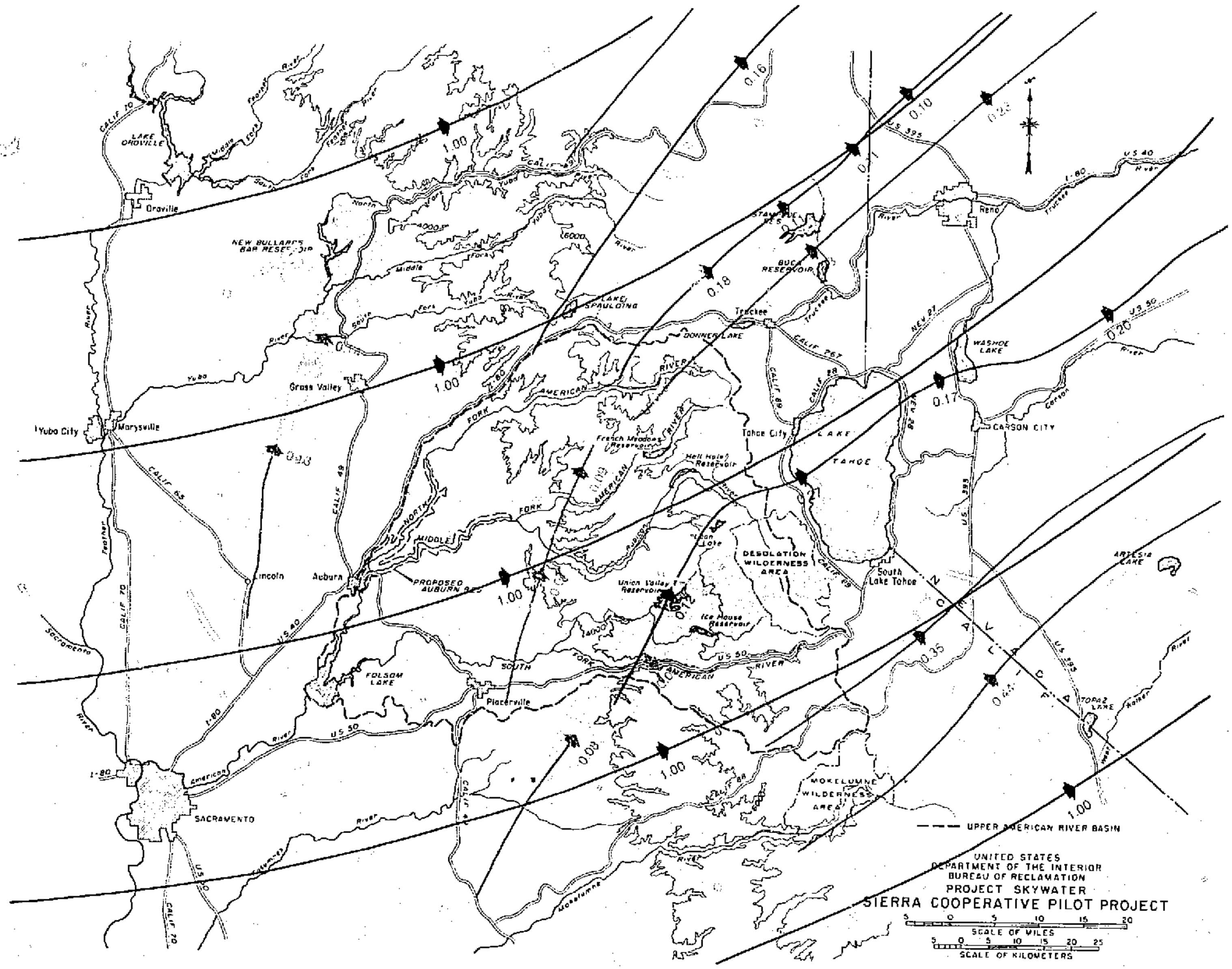

Figure 28.—Ground seeder trajectories, 245° wind, during storm.

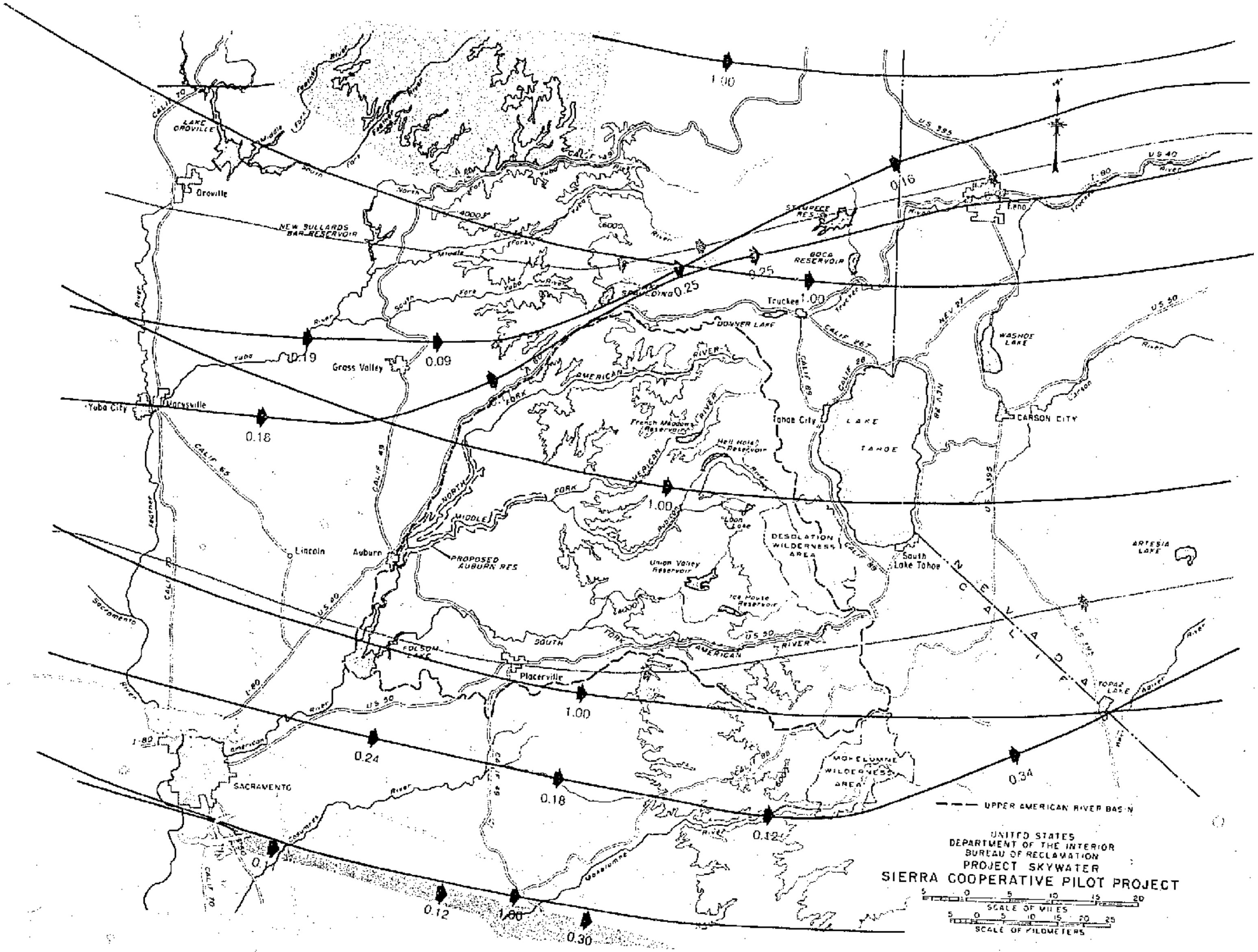

Figure 29.—Airborne seeder trajectories, 275° wind, during storm.

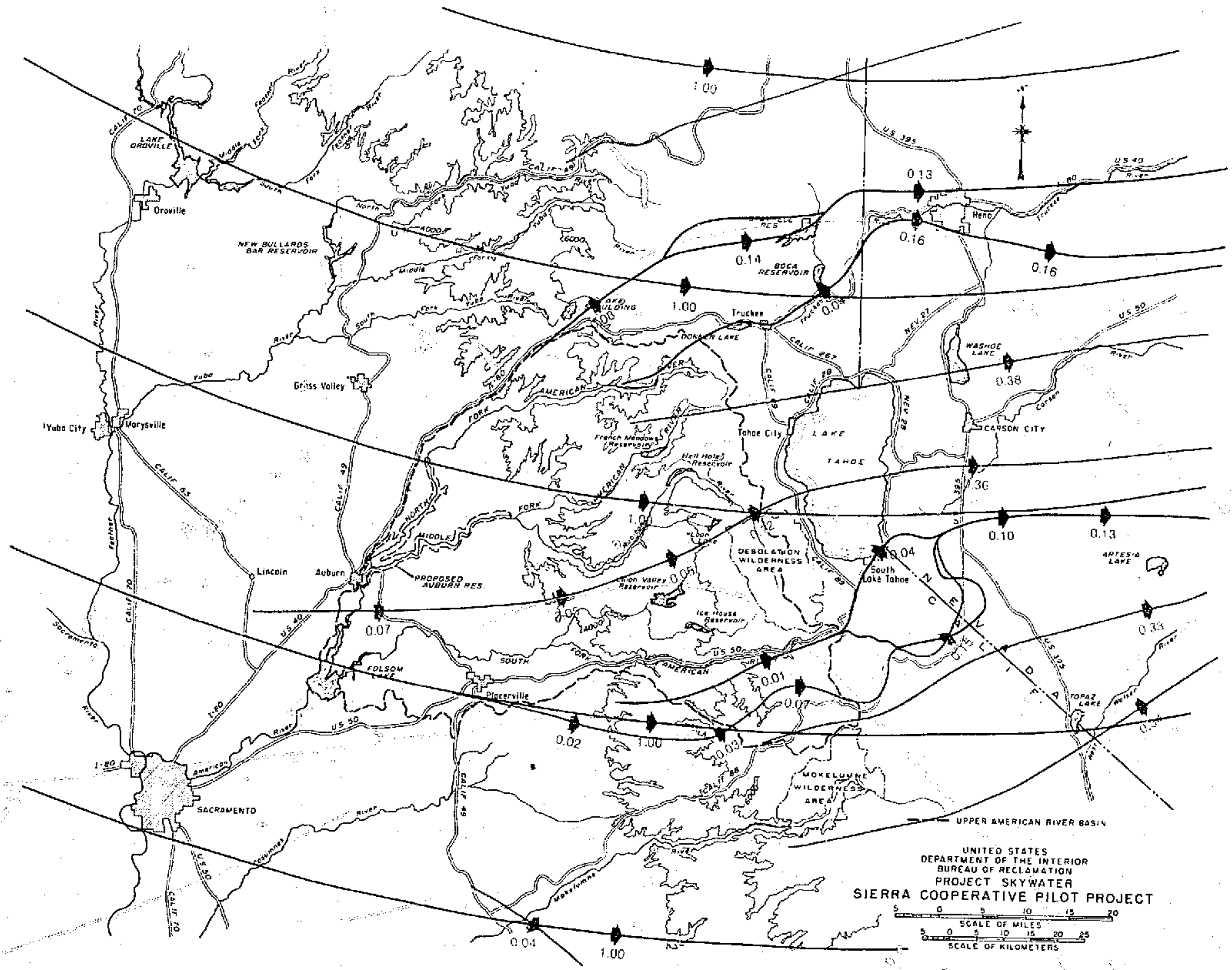

Figure 30.—Ground seeder trajectories, 275° wind, during storm.

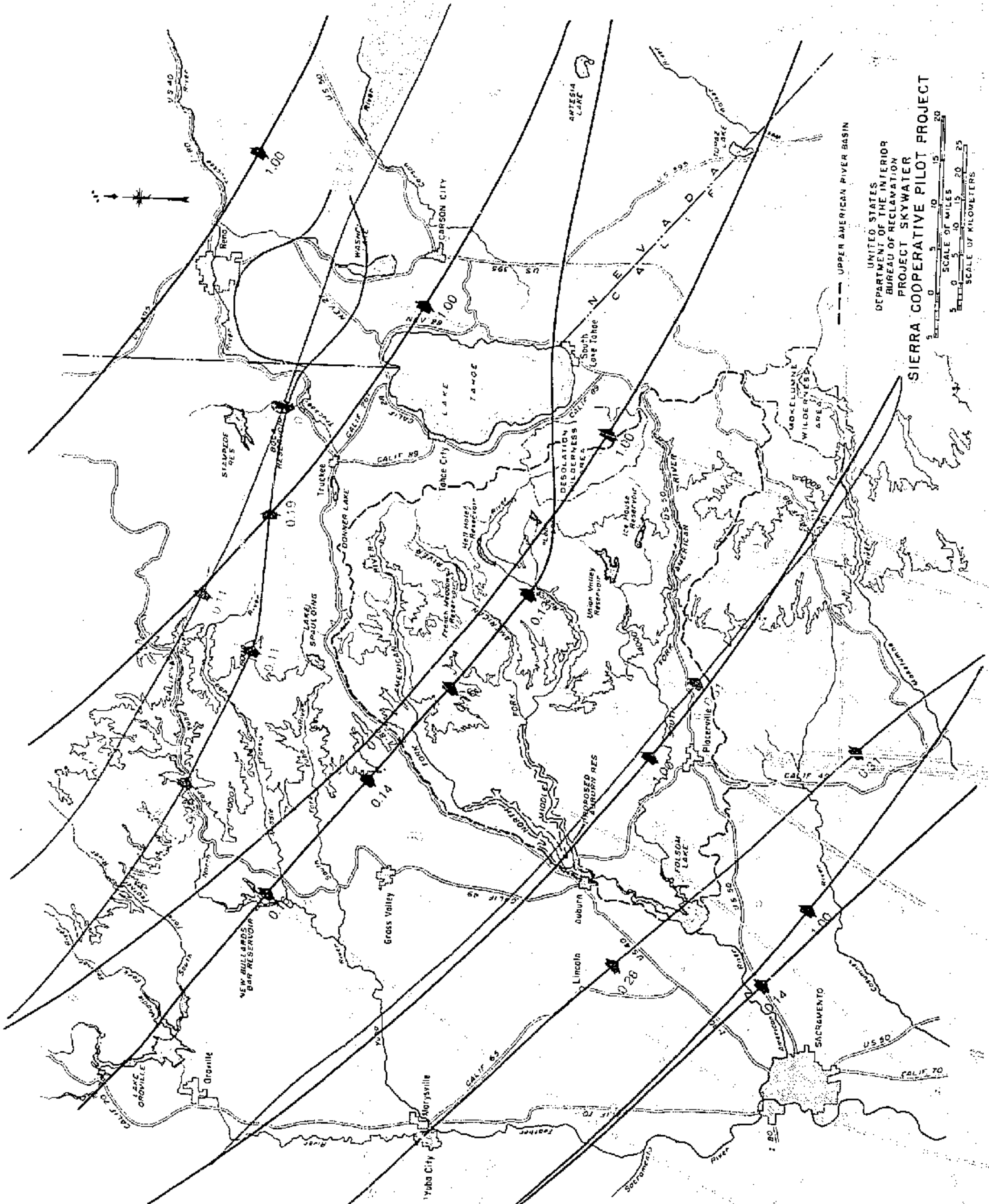

Figure 31.—Airborne seeder trajectories, 305° wind, during storm.

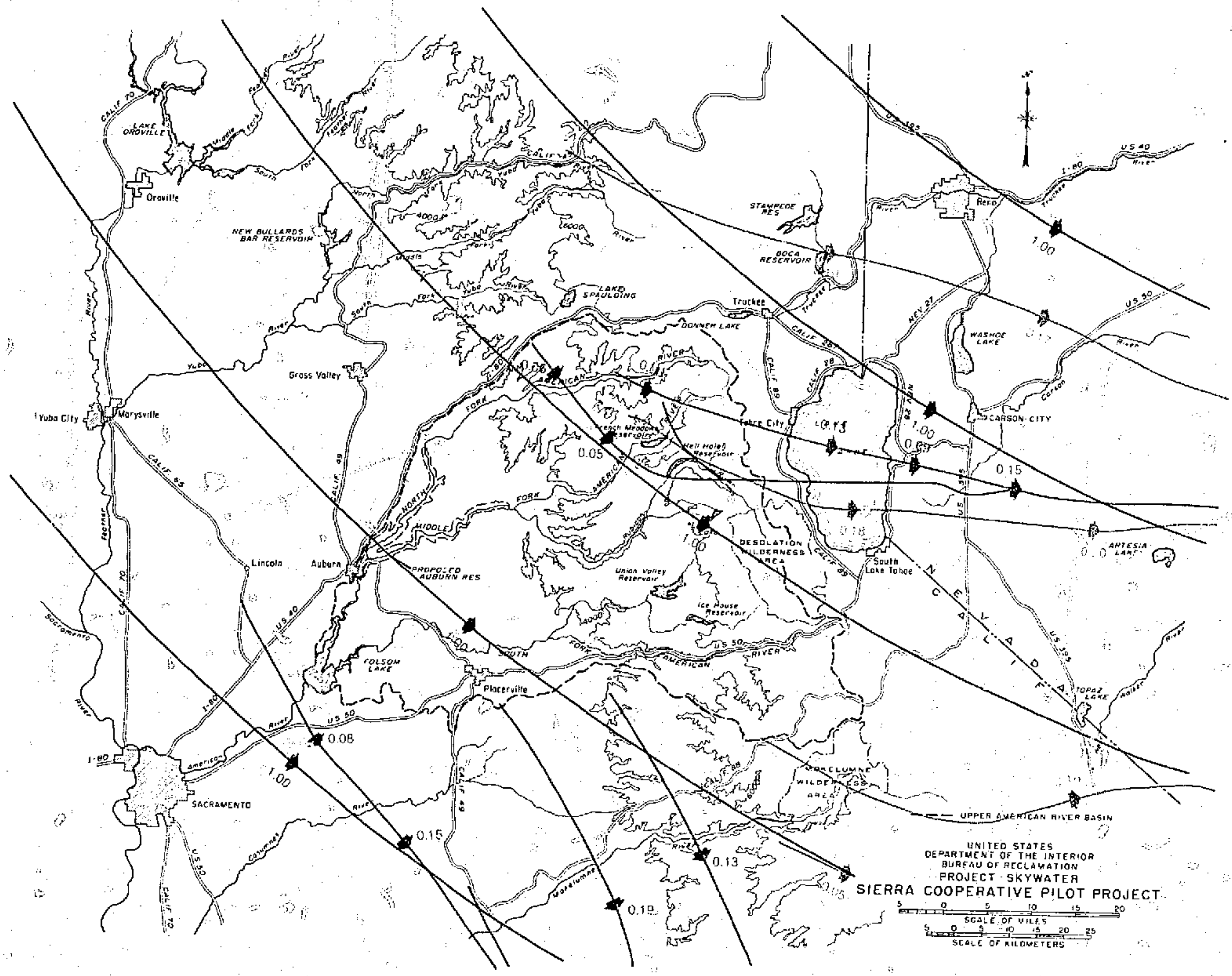

Figure 32.--Ground seeder trajectories, 305° wind, during storm.

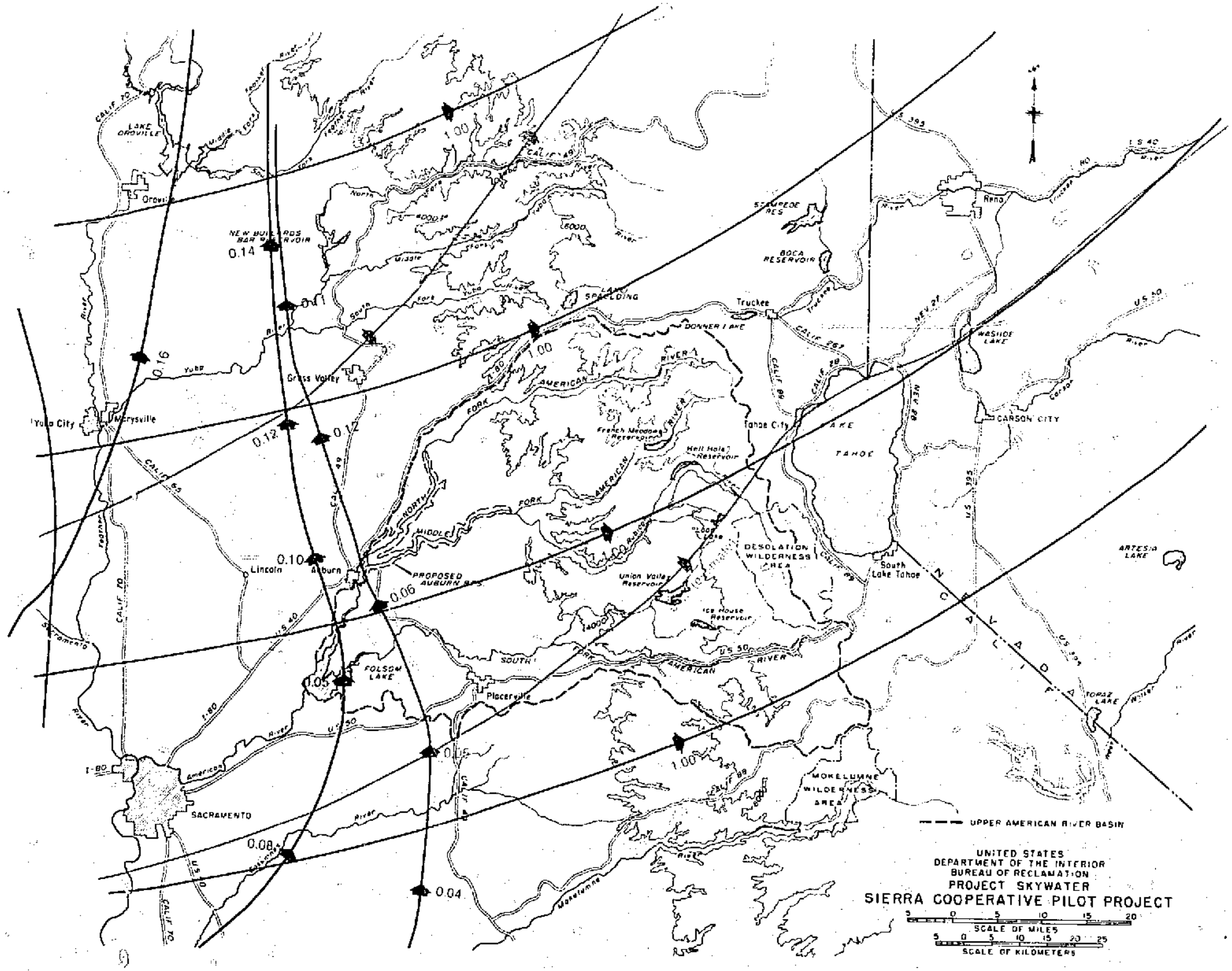

Figure 33.—Airborne seeder trajectories, 245° wind, poststorm.

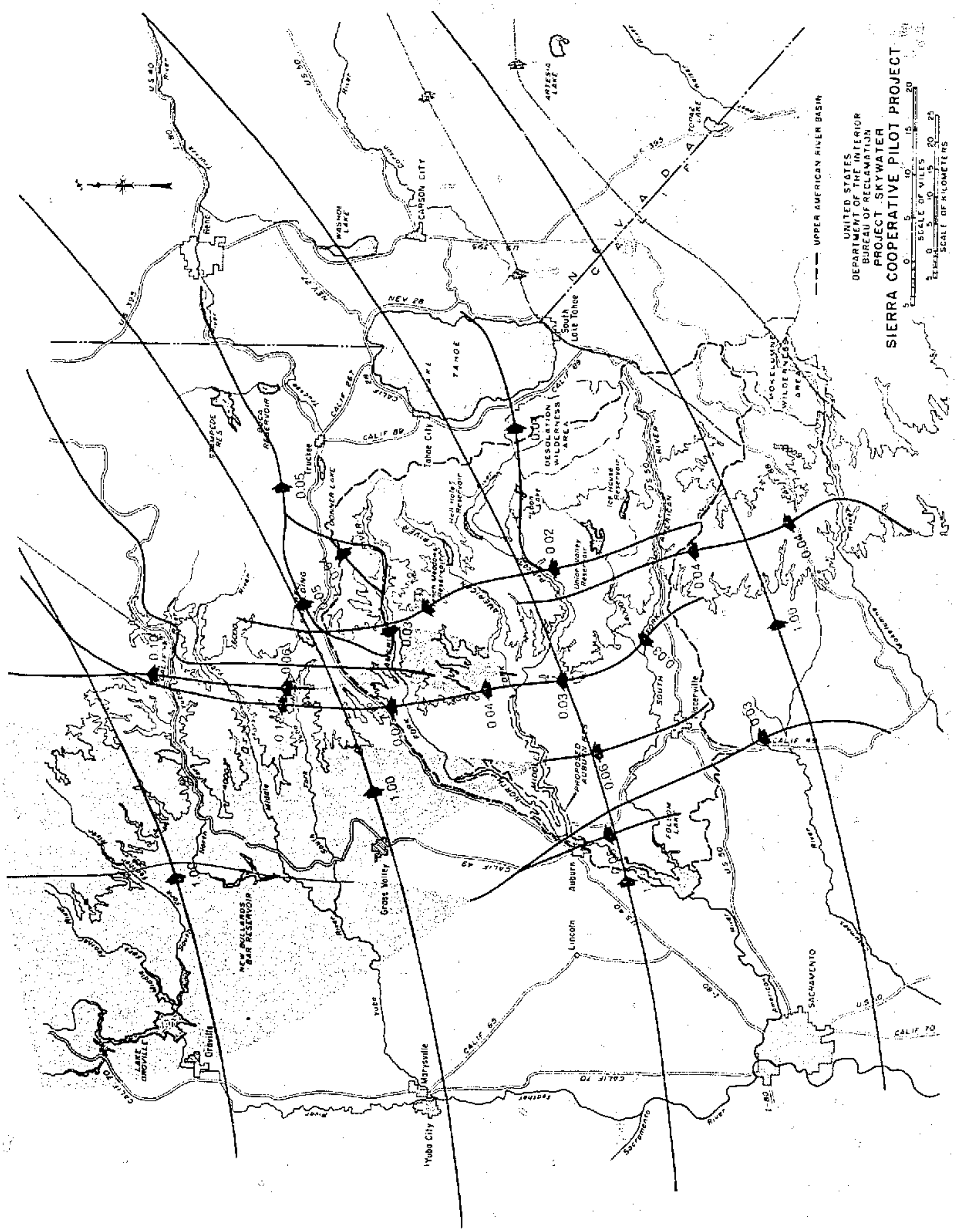

Figure 34.–Ground seeder trajectories, 245° wind, poststorm.

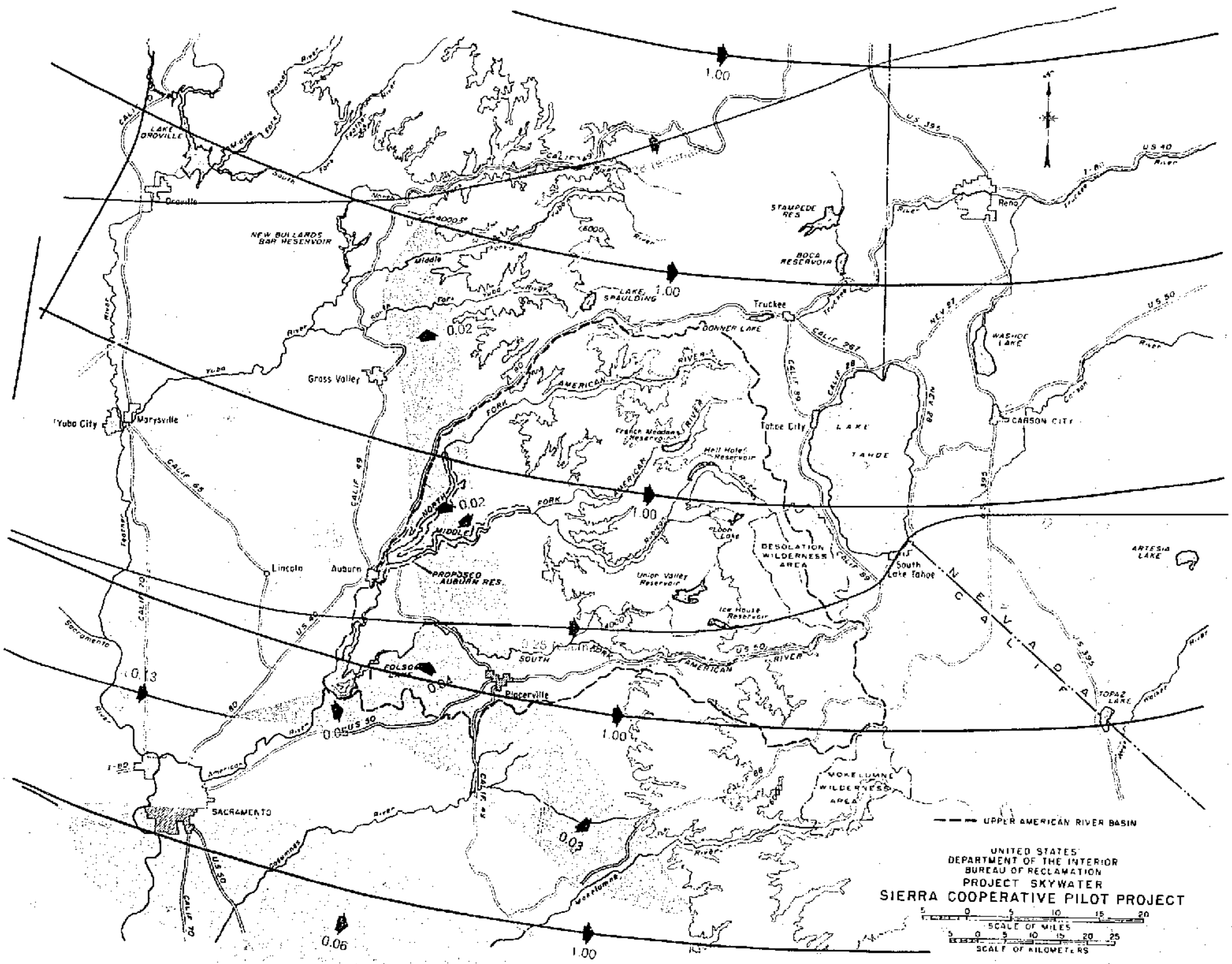

Figure 35.–Airborne seeder trajectories, 275° wind, poststorm.

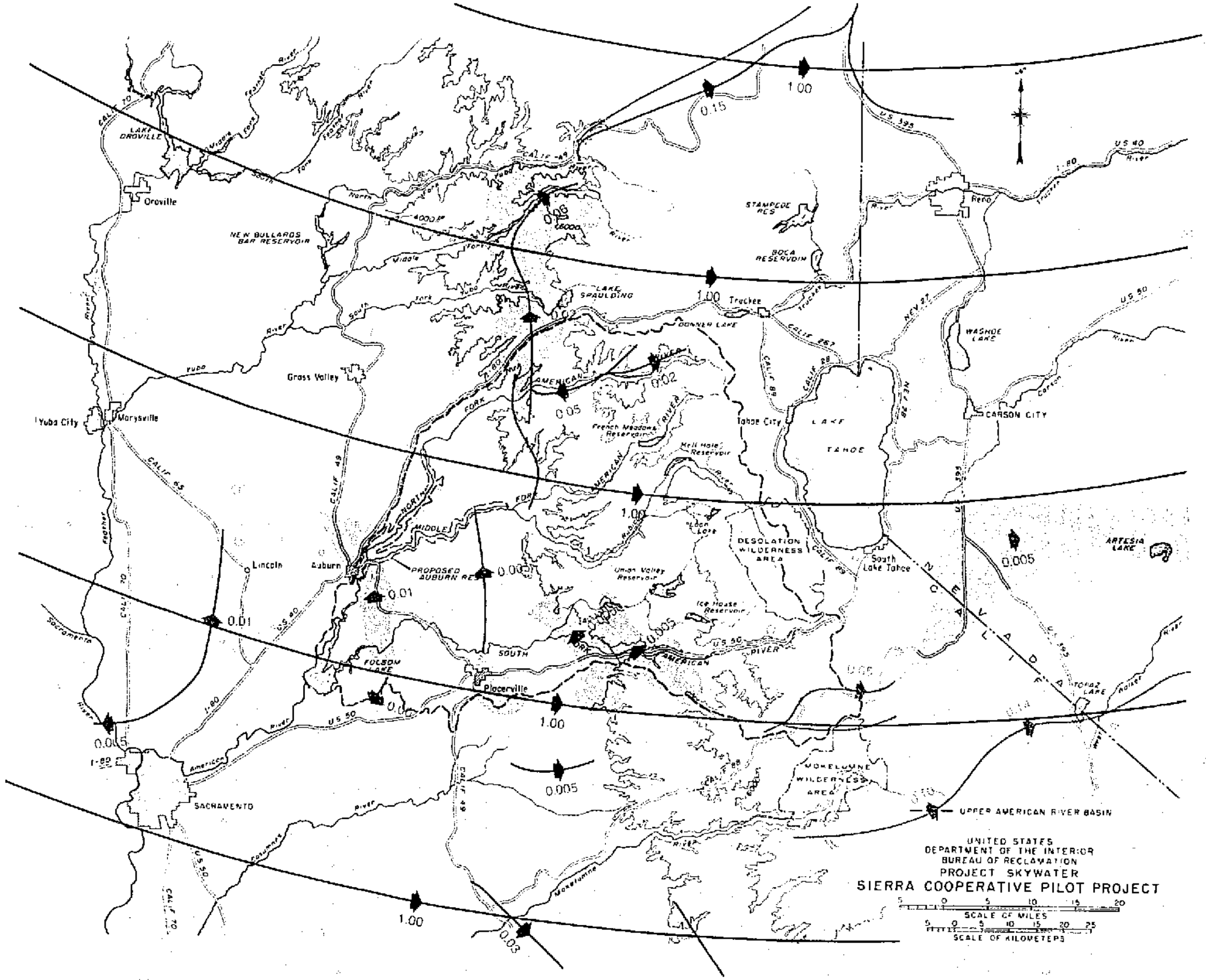

Figure 36.--Ground seeder trajectories, 275° wind, poststorm.

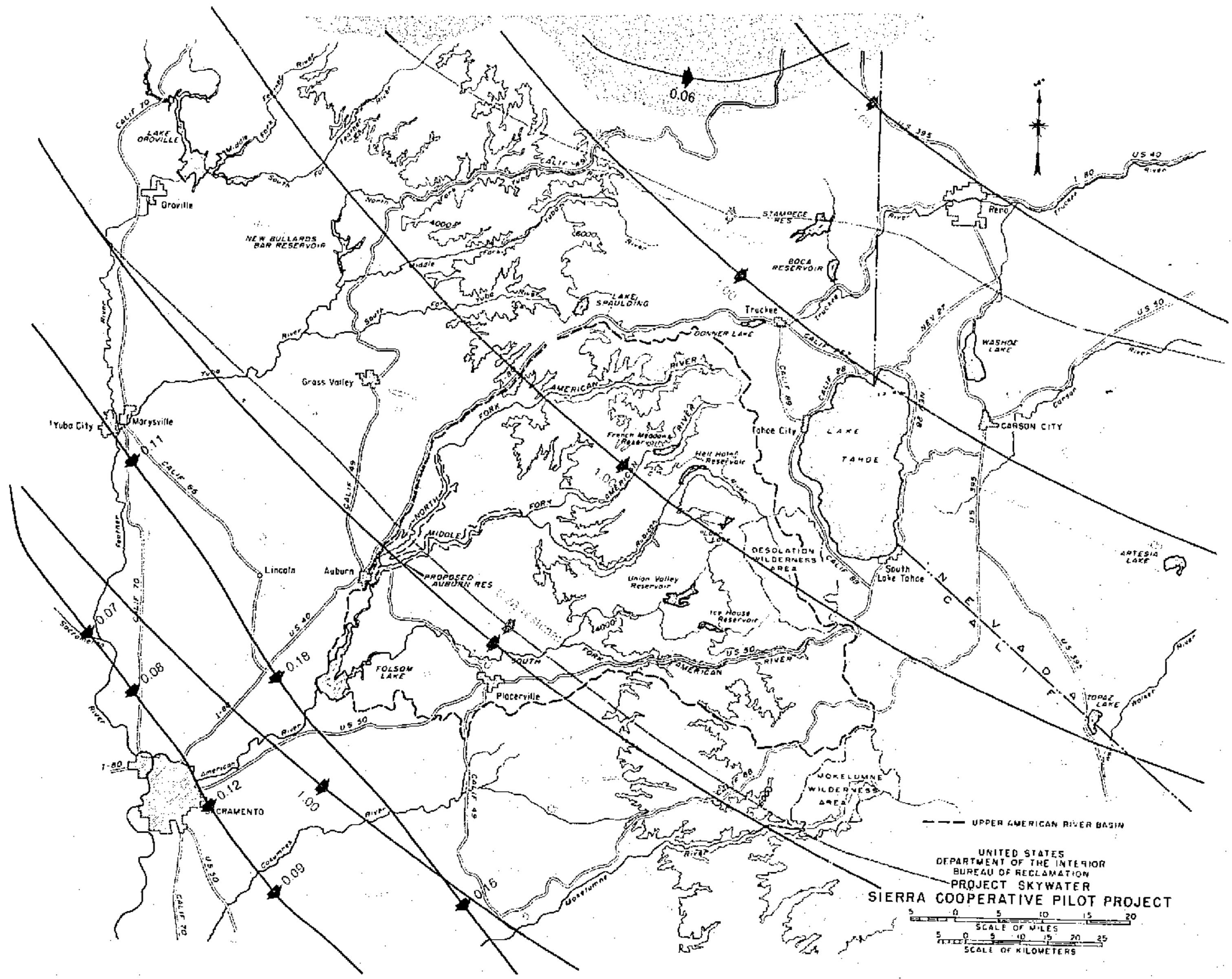

Figure 37.—Airborne seeder trajectories, 305° wind, poststorm.

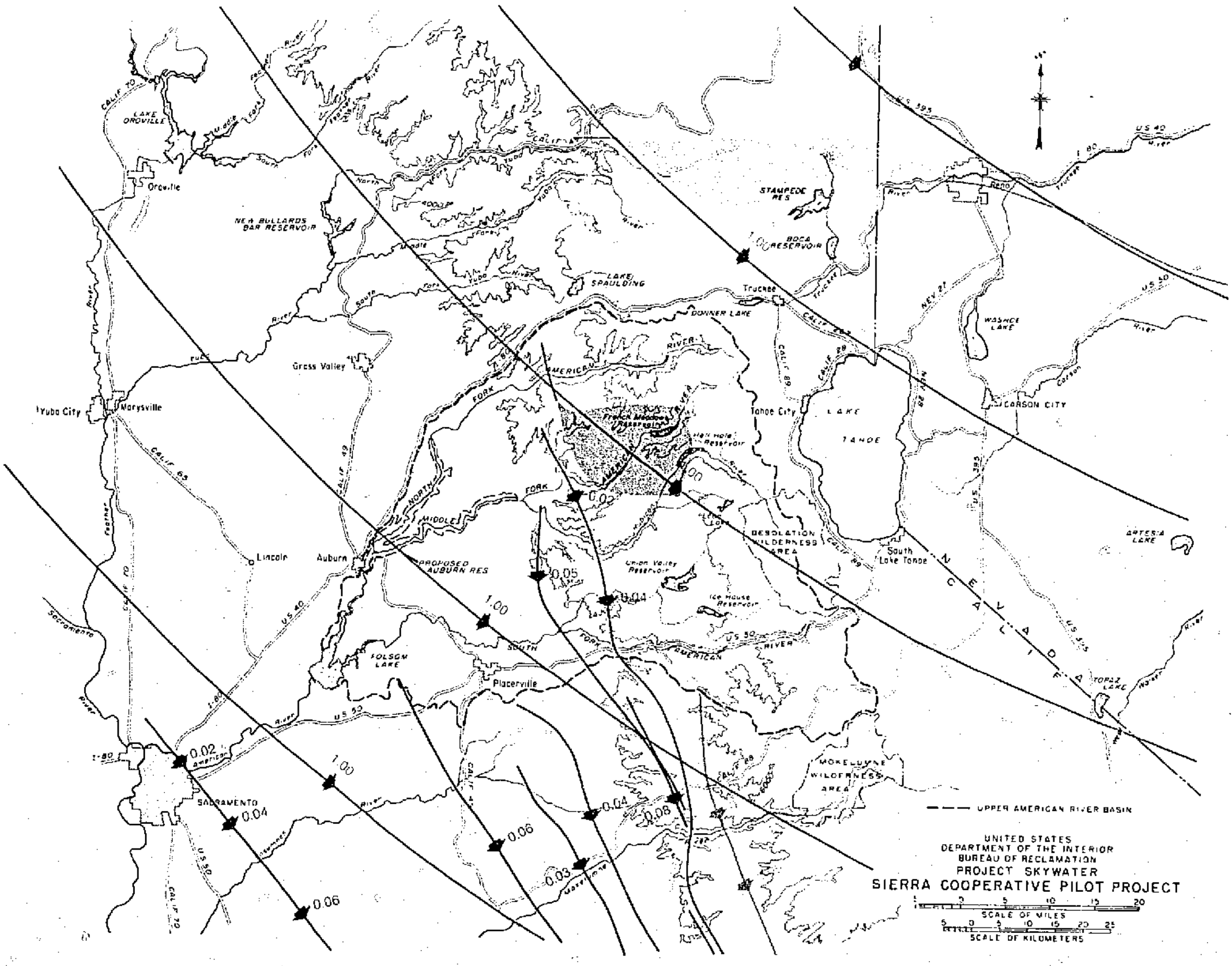

Figure 38.–Ground seeder trajectories, 305° wind, poststorm.

APPENDIX A

Optical Measurement of Density Gradients in Stratified Fluids

APPENDIX A

OPTICAL MEASUREMENT OF DENSITY GRADIENTS IN STRATIFIED FLUIDS

PURPOSE

The purpose of this appendix is to describe the optical system for determining density profiles during atmospheric simulation studies using stratified liquids.

APPLICATIONS

The material in this appendix can be used as an aid in applying the optical method for determining density gradients in stratified fluids. The computer program for computing the density from the rod photographs is included in documented form along with a sample rod photograph and sample computer output.

INTRODUCTION

In recent years, interest in studying stratified liquids has increased significantly. The investigations normally use either temperature or salinity to achieve the stratification. The density gradients in thermally stratified fluids are commonly determined from a set of temperature readings. Similarly, conductivity measurements are used to indicate density gradients in saline stratified models. Both methods use instrumentation which introduces a disturbance to the flow. In addition, the measurements are made at a series of discrete points.

With two-dimensional flow, an optical method of measuring the density gradient has been developed by Mowbray[1] which minimizes the disadvantages of temperature or conductivity measurements. The method is based on Fermat's law of stationary transit time. According to this law, the light rays passing through a density gradient will follow a path that minimizes the travel time. In general, the rays tend to travel in the less dense fluid. An inclined straight line viewed through a density gradient will appear curved, figure A-1. In layers of constant density, the light path having the minimum travel time is not refracted. Because of this phenomenon the inclined rod appears straight in areas where the density is constant.

Density gradients produce multiple images when the path length exceeds the thickness of the gradient by a fixed amount. For instance, with a diffused gradient between two fluids whose ratio of refractive indices is 0.975, multiple images are observed if the path length to thickness of gradient exceeds 3.2. For these cases, an odd number of images will be formed. With multiple images, an undistorted image is observed below the density gradient. A somewhat magnified and inverted image is observed above the undistorted image. Finally, a reduced and erect image can be observed above the inverted image, figure A-2. Multiple images in nature are known as mirages. Because the inverted image is so prominent, the smaller erect image is often not noticed in nature.

THEORY

Basic Equations

Ray path.—The equations are presented in dimensionless form with respect to quantities presented in the definition sketch, figure A-3.

[1] Mowbray, D. E., "The Use of Schlieren and Shadowgraph Techniques in the Study of Flow Patterns in Density Stratified Liquids," J. Fluid Mech., vol. 27, part 3, pp. 595-608, 1967.

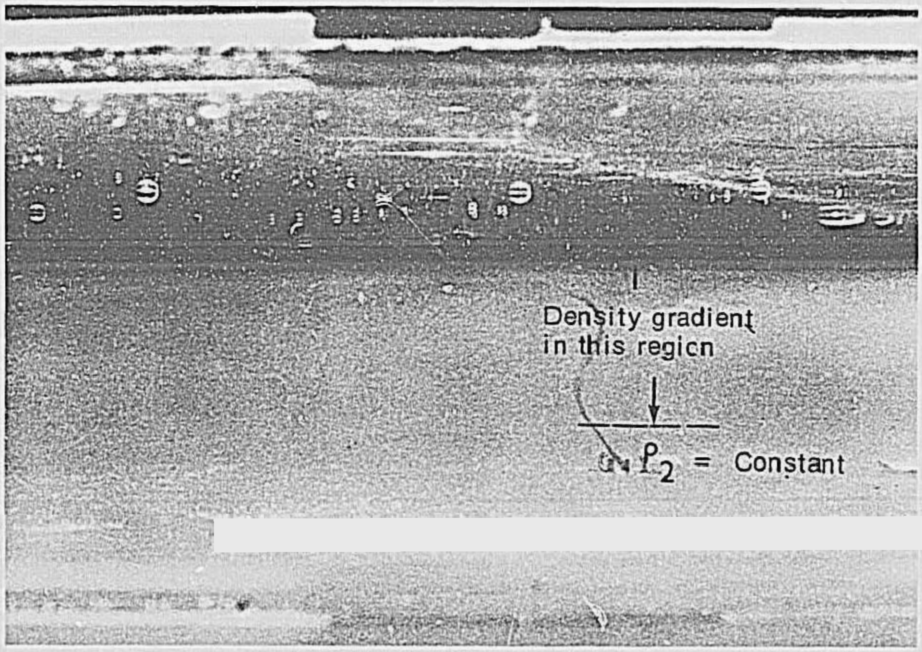

Figure A-1.—Optical distortion of straight rod when viewed through density gradient.
Photo P801-D-77863

All values can be made dimensionless by the following definitions

$$\overline{x} = x/L \qquad \overline{n} = n/n_o \qquad \overline{y} = y/H \qquad N = \overline{n}^2 \qquad \overline{z} = z/H$$

where n is the refractive index and the subscript o refers to conditions at $\overline{y} = 0$

The governing differential equations are

$$\frac{d\overline{y}}{d\overline{x}} = \frac{L}{H}\left(\frac{\alpha N}{N_f} - \beta\right)^{1/2} \tag{1a}$$

and

$$\overline{z} = \overline{z}_f + \left(\frac{d\overline{z}}{d\overline{x}}\right)\overline{x} \tag{1b}$$

The subscript f refers to conditions at the side of the viewing window where the ray is observed. The Greek letters are defined as

$$\alpha = \left[1 + (H/L)^2\,(d\overline{z}/d\overline{x})^2_{\overline{y}_f} + (H/L)^2\,(d\overline{y}/d\overline{x})^2_{\overline{y}_f}\right]^{1/2} \tag{2}$$

$$\beta = \left[1 + (H/L)^2\,(d\overline{z}/d\overline{x})^2_{\overline{y}_f}\right]^{1/2} \tag{3}$$

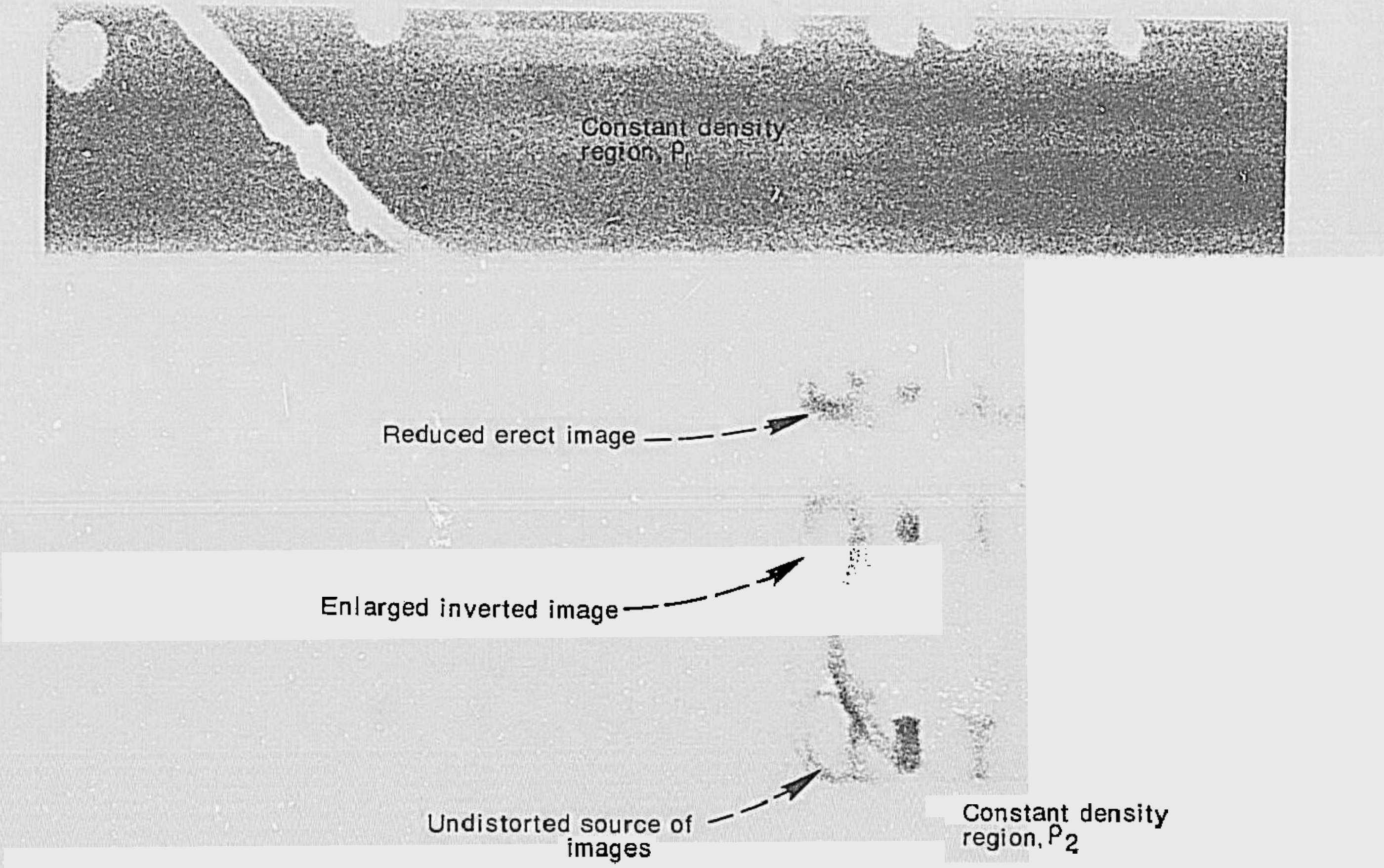

Figure A-2.—Multiple images. Photo P801-D-77870

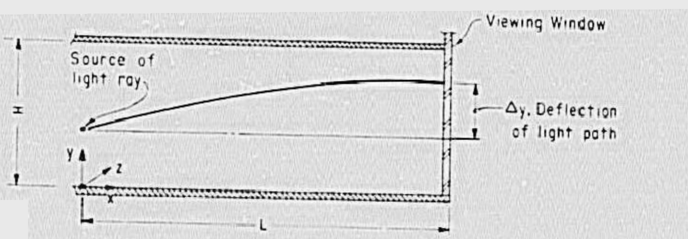

Figure A-3.—Definition sketch of ray path.

The solution of equation (1a) is

$$\bar{x} = 1.0 - \frac{H}{L} \int_{\bar{y}}^{\bar{y}_f} \left[\frac{d\bar{y}}{\alpha^2 N/N_f - \beta^2} \right]^{1/2} \qquad (4)$$

The boundary conditions used with equation (4) are different from those used by Mowbray. He assumed a test section was contained between two parallel walls, one wall transparent and the other translucent. A line at approximately 45° with the horizontal was scribed on the inside of the transparent wall. Parallel light rays, generated by a suitable lens system, passed through the transparent wall to cast an image on the inside of the translucent wall.

The formulation of equation (4) assumes that the light rays emanate from a slender rod located in the fluid. The rod is also inclined at an angle of about 45°. The boundary conditions necessary for this assumption complicate the interpretation of the results. However, an expensive lens system is not required if the model depth is large. In addition, with their formulation, two-dimensional rotational flow can be studied.

Refractive indices.—For a saline solution, the index of refraction n at 18 °C for a wave length of 589.3 nanometres (yellow band near sodium) is given approximately by

$$n = 1.33317 + 0.1397G \tag{5}$$

where G is the concentration in grams of NaCl per millilitre of solution.

For temperature stratification, the index of refraction is given approximately by

$$n = 1.33467 - 0.0000841T \tag{6}$$

where T is temperature in °C.

Combining temperature and salinity into one equation gives:

$$n = 1.33467 - 0.0000841T + 0.1397G \tag{7}$$

Once the refractive index of the fluid at a point is known, the relative density at that point can be computed from the equation:

$$\sigma = \left(\sigma_o - \sigma_1\right)\left(\frac{\bar{n} - \bar{n}_1}{1 - n_1}\right) + \sigma_1 \tag{8}$$

The relative density σ is defined as:

$$\sigma = \rho / \rho_{4^\circ C} \tag{9}$$

In practice, both the relative density and refractive index should be measured using the salt and water actually used in the model. It has been found that the measured values can deviate from the handbook values, especially if the salt contains additives and if the water is not distilled, figures A-4 and A-5.

Computer Program

The fully documented computer program that computes the terms for the basic equation (4) is included at the end of this appendix. A definition sketch of the required parameters (fig. A-10) and a sample photograph (fig A-11) showing how the x and y values were measured are also included. The computer output is based upon the measured values.

Design of Measuring System

Maximum deflection of light ray.—To obtain accurate results, the maximum deflection of the ray path should be significant with respect to the thickness of the gradient layer. In general, maximum deflections of about 0.2 H to 0.4 H will give reasonably accurate results. The maximum deflection depends upon the magnitude of the density gradient, the shape of the gradient, and the relative travel length of the ray path. The maximum deflections were obtained for a linear profile, figure A-6, and a profile caused by molecular diffusion between two layers, figure A-7.

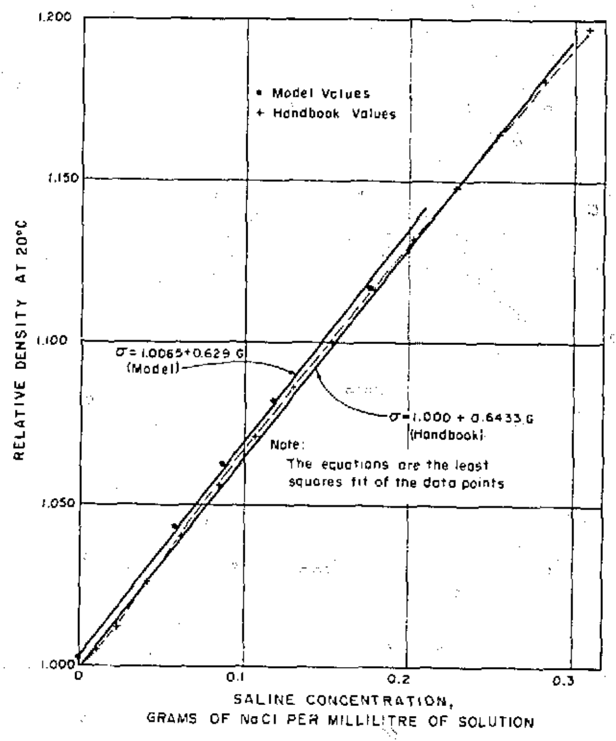

Figure A-4.—Measured relative density.

The curves shown on figures A-6 and A-7 can be used to estimate the maximum deflections to be obtained for a given magnitude of gradient and a given ray path length to gradient thickness ratio.

Recording camera criteria.—The location, aperture (f-stop), and focal length of the recording camera should be carefully chosen, figure A-8.

The camera should be placed as far from the viewing window as possible to minimize the offset, *A*. If the offset is large, then the density distribution near the edges of the gradient cannot be accurately determined. In general, the ratio *D/R* (fig. A-8) should not be less than 50. To keep the image sharp, the aperture of the camera should be as small as possible. This is equivalent to using large values for the f-stop. Finally, the focal length of the lens should be as large as possible to maximize the size of the image on the film plate. The focal length *F* required to produce a given image height *H* can be approximated from:

$$F = \frac{DB/H}{1 + B/H}$$

where *B* is the desired image height.

Density Gradient Over Entire Depth

If the density gradient occupies only a portion of the depth, it is not difficult to determine the origin of the light rays on the rod. For example, in figure A-1 the location of the undistorted rod can be determined by connecting the straight portion of the rod in the two constant density portions of the depth.

When the gradient fills the depth, the undistorted location of the rod can no longer be determined from a single photograph. Instead, the following procedure is recommended. First, it is necessary to photograph the distorted rod. At the completion of the experiments, the fluid is mixed to eliminate all density gradients. The rod is then

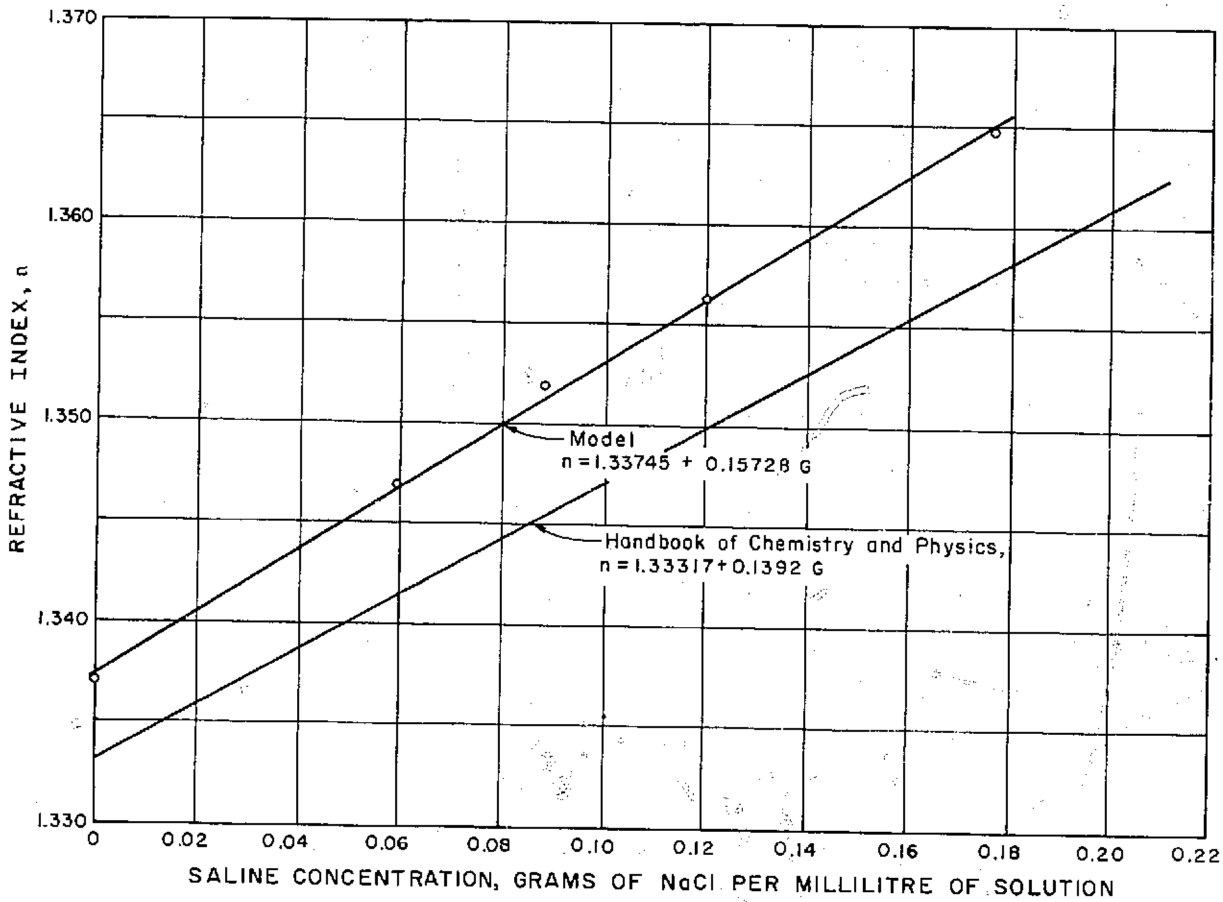

Figure A-5.—Measured refractive index.

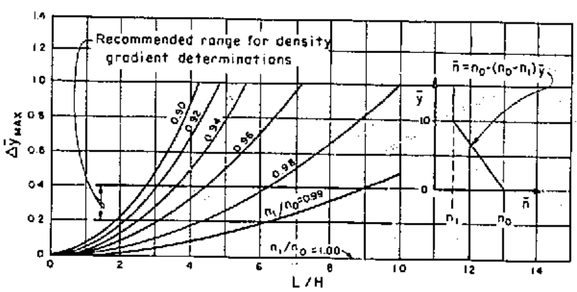

Figure A-6.—Maximum deflection of ray path with linear density profile.

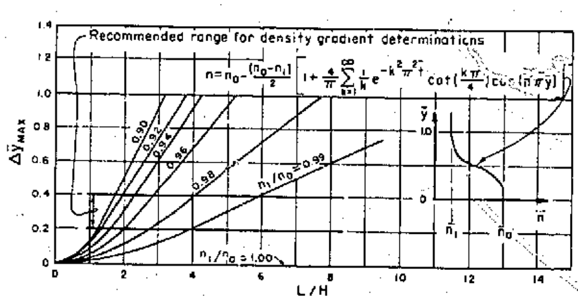

Figure A-7.—Maximum deflection of ray path with diffused density profile.

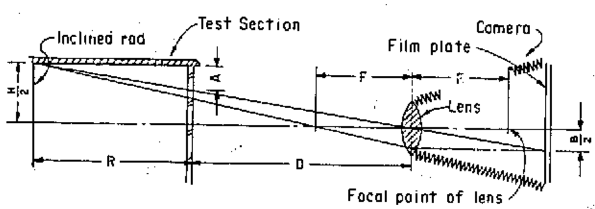

Figure A-8.—Light paths to camera.

rephotographed. By making a print of the two negatives superimposed, it is possible to obtain an image of both the distorted and the undistorted rod, figure A-9.

The superposition of the two negatives is facilitated if a target is included in the photographs. Since the distortion is only in the vertical plane, the width of the target in the two photographs must be identical. Targets were drawn on the wall of the tank and were also placed in the plane of the rod. Those placed at the rod gave sharper images, but they tended to disturb the density gradient if extreme care was not exercised during their placement.

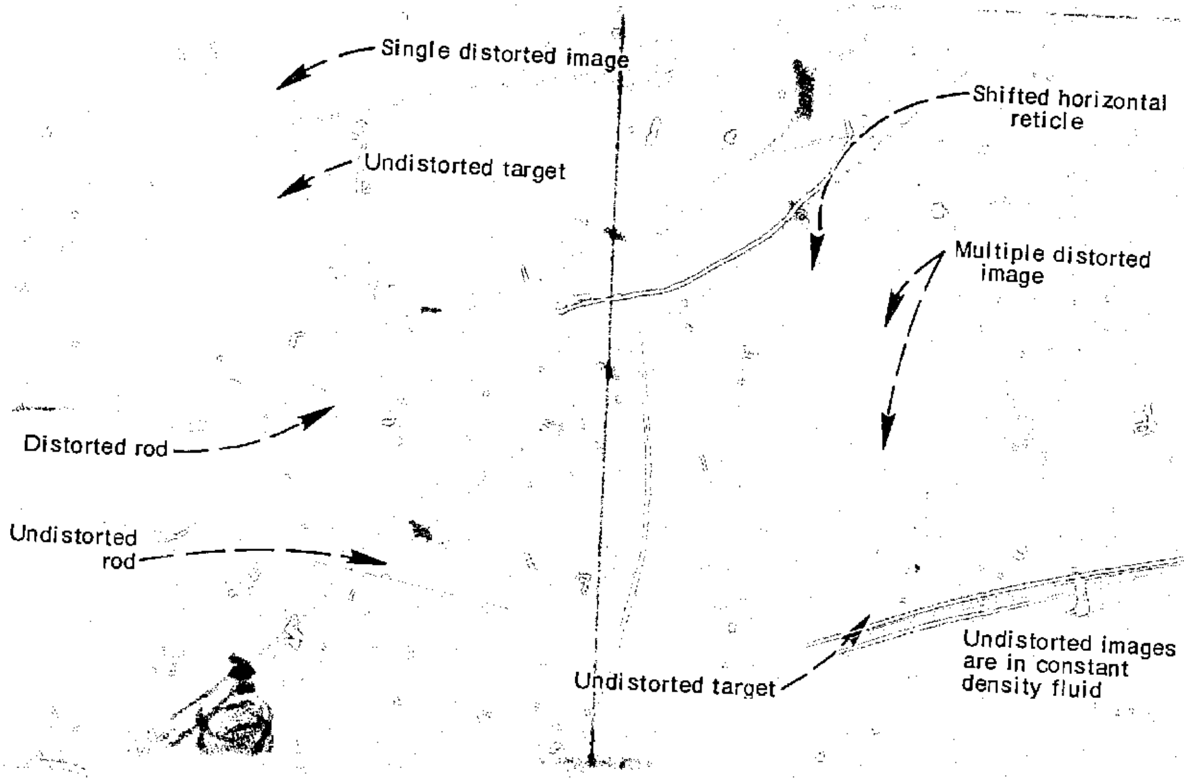

Figure A-9.—Superposition of image in constant density fluid with image in density gradient. Photo P801-D-77861

CONCLUSIONS

During the use of the optical method for measuring stratified density gradients, the following conclusions were noted:

1. The method provides a photographic record that is continuous with respect to height.

2. To determine density gradients, cumbersome numerical integration is required. Therefore, a computer program greatly reduces analysis time.

3. The method does not noticeably disturb stratified flow.

4. Measurement of refractive indexes was necessary because of impurities in the water and additives in the commercially available salt.

5. The distance from the window wall to the rod should be selected so that maximum image deflection is between 0.2 and 0.4 of the height of image.

6. Careful referencing and scaling on the observation window are required so that the actual location and size of the rod can be accurately determined relative to the distorted photographed image of the rod.

7. The camera must be carefully set with respect to the rod and window regarding distance, alinement, and elevation.

8. The camera should be placed as far from the viewing window as possible to minimize parallax. Parallax is negligible when the ratio of the camera distance from the wall to the rod distance from the wall is greater than 50.

9. The focal length of the camera lens should be as large as possible to produce a sufficiently large image so that rod deflections can be measured accurately.

BUREAU OF RECLAMATION ENGINEERING COMPUTER SYSTEM
****

CLASSIFICATION - HYDRAULICS

PROGRAM DESCRIPTION - PRO 1532 - DENGRA
****

PROGRAM BY

H.T. FALVEY

DOCUMENTATION BY

H.T. FALVEY

UNITED STATES DEPARTMENT OF THE INTERIOR
BUREAU OF RECLAMATION
DIVISION OF GENERAL RESEARCH
HYDRAULICS BRANCH
ENGINEERING AND RESEARCH CENTER
DENVER, COLORADO

77/07/12.

PROGRAM DESCRIPTION - PRO 1532 - DENGRA

PROGRAM TITLE

OPTICAL MEASUREMENT OF LIQUID DENSITY GRADIENT

PURPOSE

TO MEASURE THE INSITU DENSITY GRADIENT OF A STRATIFIED LIQUID

METHOD

BASED ON THE REFRACTION OF A LIGHT RAY WHEN IT PASSES THRU A DENSITY GRADIENT. THE PROGRAM INTEGRATES THE FIRST DERIVATIVE OF THE LIGHT PATH FROM A KNOWN POINT IN THE LIQUID TO THE WALL OF THE CONTAINER. THE REFRACTIVE INDEX OF THE FLUID IS AJUSTED UNTIL THE EMERGENT RAY MATCHES THE OBSERVED DISTORTION. THEORY BY D.E.MOWBRAY, JOURNAL FLUID MECHANICS, VOL 27, PART 3, 1967.

INPUT-OUTPUT

THE INPUT CONSISTS OF:

LENGTH OF LIGHT PATH, THICKNESS OF INTERFACE, 26 LIGHT RAY EMERGENCE POINTS, SCALE FACTOR TO CONVERT PHOTO MEASUREMENTS TO REAL DIMENSIONS, NUMBER OF INCREMENTS ON INTEGRATED LIGHT PATH, REFRACTIVE INDEX OF LOWER FLUID LAYER, 26 LIGHT RAY BEGINNING POINTS.

THE OUTPUT CONSISTS OF:

THE REAL HEIGHT, THE REFRACTIVE INDEX AT THAT HEIGHT, SPECIFIC GRAVITY AT THAT HEIGHT

LIMITATIONS

THE RELATIONSHIP BETWEEN DENSITY AND REFRACTIVE INDEX OF FLUID MUST BE KNOWN. THE PATH MUST HAVE A SINGLE EMERGENCE POINT. THE PROGRAM REQUIRES SUBROUTINES 1532-ABINT AND 1532-SIMSOL

BUREAU OF RECLAMATION ENGINEERING COMPUTER SYSTEM
****

CLASSIFICATION - HYDRAULICS

USER'S MANUAL - PRO 1532 - DENGRA
****

PROGRAM BY

H.T. FALVEY

DOCUMENTATION BY

H.T. FALVEY

UNITED STATES DEPARTMENT OF THE INTERIOR
BUREAU OF RECLAMATION
DIVISION OF GENERAL RESEARCH
HYDRAULICS BRANCH
ENGINEERING AND RESEARCH CENTER
DENVER, COLORADO

77/07/12.

DISCLAIMER STATEMENT

COMPUTER PROGRAMS DEVELOPED BY THE BUREAU OF RECLAMATION ARE SUBJECT TO THE FOLLOWING CONDITIONS: CONSULTING SERVICE AND ASSISTANCE WITH CONVERSION CANNOT BE PROVIDED. THE PROGRAMS HAVE BEEN DEVELOPED FOR USE AT THE "USBR" AND NO WARRANTY AS TO ACCURACY, USEFULNESS, OR COMPLETENESS IS EXPRESSED OR IMPLIED.

PERMISSION IS GRANTED TO REPRODUCE OR QUOTE FROM THE PROGRAM; HOWEVER, IT IS REQUESTED THAT CREDIT BE GIVEN TO THE BUREAU OF RECLAMATION, U.S. DEPARTMENT OF INTERIOR, AS THE OWNER.

PROGRAM TITLE

DENSITY DETERMINATION IN A STRATIFIED FLUID.

GENERAL INFORMATION

THE LIGHT PATH THROUGH A STRATIFIED FLUID OBEYS FERMAT'S LAW OF STATIONARY TRANSIT TIME. THE PATH TAKEN BY A LIGHT RAY IS ONE WHICH MINIMIZES THE TRAVEL TIME. SINCE THE SPEED OF LIGHT IS INVERSELY PROPORTIONAL TO THE FLUID DENSITY, THE SHORTEST TIME PATH TENDS TO BE ONE WHICH TENDS TO PASS THROUGH THE LESS DENSE FLUID. THUS, A STRAIGHT LINE VIEWED THROUGH A DENSITY GRADIENT APPEARS TO BE CURVED. ABOVE AND BELOW THE GRADIENT THE LINE IS STRAIGHT.

DATA FROM PHOTOGRAPHS OF THE INCLINED ROD ARE USED TO DETERMINE THE ACTUAL DEFLECTIONS. THE PROGRAM INTEGRATES THE DIFFERENTIAL EQUATIONS WHICH DESCRIBE THE LIGHT PATH TO OBTAIN A COMPUTED DEFLECTION. THE REFRACTIVE INDEX AT 26 EQUALLY SPACED POINTS IN THE GRADIENT IS ADJUSTED UNTIL THE COMPUTED DEFLECTION MATCHES THE MEASURED DEFLECTION. FROM THE COMPUTED REFRACTIVE INDICES THE RELATIVE DENSITY AND SPECIFIC GRAVITY OF THE FLUID ARE COMPUTED.

IN GENERAL THE RECORDING CAMERA SHOULD BE LOCATED A DISTANCE FROM THE VIEWING WINDOW OF AT LEAST 50 TIMES THE DISTANCE OF THE INCLINED ROD FROM THE WINDOW. IF THE DISTANCE IS CLOSER, OR IF THE FLUID IS UNSTABLE (DENSITY INCREASING IN AN UPWARD DIRECTION), LARGE ERRORS IN THE COMPUTED DENSITY GRADIENT WILL OCCUR. IN ADDITION, THE F-STOP OF THE CAMERA SHOULD BE AS LARGE AS POSSIBLE.

INPUT

NINE CARDS ARE NEEDED TO INPUT THE DATA FOR EACH ANALYSIS. THESE CARDS CONSIST OF A TITLE CARD, A MODEL GEOMETRY CARD, A FLUID PROPERTIES CARD, AND SIX ROD COORDINATE CARDS.

TITLE CARD

THE TITLE OF THE RUN OR THE NUMBER OF THE PHOTOGRAPH BEING ANALYZED SHOULD BE CENTERED IN COLUMNS 9-63.

MODEL GEOMETRY CARD

THE MODEL GEOMETRY CARD IS FILLED OUT AS FOLLOWS:

COLUMNS

1- 8 A - DEPTH OF TEST SECTION

9-16 R - ROD TO AIR SIDE OF VIEWING WINDOW

17-24 D - AIR SIDE WINDOW TO CAMERA LENS

25-32 RAD - RADIUS OF CURVATURE OF VIEWING WINDOW

33-40 TW - THICKNESS OF VIEWING WINDOW

41-48 RIP - REFRACTIVE INDEX OF VIEWING WINDOW

49-56 CL - HEIGHT OF LENS CENTERLINE / A

57-80 BLANK

ALL DIMENSIONS MUST BE IN THE SAME UNITS (IE, MM, INCHES, OR FEET AND TENTHS).

FLUID PROPERTIES CARD

THE FLUID PROPERTIES CARD IS FILLED OUT AS FOLLOWS:

COLUMNS

1- 8 YS - DISTANCE FROM FLOOR OF TEST SECTION TO BOTTOM OF GRADIENT

9-16 YB - DISTANCE FROM FLOOR OF TEST SECTION TO TOP OF GRADIENT

17-24 TEMP- TEMPERATURE OF FLUID IN DEGREES CELSIUS

25-32 CON - MAXIMUM SALT CONCENTRATION IN GRAMS NACL/MILLILITER SOLUTION

33-80 BLANK

THE DIMENSIONS MUST BE CONSISTENT WITH THOSE USED ON THE MODEL GEOMETRY CARD.

ROD COORDINATE CARDS

THE THICKNESS OF THE DENSITY GRADIENT IS DIVIDED INTO 25 EQUAL INCREMENTS. THIS FORMS AN ARBITRARY SCALE WHICH RUNS BETWEEN 0 AT THE BOTTOM OF THE GRADIENT TO 1.0 AT THE TOP. ALL X AND Y COORDINATES ARE MEASURED WITH THIS SCALE. X COORDINATES ARE MEASURED RELATIVE TO A VERTICAL CENTERLINE PASSING THROUGH THE ROD. POSITIVE VALUES OF X ARE MEASURED TO THE RIGHT OF THE CENTERLINE. THE X COORDINATES CORRESPOND TO THE POINTS WHERE THE EQUAL INCREMENT LINES CUT THE IMAGE OF THE ROD. THE Y COORDINATES CORRESPOND TO THE ELEVATION OF THE ROD AT WHICH THE X COORDINATE OF THE IMAGE ORIGINATED.

THE CARDS ARE FILLED OUT IN FIELDS OF 8 DIGITS AS FOLLOWS:

FIRST CARD

COLUMNS

1-80 X - VALUES 1 THRU 10 OF THE X COORDINATES

SECOND CARD

COLUMNS

1-80 X - VALUES 11 THRU 20 OF THE X COORDINATES

THIRD CARD

COLUMNS

1-48 X - VALUES 21 THRU 26 OF THE X COORDINATES

49-80 Y - VALUES 1 THRU 4 OF THE Y COORDINATES

FOURTH CARD

COLUMNS

1-80 Y - VALUES 5 THRU 14 OF THE Y COORDINATES

FIFTH CARD

COLUMNS

1-80 Y - VALUES 15 THRU 24 OF THE Y COORDINATES

SIXTH CARD

COLUMNS

1-16 Y - VALUES 25 AND 26 OF THE Y COORDINATES

17-80 BLANK

SUBMITTAL INSTRUCTIONS

THE NUMBER OF SETS OF DATA SUBMITTED IS NOT LIMITED. HOWEVER, EACH SET MUST CONSIST OF NINE CARDS IN THE ORDER GIVEN IN THE INPUT CHAPTER. THE LAST CARD MUST HAVE A 6/7/8/9 MULTIPUNCHED IN COLUMN 1.

OUTPUT

THE OUTPUT CONSISTS OF A SET OF DATA WHICH CAN BE USED FOR DETAILED ANALYSIS AND THE FOLLOWING MORE PERTINENT DATA:

1) A SET OF Y VALUES THROUGH THE GRADIENT (Y=0. IS AT THE FLOOR),

2) THE CORRESPONDING REFRACTIVE INDICES,

3) SPECIFIC GRAVITIES OF THE FLUID, AND

4) RELATIVE DENSITIES. THE RELATIVE DENSITY IS DEFINED AS THE SPECIFIC GRAVITY AT A PARTICULAR Y VALUE DIVIDED BY THE SPECIFIC GRAVITY AT Y= 0.

SPECIAL OPERATING REQUIREMENTS

NONE

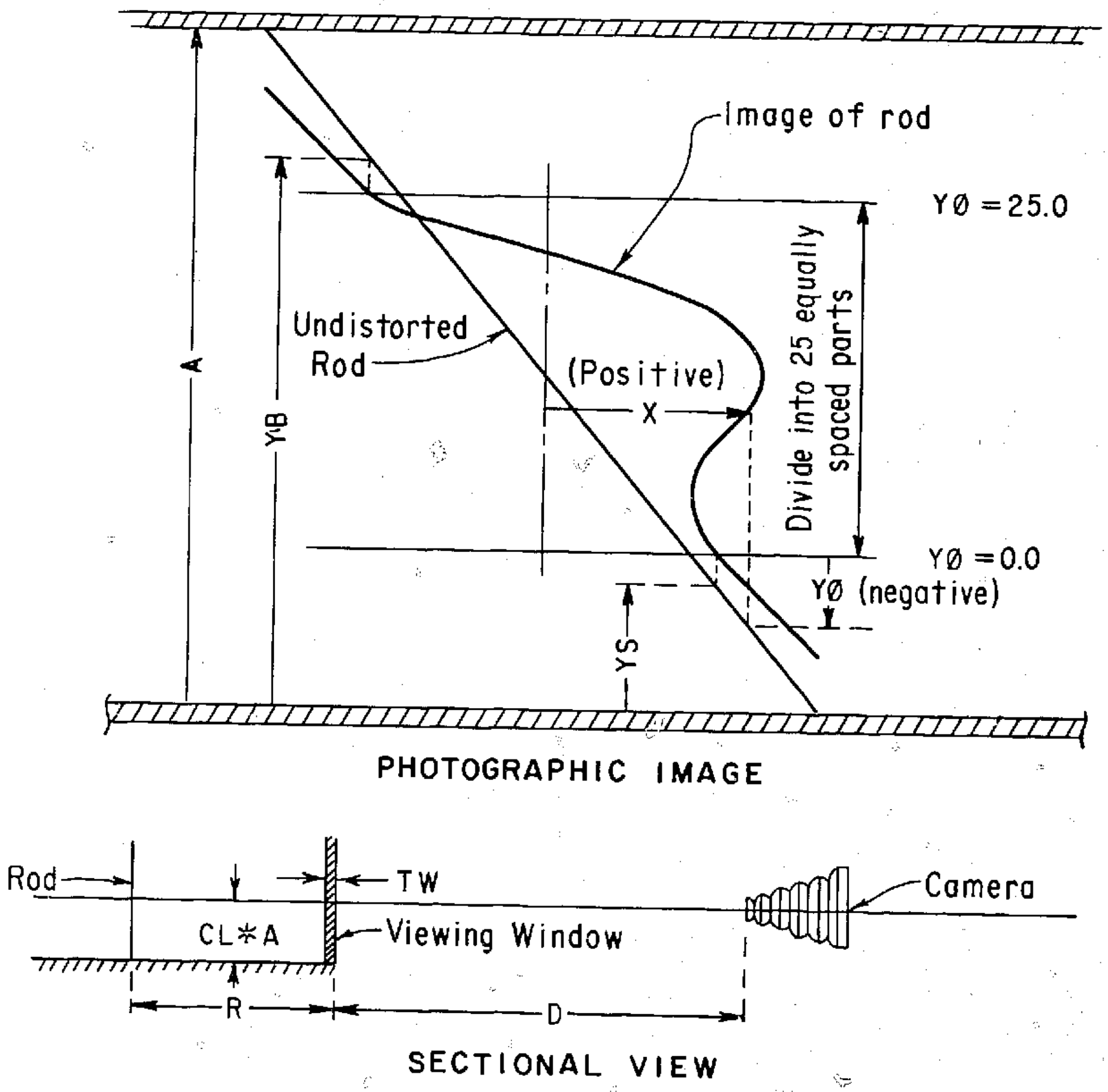

Figure A-10.—Definition sketch.

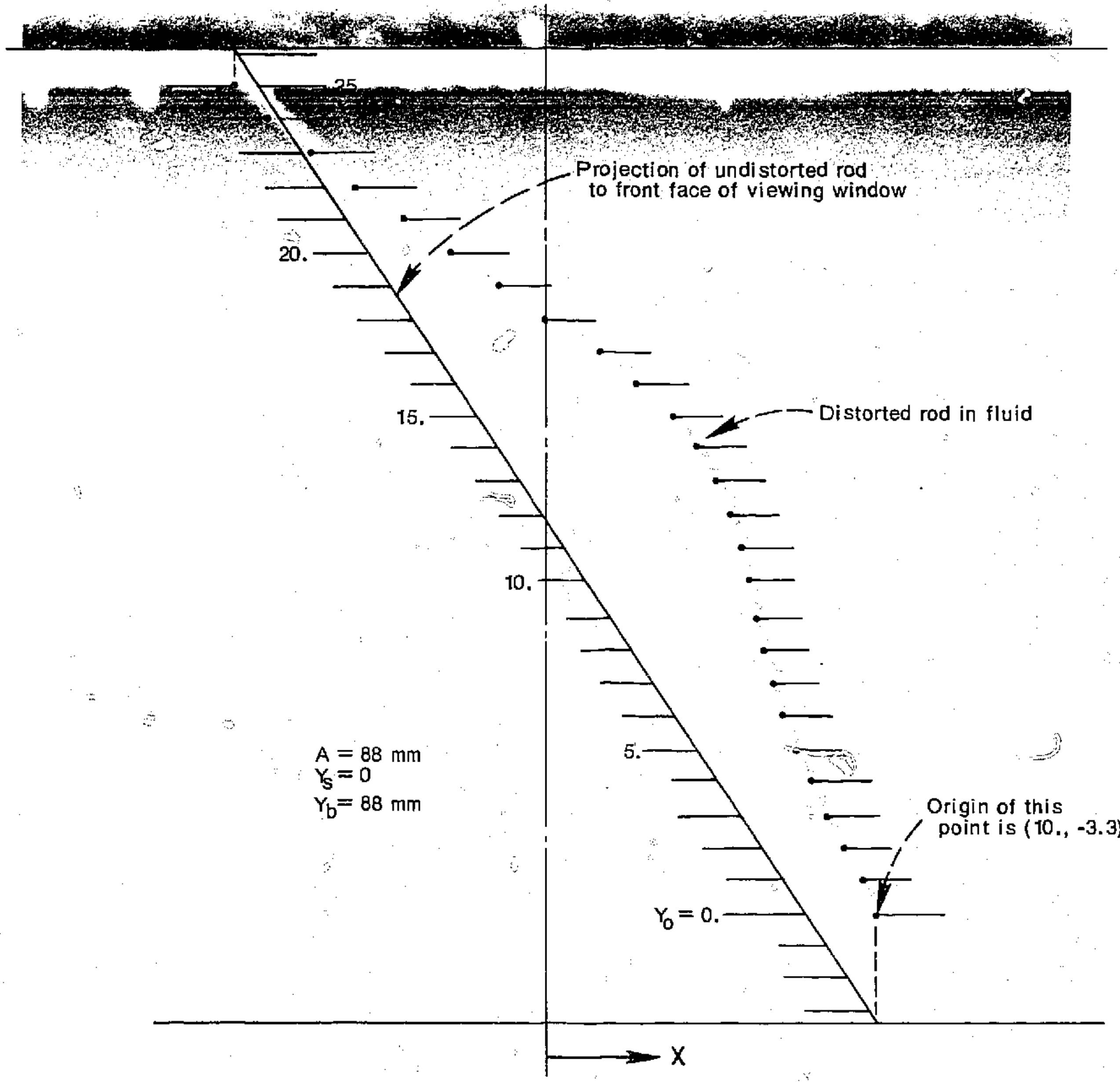

Figure A-11.—Sample rod photograph. Photo P801-D-77871

FORTRAN LISTING

```
      PROGRAM HFDEN(INPUT,OUTPUT,TAPE2=INPUT,TAPE3=OUTPUT)
C     PROGRAM TO DETERMINE THE DENSITY GRADIENT OF A STRATIFIED LIQUID
C     USING FERMATS PRINCIPLE OF LIGHT REFRACTION
C
      DIMENSION DELY(26),RIN(26),RN(10),YO(26),RI(26)
     1,YD(26),XE(26),YE(26),TIT(11),SG(26),RD(26),AR(26)
C
C     INPUT TO PROGRAM
C
    1 READ(2,2)(TIT(I),I=1,11),A,R,D,RAD,TW,RIP,CL,YS,YB,TEMP,CON,
     1(XE(I),I=1,26),(YO(I),I=1,26)
    2 FORMAT(11A5/7F8.4/4F8.4/10F8.4/10F8.4/10F8.4/10F8.4/10F8.4/2F8.4)
      NO= EOF(2)
      IF(NO.NE.0)CALL EXIT
      WRITE(3,20)(YO(I),I=1,26),(XE(I),I=1,26),A,R,D,RAD,TW
   20 FORMAT(1H1/25X,38HORIGIN OF RAYS EXITING AT EQUAL DEPTHS/
     12(8X,9F8.4/),8X,8F8.4/28X,33HDISTANCE FROM VERTICAL CENTERLINE/
     22(8X,9F8.4/),8X,8F8.4/9X,3HA =,F8.2,3X,3HR =,F8.2,3X,3HD =,F8.2,
     33X,5HRAD =,F8.2,3X,4HTW =,F8.2//
     48X,70H    YO          X1          X2          RI         RIN        DELN
     5   DELY    /)
C
C     INITIALIZATION
C
      RFIF= 1.33871-.0000841*TEMP
      RFIS= RFIF+.00252*CON
      SF= (YB-YS)/(A*(YO(26)-YO(1)))
      HL= A/(R-TW)
      YEE= YB/A
      YSS= YS/A
      YD(1)= YSS+SF*ABS(YO(1))
      GAMA= 3.14159*(YSS+(YEE-YSS)/2.-YD(1))/(YEE-YSS)
      RI(1)= 1.+(1.-RFIF/RFIS)*(SIN(GAMA)-1.)/2.
      YD(26)= YEE-SF*ABS(YO(26)-25.)
      GAMA= 3.14159*(YSS+(YEE-YSS)/2.-YD(26))/(YEE-YSS)
      RI(26)= 1.+(1.-RFIF/RFIS)*(SIN(GAMA)-1.)/2.
      RIN(26)= RI(26)*RI(26)
      C= (CL-YD(1))/(RFIS*RI(1)*SQRT((D/A)*(D/A)+(CL-YD(1))*(CL-YD(1))))
      YE(1)= C/SQRT(1.-C*C)
      AW= ATAN(XE(1)*SF/(D/A))
      AT= ATAN(XE(1)*SF/SQRT(RAD*RAD-XE(1)*SF*XE(1)*SF))
      ST2= SIN(AW+AT)/(RFIS*(1.-(1.-RFIF/RFIS)*SIN(1.57079*(YD(1)-YSS)
     1/(YEE-YSS))))
      T2= ATAN(ST2/SQRT(1.-ST2*ST2))
      DEL= T2-AT
      XE(1)= SIN(DEL)/SQRT(1.-SIN(DEL)*SIN(DEL))
      ALPH= 1.+YE(1)*YE(1)+XE(1)*XE(1)
      RISAV= RI(1)
      RMAX= 1.0
      DO 22 NI=1,10
      RIN(1)= RI(1)*RI(1)
      RHEQ= SF*ABS(YO(1))*RI(1)/(ALPH*(1.-RIN(1)))*
     1(SQRT((1.-RIN(1))*ALPH+YE(1)*YE(1)*RIN(1))-YE(1)*RI(1))
      EQLH= 0.5/HL
      DIFF= ABS((RHEQ-EQLH)/EQLH)
      IF(DIFF.LE.0.01)GO TO 18
      IF(RHEQ.LT.EQLH)DELR=(RMAX-RISAV)/2.
```

```
      IF(RHEQ.GT.EQLH)DELR= (-.5)*ABS(DELR)
      RISAV= RI(1)
      RI(1)= RISAV+DELR
      IF(RI(1).GE.RMAX)RI(1)= RMAX
   22 CONTINUE
C
C     COMPUTE DIMENSIONLESS Y VALUES
   18 YORIG= YO(1)
      YO(1)= YSS
      CCA= YEE-YD(1)-SF*(YO(26)-25.)
      DO 3 IN=1,25
      RC= IN
      RC= RC/25.
      YD(IN+1)= YD(1)+RC*CCA
      YO(IN+1)= YO(1)+SF*(YO(IN+1)-YORIG)
      PHI= ATAN((.5-YD(IN+1))/(D/A))
      PHIP= SIN(PHI)/RIP
      DELP= (TW/A)*SIN(PHIP)/SQRT(1.-SIN(PHIP)*SIN(PHIP))
      DELY(IN)= YD(IN+1)-DELP-YO(IN+1)
      GAMA= 3.14159*(YSS+(YEE-YSS)/2.-YD(IN+1))/(YEE-YSS)
      B= RFIS*(1.+(1.-RFIF/RFIS)*(SIN(GAMA)-1.)/2.)
      C= (CL-YD(IN+1))/(B*SQRT((D/A)*(D/A)+(CL-YD(IN+1))*
     1(CL-YD(IN+1))))
      YE(IN+1)= C/SQRT(1.-C*C)
      AW= ATAN(XE(IN+1)*SF/(D/A))
      AT= ATAN(XE(IN+1)*SF/SQRT(RAD*RAD-XE(IN+1)*SF*XE(IN+1)*SF))
      ST2= SIN(AW+AT)/B
      T2= ATAN(ST2/SQRT(1.-ST2*ST2))
      DEL= T2-AT
      XE(IN+1)= SIN(DEL)/SQRT(1.-SIN(DEL)*SIN(DEL))
    3 CONTINUE
C
C     MAIN PROGRAM
C
      DO 12 I=2,25
      IN= I-1
      ALPH= 1.+XE(I)*XE(I)+YE(I)*YE(I)
      BETA= 1.+XE(I)*XE(I)
      DELN= 2.0*((DELY(I-1)-YE(I))*HL)**2
      IF(I.EQ.3)DELN= RIN(1)-RIN(2)
      IF(I.GE.4)DELN= 3.*RIN(I-2)-2.*RIN(I-1)-RIN(I-3)
      IF(DELN.LE.0.)DELN=DELN1/2.
      NCT= 0
      NH= 2
    4 RIN(I)= RIN(I-1)-DELN
      FN= RIN(I)
      YN= FN
C
C     INTEGRATION OF LIGHT PATH
   15 DYX= DELY(I-1)/10.
C     COMPUTATION OF N RATIOS ALONG LIGHT PATH
      YF= YO(I)
      DO 8 M=1,10
      RM= M
      Y= YF-RM*DYX
      YNSAV= YN
C
```

```
C     DETERMINATION OF REFRACTIVE INDEX RATIO AT Y USING LINEAR INTERP
      DO 7 N=1,IN
      NK= I-N
      NKT= I-N+1
      YTST= YD(NK)
      IF(Y.GE.YTST)GO TO 6
    7 CONTINUE
    6 YN= RIN(NK)-(Y-YD(NK))*(RIN(NK)-RIN(NKT))/(YD(NKT)-YD(NK))
      IF(Y.LE.YD(1))YN=1.
      YX= YN*ALPH/FN-BETA
      IF(YX.LE.0.)GO TO 14
      RN(M)= 1./SQRT(YX)
      GO TO 8
   14 RN(M)= RN(M-1)
      YN= YNSAV
      WRITE(3,100)RN(M),YN,FN,DELN,Y,YF,YO(I)
    8 CONTINUE
C
C     COMPUTATION OF FIRST INTERVAL
      BP= 0.1*DELY(I-1)*(ALPH-BETA)/(ALPH*(YN/FN-1.))
      IF(ABS(YE(I)).GE.(.00001))X1= .2*DELY(I-1)/(YE(I)+1./RN(1))
      IF(ABS(YE(I)).GE.(.00001))GO TO 17
      IF(BP.LE.ABS(DELY(I-1)).AND.DELY(I-1).LE.(0.))
     1COEF= 2.*ABS(DELY(I-1))/(YE(I)   +SQRT(YN*ALPH/FN-BETA))
      IF(BP.LE.ABS(DELY(I-1)).AND.DELY(I-1).LE.(0.))GO TO 16
      AP= SQRT((ALPH*YN/FN-BETA)/(.1*DELY(I-1)+BP))
      X1= 2.*(SQRT(.1*DELY(I-1)+BP)-SQRT(BP))/AP
      IF(YE(I).LE.(0.).AND.DELY(I-1).GT.(0.))X1= 2.*(SQRT(.1*DELY(I-1)
     1+BP)+SQRT(BP))/AP
      IF(DELY(I-1).LT.(0.))GO TO 5
C
C     COMPUTATION OF SECOND INTERVAL USING NEWTON-COTES COEFFICIENTS
C     AT EQUAL INTERVALS
   17 X2= 0.9*DELY(I-1)*(.0319*(RN(1)+RN(10))+.1757*(RN(2)+RN(9))
     1+.0121*(RN(3)+RN(8))+.2159*(RN(4)+RN(7))+.0645*(RN(5)+RN(6)))
      COEF= X1+X2
      GO TO 16
    5 X11= 2.*SQRT(BP)/AP
      RLH= 1./HL
      IF(X11.GE.RLH)COEF= 2.*(SQRT(BP)-SQRT(DELY(I-1)+BP))/AP
      IF(X11.LT.RLH)COEF= X11+2.*SQRT(DELY(I-1)+BP)/AP
      YCK= YD(I)+BP
      IF(YCK.GE.YEE)COEF= DELY(I-1)*RI(I)*RFIF/(B*YE(I)*RI(26))
   16 X= ABS(HL*COEF)
C
C     TESTS TO DETERMINE IF DO LOOP IS SATISFIED AND RECOMPUTE DELN
      IF(ABS(1.-X).LE.0.001)GO TO 11
      NCT= NCT+1
      DIF=ABS(RIN(I)-RIN(26))
      IF(DIF.LE.(.0001))GO TO 11
      IF(NCT.GE.10)GO TO 9
      IF(NCT.EQ.1)GO TO 200
      IF(NH.EQ.1)GO TO 150
      IF((X.LE.1.).AND.(DSAV.LE.0.))GO TO 200
      IF((X.GE.1.).AND.(DSAV.GE.0.))GO TO 200
      DSAV= ABS(DSAV)
  150 IF(X.LE.1.)DELN1= DELN-DSAV/2.
```

```
      IF(X.GE.1.)DELN1= DELN+DSAV/2.
      DCK= RIN(I-1)-RIN(26)
      IF(DELN1.GE.DCK)DELN1= DCK
      IF(DELN1.LE.0.)DELN1= 0.
      DSAV= ABS(DELN1-DELN)
      DELN= DELN1
      NH= 1
      GO TO 4
  200 IF(X.LE.1.)DELN1= 0.5*DELN
      IF(X.GE.1.)DELN1= 2.0*DELN
      DCK= RIN(I-1)-RIN(26)
      IF(DELN1.GE.DCK)DELN1= DCK
      IF(DELN1.LE.0.)DELN1= 0.
      DSAV= DELN1-DELN
      DELN= DELN1
      GO TO 4
    9 WRITE(3,10)X,DELN,(YD(N),RIN(N),N=1,I)
   10 FORMAT(1H1/10X,48HAFTER 10 TRIES DELN COULD NOT BE MADE TO SATISFY
     1/10X,48HTHE REQUIRED LIMITS ON X. THE LAST VALUES WERE - /
     218X, 2HX=,E10.3, 5X,5HDELN=,E10.3 //17X,33HTHE VALUES COMPUTED THU
     3S FAR ARE  /17X,33H          Y                  N*N          /
     4(22X,F5.2,10X,F7.4))
   11 RI(I)= SQRT(RIN(I))
      WRITE(3,100)YD(I),X1,X2,RI(I),RIN(I),DELN,DELY(I)
  100 FORMAT(8X,7E10.3)
   12 CONTINUE
      RIMAX= RI(25)
      DO 19 NO=1,26
      SG(NO)= 1.00405+4.113*RFIS*(RI(NO)-RIMAX)
      RD(NO)= SG(NO)/SG(1)
      AR(NO)= (RI(NO)-RFIF/RFIS)/(1.-RFIF/RFIS)
   19 CONTINUE
      WRITE(3,13) (TIT(N),N=1,11),HL,(YD(N),RI(N),SG(N),RD(N),AR(N),
     1N=1,26)
   13 FORMAT(1H1,8X,11A5/13X,39HVALUES OF THE REFRACTIVE INDEX FOR H/L=
     1  ,F6.4/11X,48H   Y              N              SG         RD      PCT N /
     2(11X,F5.2,4X,F8.5,4X,F7.4,4X,F7.4,4X,F7.4))
      WRITE(3,23)YEE,YSS
   23 FORMAT(3X//23X,17HTOP OF GRADIENT =,F7.4/22X,
     120HBOTTOM OF GRADIENT =,F7.4/)
      WRITE(3,21)(YE(N),N=1,26),(XE(N),N=1,26),(YD(N),N=1,26),
     1(YO(N),N=1,26)
   21 FORMAT(1H1,/35X,11HDYDZ VALUES/3(8X,8F8.4/),8X,2F8.4/35X,
     111HDXDZ VALUES/3(8X,8F8.4/),8X,2F8.4/35X,11H YD VALUES /3(8X,
     28F8.4/),8X,2F8.4/35X,11H YO VALUES /3(8X,8F8.4/),8X,2F8.4)
      GO TO 1
      END
```

H1683-78

VALUES OF THE REFRACTIVE INDEX FOR H/L= .2963

Y	N	SG	RD	PCT N
.31	.99969	1.0750	1.0000	.9806
.34	.99936	1.0732	.9983	.9595
.36	.99890	1.0706	.9959	.9304
.39	.99838	1.0677	.9932	.8971
.42	.99776	1.0642	.9899	.8577
.44	.99707	1.0603	.9864	.8141
.47	.99631	1.0561	.9824	.7661
.49	.99547	1.0514	.9780	.7124
.52	.99456	1.0463	.9733	.6548
.55	.99363	1.0411	.9685	.5958
.57	.99268	1.0358	.9636	.5360
.60	.99180	1.0309	.9590	.4797
.62	.99094	1.0261	.9545	.4253
.65	.99015	1.0217	.9504	.3752
.67	.98944	1.0177	.9467	.3301
.70	.98884	1.0143	.9436	.2920
.73	.98834	1.0115	.9410	.2602
.75	.98792	1.0092	.9388	.2338
.78	.98760	1.0075	.9372	.2138
.80	.98736	1.0061	.9359	.1982
.83	.98721	1.0053	.9351	.1887
.86	.98711	1.0047	.9346	.1826
.88	.98707	1.0045	.9344	.1798
.91	.98703	1.0043	.9342	.1774
.93	.98699	1.0041	.9340	.1751
.96	.98435	.9893	.9202	.0074

TOP OF GRADIENT = 1.0000

BOTTOM OF GRADIENT = .2455

APPENDIX B

Computer Program to Convert Atmosphere to Equivalent Liquid Density

APPENDIX B

COMPUTER PROGRAM TO CONVERT ATMOSPHERE TO EQUIVALENT LIQUID DENSITY

DETERMINATION OF POTENTIAL DENSITY FROM RADIOSONDE DATA

To properly simulate the atmosphere, the density gradient in the stratified liquid must be identical with the potential density gradient in the atmosphere. The potential density gradient can be computed from:

$$\frac{\rho_{pot}}{(\rho_{pot})_o} = \left(\frac{T_o}{T} \cdot \frac{p}{p_o}\right)^{(k-n)/k} \tag{1}$$

if the polytropic gas constant, n, is known at each elevation for which temperature and pressure data are available from a radiosonde.

In equation (1),

T = temperature
p = pressure
k = isentropic gas constant = 1.4
ρ = density

The subscript o refers to conditions at a reference elevation which can be either sea level or the elevation at a fixed ground location.

Prandtl and Tietjens[1] show that n can be determined from

$$n = \frac{1}{1 + \dfrac{R}{g}\dfrac{dT}{dh}} \tag{2}$$

where

R = gas constant for air,
g = acceleration of gravity, and
$\dfrac{dT}{dh}$ = change in temperature per incremental change in elevation.

The value of R depends upon the constituents of the gas. For dry air, the value of the constant is 287.0 square metres per second squared-kelvin.

However, for moist air the value is dependent upon the amount of water vapor in the air. Haltiner and Martin[2] show that the moist gas constant R_m can be approximated by

$$R_m = R_d(1 + 0.606\, m_r) \tag{3}$$

---

[1] Prandtl, L., and Tietjens, O. G., "Fundamentals of Hydro- and Aerodynamics," Dover Publications, Inc., 1957.
[2] Haltiner, G. J., and Martin, F. L., "Dynamical and Physical Meteorology," McGraw-Hill, 1957.

where

R_d = dry gas constant, and
m_r = mixing ratio.

Jennings and Lewis[3] give values of the mixing ratio as a function of the dewpoint temperature, figure B-1. These values can be approximated over the range of temperatures usually found in the atmosphere by

$$m_r = \exp\left(\frac{T_d + 28.0}{40.5}\right) + 1 \tag{4}$$

where

exp = exponent to base 2.7183
T_d = dewpoint temperature, °C.

The following program uses these relationships to calculate the potential density gradient from radiosonde data. All densities are referenced to the lowest elevation given in the data.

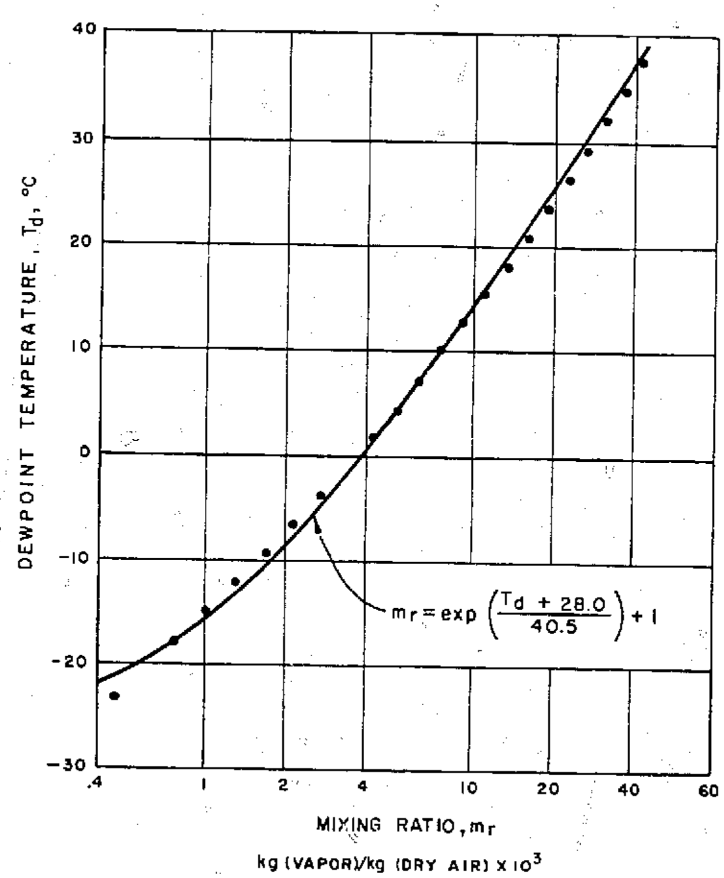

Figure B-1.—Mixing ratio—dewpoint temperature relationships.

[3] Jennings, B. H., Lewis, S. R., "Air Conditioning and Refrigeration," 4th Edition, International Textbook Co., 694 p., 1958.

BUREAU OF RECLAMATION ENGINEERING COMPUTER SYSTEM
****

CLASSIFICATION - HYDRAULICS

PROGRAM DESCRIPTION - PRO 1532 - HATM
****

PROGRAM BY

H.T. FALVEY

DOCUMENTATION BY

H.T. FALVEY

UNITED STATES DEPARTMENT OF THE INTERIOR
BUREAU OF RECLAMATION
DIVISION OF GENERAL RESEARCH
HYDRAULICS BRANCH
ENGINEERING AND RESEARCH CENTER
DENVER, COLORADO

77/07/12.

PROGRAM DESCRIPTION - PRO 1532 - HATM

PROGRAM TITLE

CONVERSION OF ATMOSPHERE TO EQUIVALENT LIQUID DENSITY

PURPOSE

THE ATMOSPHERE CAN BE SIMULATED BY A STRATIFIED LIQUID IF THE DENSITY GRADIENT OF THE LIQUID HAS BEEN PROPERLY FORMULATED. THE PURPOSE OF THE PROGRAM IS TO DETERMINE THE PROPER LIQUID DENSITY GRADIENT USING ATMOSPHERIC DATA AT SELECTED ELEVATIONS.

METHOD

THE PROGRAM DETERMINES THE POLYTROPIC GAS CONSTANT FOR DISCRETE LAYERS OF THE ATMOSPHERE FROM THE INPUT DATA. A SIMPLE MATHEMATICAL EXPRESSION IS USED TO DETERMINE THE VARIATION IN EQUIVALENT LIQUID DENSITY ACROSS THE LAYER.

INPUT-OUTPUT

THE INPUT CONSISTS OF A DESCRIPTIVE TITLE AND A SERIES OF DATA POINTS WHICH DESCRIBE THE ATMOSPHERE AT SEVERAL LEVELS. AT EACH LEVEL THE DATA INPUT CONSISTS OF THE ELEVATION, TEMPERATURE, AND PRESSURE. THE OUTPUT CONSISTS OF THE ELEVATION, POTENTIAL TEMPERATURE, THE POLYTROPIC GAS CONSTANT, AND THE EQUIVALENT OR RELATIVE DENSITY.

LIMITATIONS

THE PROGRAM WILL WORK FOR ANY ATMOSPHERIC CONDITIONS FOUND IN NATURE. THE DATA SETS MUST BE ARRANGED IN ORDER OF INCREASING HEIGHT. THE NUMBER OF DATA SETS CANNOT EXCEED 50.

BUREAU OF RECLAMATION ENGINEERING COMPUTER SYSTEM
****

CLASSIFICATION - HYDRAULICS

USER"S MANUAL - PRO 1532 HFATM
****

PROGRAM BY

H.T. FALVEY

DOCUMENTATION BY

H.T. FALVEY

UNITED STATES DEPARTMENT OF THE INTERIOR
BUREAU OF RECLAMATION
DIVISION OF GENERAL RESEARCH
HYDRAULICS BRANCH
ENGINEERING AND RESEARCH CENTER
DENVER, COLORADO

77/07/12.

DISCLAIMER STATEMENT

COMPUTER PROGRAMS DEVELOPED BY THE BUREAU OF RECLAMATION ARE SUBJECT TO THE FOLLOWING CONDITIONS: CONSULTING SERVICE AND ASSISTANCE WITH CONVERSION CANNOT BE PROVIDED. THE PROGRAMS HAVE BEEN DEVELOPED FOR USE AT THE #USBR# AND NO WARRANTY AS TO ACCURACY, USEFULNESS, OR COMPLETENESS IS EXPRESSED OR IMPLIED.

PERMISSION IS GRANTED TO REPRODUCE OR QUOTE FROM THE PROGRAM; HOWEVER, IT IS REQUESTED THAT CREDIT BE GIVEN TO THE BUREAU OF RECLAMATION, U.S. DEPARTMENT OF INTERIOR, AS THE OWNER.

PROGRAM TITLE

CONVERSION OF ATMOSPHERE TO EQUIVALENT LIQUID DENSITY

GENERAL INFORMATION

THE CONVENTIONAL METHOD FOR SIMULATION OF THE ATMOSPHERE RELIES UPON A RICHARDSON NUMBER SIMILITUDE. CLAUS (LARGE-AMPLITUDE MOTION OF A COMPRESSIBLE FLUID IN THE ATMOSPHERE,J.FLUID MECH.,19,267-289,1964) SHOWED THAT IF THE DISTRIBUTION OF DENSITY IN A LIQUID WAS IDENTICAL WITH THE DISTRIBUTION OF POTENTIAL DENSITY IN THE ATMOSPHERE, THE FLOWS COULD BE SIMILAR.

THIS PROGRAM READS ALL OF THE DATA AND PUTS IT INTO ONE DIMENSIONAL ARRAYS. THE FIRST SET OF DATA POINTS ARE THE REFERENCE VALUES. THE COMPUTATIONS PROGRESS TO SUCCESSIVELY HIGHER LAYERS. THE POLYTROPIC GAS CONSTANTS AND RELATIVE DENSITY ACROSS EACH LAYER ARE DETERMINED. IN ADDITION, THE MORE COMMONLY USED MEASURE OF STABILITY, POTENTIAL TEMPERATURE, IS DETERMINED AT EACH ELEVATION. THE REFERENCE PRESSURE FOR DETERMINING THE POTENTIAL PRESSURE IS 1013 MILLIBARS.

INPUT

THE DATA ARE INPUT IN A FILE CALLED DATA1. THE FILE CONTAINS THE TITLE AND THE ATMOSPHERIC PARAMETERS.

SUBMITTAL INSTRUCTIONS

THE DATA FILE IS PREPARED AS FOLLOWS:

THE TITLE SHOULD BE CENTERED IN A FIELD OF 27 CHARACTERS. THIS FILE CONTAINS THE ELEVATION IN METERS, THE PRESSURE IN MILLIBARS, AND THE TEMPERATURE IN DEGREES CELSIUS, THE DEWPOINT TEMPERATURE IN DEGREES CELSIUS, AND THE WIND DIRECTION AND WIND VELOCITY IN KNOTS. THE LAST ENTRY IN THE DATA MUST BE AN ELEVATION OF -1 METER. THE VARIABLES ARE READ WITH A 6F8.2 FORMAT.

OUTPUT

THE OUTPUT CONSISTS OF THE FOLLOWING:

THE TITLE
HEIGHT (METERS)
TEMPERATURE (DEGREES KELVIN)
POTENTIAL TEMPERATURE (DEGREES KELVIN)
POLYTROPIC GAS EXPONENT
RELATIVE DENSITY

SPECIAL OPERATING REQUIREMENTS

NONE

FORTRAN LISTING

```
      PROGRAM HFATM(DATA1,OUTPUT,TAPE1=DATA1,TAPE3=OUTPUT)
C
C
C      PROGRAM TO CONVERT METEOROLOGICAL DATA TO MODEL DENSITIES
C
C      H= ELEVATION,METERS
C      AP= ATMOSPHERIC PRESSURE,MILLIBARS
C      APREF= REFERENCE PRESSURE
C      T= TEMPERATURE,DEG CELSIUS
C      TR= TEMPERATURE,DEG KELVIN
C      TREF= REFERENCE TEMPERATURE
C      ADN= N VALUE FOR POLYTROPIC GAS
C      RELD= RELATIVE DENSITY IN INCOMPRESSIBLE FLUID
C      POTT= POTENTIAL TEMPERATURE
C      DIR= WIND DIRECTION, AZIMUTH
C      VEL= WIND VELOCITY, KNOTS (INPUT), M/S (OUTPUT)
C      DPT= DEW POINT TEMPERATURE, DEGREES CELSIUS
C
C
C
C     THE DATA IS ENTERED FROM A FILE CALLED DATA1. THE FIRST
C     LINE IS THE TITLE IN AN 9A3 FORMAT. THE NEXT LINES CONSIST
C     OF THE DATA.  EACH LINE CONTAINS THE FOLLOWING:
C     THE HEIGHT IN METERS, THE PRESSURE IN MILLIBARS, THE
C     TEMPERATURE IN DEGREES CELSIUS, THE DEW POINT TEMPERATURE IN
C     DEGREES CELSIUS, THE WIND DIRECTION IN AZIMUTH, AND THE WIND
C     VELOCITY IN KNOTS. (THE OUTPUT VELOCITY IS IN METERS PER
C     SECOND.)  THE INPUT IS READ WITH A 6F8.2 FORMAT.
C     THE LAST LINE IN THE DATA MUST BE SET EQUAL TO A NEGATIVE NUMBER.
C     THIS TELLS THE COMPUTER THAT THE END OF THE DATA HAS
C     BEEN REACHED.  UP TO 100 LINES OF DATA CAN BE ENTERED.
C
C
      DIMENSION H(100),AP(100),T(100),TIT(9),TR(100),ADN(100),RELD(100)
     1,POTT(100),DIR(100),VEL(100),DPT(100)
    3 READ (1,1) (TIT(J),J=1,9)
    1 FORMAT(9A3)
      IF(EOF(1))30,40
   40 WRITE(3,8)(TIT(J),J=1,9)
    8 FORMAT(1H1,19X,10HINPUT DATA//9A3)
      DO 20 J=1,100
      READ (1,2) H(J),AP(J),T(J),DPT(J),DIR(J),VEL(J)
    2 FORMAT(6F8.2)
      WRITE(3,6)H(J),AP(J),T(J),DPT(J),DIR(J),VEL(J)
    6 FORMAT(1X,6F8.2)
      IF(H(J).LT.0.)GO TO 4
   20 CONTINUE
    4 L= J-1
      WRITE(3,7)
    7 FORMAT(1X,/////)
      TREF= T(1)+273.15
      TR(1)= TREF
      RELD(1)= 1.
      VEL(1)= 0.515*VEL(1)
      DO 10 K=2,L
    5 TR(K)= T(K)+273.15
      DELT= TR(K)-TR(K-1)
```

REC-ERC-77-8

ATMOSPHERIC SIMULATION USING STRATIFIED LIQUID MODELS

Engineering and Research Center
Bureau of Reclamation

July 1977

```
      DELH= H(K)-H(K-1)
      SPH= (EXP((DPT(K)+28.)/40.5)+1.)*0.001
      R=  29.266*(1.+0.606*SPH)
      ADN(K)= 1./(1.+R*DELT/DELH)
      COEF= (1.4-ADN(K))/1.4
      PR= AP(K)/AP(K-1)
      RT= TR(K-1)/TR(K)
      DR= (RT*PR)**COEF
      RELD(K)= DR*RELD(K-1)
      POTT(K)= TR(K)*(1000./AP(K))**.2857
      VEL(K)= 0.515*VEL(K)
   10 CONTINUE
      ADN(1)= ADN(2)
      POTT(1)= TR(1)*(1000./AP(1))**.2857
      L= K-1
      WRITE(3,70)(TIT(J),J=1,9)
   70 FORMAT(1H1,19X,9A3,/
     A73X,4HWIND/
     111X,52H  HEIGHT       TEMP    POT TEMP    POLYTROPIC  RELATIVE
     A22H DIRECTION   VELOCITY /
     211X,52H (METERS)    (KELVIN) (KELVIN)     GAS COEFF   DENSITY
     A,22H    (DEG)        (M/S)     /)
      WRITE(3,75)(H(M),TR(M),POTT(M),ADN(M),RELD(M),DIR(M),VEL(M),
     1M=1,L)
   75 FORMAT(11X,F8.0,1X,F9.1,F10.1,F10.2,F11.3,2F11.2)
      GO TO 3
   30 CALL EXIT
      END
```

DURING STORM

HEIGHT (METERS)	TEMP (KELVIN)	POT TEMP (KELVIN)	POLYTROPIC GAS COEFF	RELATIVE DENSITY	WIND DIRECTION (DEG)	WIND VELOCITY (M/S)
0.	283.2	282.1	1.40	1.000	0.00	0.00
1000.	273.4	282.5	1.40	1.000	0.00	0.00
2000.	263.7	282.0	1.40	1.000	0.00	0.00
3000.	254.1	281.4	1.39	1.000	0.00	0.00
3500.	249.1	280.7	1.41	1.000	0.00	0.00
4000.	246.1	282.4	1.21	.993	0.00	0.00
5000.	238.9	285.3	1.27	.983	0.00	0.00
6000.	232.2	287.5	1.24	.972	0.00	0.00
7000.	225.7	290.7	1.24	.960	0.00	0.00
8000.	218.8	293.8	1.25	.948	0.00	0.00
9000.	211.9	296.6	1.25	.937	0.00	0.00
10000.	205.2	299.8	1.24	.925	0.00	0.00
11000.	197.7	302.3	1.28	.915	0.00	0.00

INPUT DATA

DURING STORM

0.00	1013.00	10.00	10.00	0.00	0.00
1000.00	891.00	.20	.20	0.00	0.00
2000.00	790.00	-9.50	-9.50	0.00	0.00
3000.00	699.00	-19.10	-19.10	0.00	0.00
3500.00	658.00	-24.10	-24.10	0.00	0.00
4000.00	617.00	-27.10	-27.10	0.00	0.00
5000.00	537.00	-34.30	-34.30	0.00	0.00
6000.00	473.00	-41.00	-41.00	0.00	0.00
7000.00	412.00	-47.50	-47.50	0.00	0.00
8000.00	356.00	-54.40	-54.40	0.00	0.00
9000.00	308.00	-61.30	-61.30	0.00	0.00
10000.00	265.00	-68.00	-68.00	0.00	0.00
11000.00	226.00	-75.50	-75.50	0.00	0.00
-100.00	0.00	0.00	0.00	0.00	0.00

APPENDIX C

Computer Program to Calculate the Diffusion Between Two Fluid Layers

APPENDIX C

COMPUTER PROGRAM TO CALCULATE THE DIFFUSION BETWEEN TWO FLUID LAYERS

DETERMINATION OF TIMEWISE DIFFUSION BETWEEN FLUIDS OF DIFFERENT DENSITIES

The assumption is made that the diffusion process between two fluids of different densities can be described by:

$$\frac{\partial C_a}{\partial t} = k \frac{\partial^2 C_a}{\partial y^2} \tag{1}$$

where

C_a = concentration of fluid A in fluid B,
t = time,
k = diffusion coefficient, and
y = vertical axis.

Equation (1) can be made dimensionless by defining:

$$\overline{C} = \frac{C_a}{C_{max}}, \qquad \overline{y} = \frac{y}{H}, \text{ and} \qquad \overline{t} = \frac{H^2 t}{k}$$

Using these definitions and dropping the subscript a, equation (1) can be written in finite elements as:

$$\frac{\Delta \overline{C}}{\Delta \overline{t}} = \frac{\Delta^2 \overline{C}}{\Delta \overline{y}^2} \tag{2}$$

Equation (2) can be solved for various initial conditions. For instance, one set of initial conditions could be:

$$\overline{C}(0,\overline{y}) = 1 \text{ for } 0 \leqq \overline{y} < 0.5, \text{ and}$$

$$\overline{C}(0,\overline{y}) = 0 \text{ for } 0.5 < \overline{y} \leqq 1.0.$$

The boundary conditions are:

$$\left.\frac{\Delta \overline{C}}{\Delta \overline{y}}\right|_{\overline{y}=0} = 0, \text{ and } \left.\frac{\Delta \overline{C}}{\Delta \overline{y}}\right|_{\overline{y}=1} = 0.$$

The following computer program solved this problem for a series of equal time increments. The value of each time increment is:

$$\Delta \overline{t} = \frac{(\Delta y)^2}{k}$$

As an alternative method, Mowbray[1] shows that the dimensionless concentration at any elevation is given by:

$$\bar{C} = \frac{1}{2}\left[1 + \frac{4}{\pi}\sum_{n=1}^{\infty}\frac{1}{n}\exp\left(-n\pi^2\bar{t}\right)\cot\left(\frac{n\pi}{4}\right)\cos\left(n\pi\bar{y}\right)\right] \tag{3}$$

In terms of a finite number of elevations, the series runs between $n = 1$ and $n = N$, where N equals the number of increments plus 1.

The results of the computer program are plotted in figure C-1 for selected time intervals. These results can be applied to a specific depth of fluid by setting H equal to the total fluid depth and using a diffusion coefficient of 0.00109 mm^2/s.

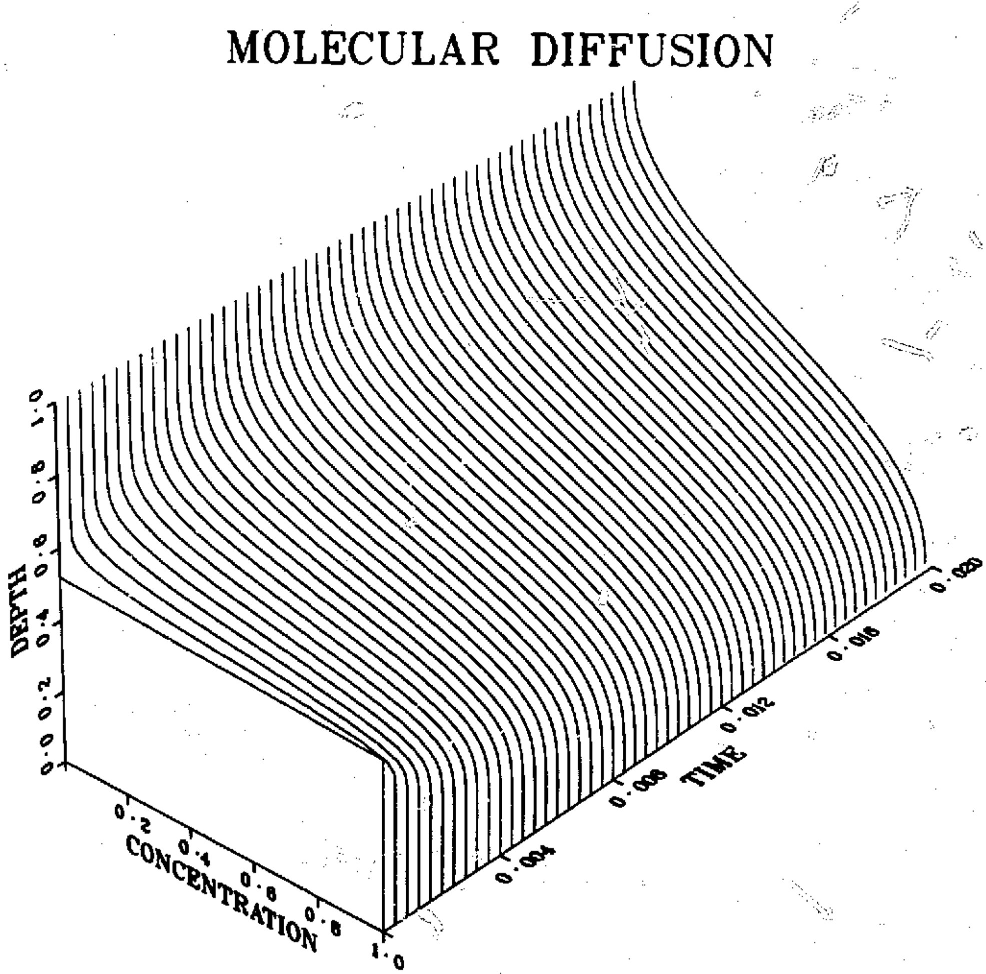

Figure C-1.—Fickian concentration distribution.

[1] Mowbray, D. E., "The Use of Schlieren and Shadowgraph Techniques in the Study of Flow Patterns in Density Stratified Liquids," J. Fluid Mech., vol. 27, part 3, pp. 595-608, 1967.

```
      PROGRAM HFDIFF(INPUT,OUTPUT,TAPE3=OUTPUT,PLFILE)
C
C     PROGRAM TO STUDY MOLECULAR DIFFUSION BETWEEN A SALINE LAYER
C             AND A FRESH WATER LAYER.
C
      DIMENSION Y(51),T(51),D(51),MESG(4)
      DATA(MESG(1)=6HFALVEY)
      DATA(MESG(2)=7HMC 1530)
      DATA(MESG(3)=9HEXT. 3760)
      DATA(MESG(4)=4HPLOT)
      DATA D/25*1.,0.5,25*0./
C
C     SET UP OF GRAPH PAPER
C
      CALL CCMPRS(30)
C     CALL DISSID(MESG)
      CALL BGNPL(-1)
      CALL TRIPLX
      CALL TITL3D("MOLECULAR DIFFUSION",19,7,7)
      CALL AXES3D("CONCENTRATION",13,"TIME",4,
     1"DEPTH",5,1.,2.,1.)
      CALL VUABS(10.,-10.,10.)
      CALL GRAF3D(0.,0.2,1.0,0.,0.04,0.2,0.,0.2,1.0)
C
C     INITIALIZATION OF DATA
C
      DO 10 J=1,51
      RJ=J
      Y(J)= 0.02*(RJ-1.)
      T(J)= 0.
   10 CONTINUE
C
C     OUTPUT OF RESULTS
C
      WRITE(3,1)
    1 FORMAT(1H1,/20X,34HDIFFUSION BETWEEN TWO FLUID LAYERS //
     119X,36HCONCENTRATIONS ARE REFERENCED TO THE /
     224X,26HINITIAL SALT CONCENTRATION //
     318X,38HGROUPS OF CONCENTRATIONS ARE SEPARATED /
     415X,45HBY A TIME INCREMENT EQUAL TO 10((H/50)**2)/D /
     517X,38HWHERE H= TOTAL DEPTH OF BOTH LAYERS,MM /
     623X,35HD=DIFFUSION COEFFICIENT, MM*MM/SEC //
     717X,39HINDIVIDUAL CONCENTRATIONS ARE SEPARATED /
     819X,35HBY A HEIGHT INCREMENT EQUAL TO H/50 //)
      WRITE(3,2)T(1),(Y(I),D(I),Y(I+1),D(I+1),Y(I+2),D(I+2),I=1,51,3)
      L=0
C
C     PLOT OF FIRST CURVE
C
      CALL CURV3D(D,T,Y,51,0)
      NT=0
C
C     COMPUTATION OF DATA POINTS
C
      DO 100 J=2,2501
      T(1)= T(1)+0.0008
      L=L+1
```

```
      NT= NT+1
      DO 50 K=2,50
      T(K)= T(K)+0.0008
C
C     INTERIOR POINTS
C
      D(K)= 0.2*(D(K+1)-2.*D(K)+D(K-1))+D(K)
   50 CONTINUE
C
C     EXTERIOR POINTS
C
      D(1)= 40.*(D(2)-D(1))+D(1)
      D(51)= 40.*(D(50)-D(51))+D(51)
      T(51)= T(51)+0.0008
C
C     OUTPUT OF RESULTS
C
      IF(L.EQ.10)WRITE(3,3)
    3 FORMAT(1H1,///,///,20X,
     1 34HDIFFUSION BETWEEN TWO FLUID LAYERS ///)
      IF(L.EQ.10)L=0
      IF(NT.EQ.50)WRITE(3,2)T(1),(Y(I),D(I),Y(I+1),D(I+1)
     1,Y(I+2),D(I+2),I=1,51,3)
    2 FORMAT(26X,20HDIMENSIONLESS TIME =,F8.4/
     1 8X,64HDEPTH  CONCENTRATION  DEPTH  CONCENTRATION  DEPTH  CONCENTR
     2ATION/
     317(1X,F12.3,F10.3,F12.3,F10.3,F12.3,F10.3/)
     4,//)
C
C     PLOT OF CURVES
C
      IF(NT.EQ.50)CALL CURV3D(D,T,Y,51,0)
      IF(NT.EQ.50) NT=0
  100 CONTINUE
      CALL ENDPL(0)
      CALL DONEPL
      CALL EXIT
      END
```

GPO 842-793

ABSTRACT

Analytical and laboratory studies were made to demonstrate the feasibility of using stratified liquids and distorted scale maps of an area to simulate mesoscale (2 to 20 kilometres) atmospheric phenomena. Techniques and instrumentation were developed for creating velocity gradients, creating density gradients, for visualization, and for making measurements. The effectiveness of both aerial and ground seeding station locations was investigated for various pilot study areas of Project Skywater.

ABSTRACT

Analytical and laboratory studies were made to demonstrate the feasibility of using stratified liquids and distorted scale maps of an area to simulate mesoscale (2 to 20 kilometres) atmospheric phenomena. Techniques and instrumentation were developed for creating velocity gradients, creating density gradients, for visualization, and for making measurements. The effectiveness of both aerial and ground seeding station locations was investigated for various pilot study areas of Project Skywater.

ABSTRACT

Analytical and laboratory studies were made to demonstrate the feasibility of using stratified liquids and distorted scale maps of an area to simulate mesoscale (2 to 20 kilometres) atmospheric phenomena. Techniques and instrumentation were developed for creating velocity gradients, creating density gradients, for visualization, and for making measurements. The effectiveness of both aerial and ground seeding station locations was investigated for various pilot study areas of Project Skywater.

ABSTRACT

Analytical and laboratory studies were made to demonstrate the feasibility of using stratified liquids and distorted scale maps of an area to simulate mesoscale (2 to 20 kilometres) atmospheric phenomena. Techniques and instrumentation were developed for creating velocity gradients, creating density gradients, for visualization, and for making measurements. The effectiveness of both aerial and ground seeding station locations was investigated for various pilot study areas of Project Skywater.

REC-ERC-77-8
Falvey, H T and Dodge, R A
ATMOSPHERIC SIMULATION USING STRATIFIED LIQUID MODELS
Bur Reclam Rep REC-ERC-77-8, Div Gen Res, July 1977, Bureau of Reclamation, Denver, 96 p, 51 fig, 1 tab

DESCRIPTORS—/ *atmospheric research/ *model studies/ *field investigations/ weather modification/ cloud seeding/ similitude
IDENTIFIERS—/ Project Skywater/ Leadville-Climax Pilot Project/ Sierra Cooperative Pilot Project/ Colorado River Basin Pilot Project

REC-ERC-77-8
Falvey, H T and Dodge, R A
ATMOSPHERIC SIMULATION USING STRATIFIED LIQUID MODELS
Bur Reclam Rep REC-ERC-77-8, Div Gen Res, July 1977, Bureau of Reclamation, Denver, 96 p, 51 fig, 1 tab

DESCRIPTORS—/ *atmospheric research/ *model studies/ *field investigations/ weather modification/ cloud seeding/ similitude
IDENTIFIERS—/ Project Skywater/ Leadville-Climax Pilot Project/ Sierra Cooperative Pilot Project/ Colorado River Basin Pilot Project

REC-ERC-77-8
Falvey, H T and Dodge, R A
ATMOSPHERIC SIMULATION USING STRATIFIED LIQUID MODELS
Bur Reclam Rep REC-ERC-77-8, Div Gen Res, July 1977, Bureau of Reclamation, Denver, 96 p, 51 fig, 1 tab

DESCRIPTORS—/ *atmospheric research/ *model studies/ *field investigations/ weather modification/ cloud seeding/ similitude
IDENTIFIERS—/ Project Skywater/ Leadville-Climax Pilot Project/ Sierra Cooperative Pilot Project/ Colorado River Basin Pilot Project

REC-ERC-77-8
Falvey, H T and Dodge, R A
ATMOSPHERIC SIMULATION USING STRATIFIED LIQUID MODELS
Bur Reclam Rep REC-ERC-77-8, Div Gen Res, July 1977, Bureau of Reclamation, Denver, 96 p, 51 fig, 1 tab

DESCRIPTORS—/ *atmospheric research/ *model studies/ *field investigations/ weather modification/ cloud seeding/ similitude
IDENTIFIERS—/ Project Skywater/ Leadville-Climax Pilot Project/ Sierra Cooperative Pilot Project/ Colorado River Basin Pilot Project